

THESIS

2
2003
57296434

This is to certify that the
thesis entitled

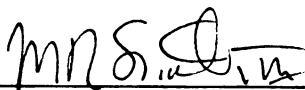
MODIFICATION OF POLYLACTIDES FOR TISSUE GROWTH

presented by

Mei Wang

has been accepted towards fulfillment
of the requirements for the

M.S. degree in Chemistry



Major Professor's Signature

5/7/04

Date

MSU is an Affirmative Action/Equal Opportunity Institution

LIBRARY

Michigan State

University

PLACE IN RETURN BOX to remove this checkout from your record.
TO AVOID FINES return on or before date due.
MAY BE RECALLED with earlier due date if requested.

DATE DUE	DATE DUE	DATE DUE
APR 23 2007		

MODIFICATION OF POLYLACTIDES FOR TISSUE GROWTH

By

Mei Wang

A THESIS

Submitted to

Michigan State University

In partial fulfillment of the requirement for the degree of

MASTER OF SCIENCE

Department of Chemistry

2004

ABSTRACT

MODIFICATION OF POLYLACTIDE COPOLYMERS FOR TISSUE GROWTH

By

Mei Wang

Poly(lactide (PLA) and its copolymers have been used as biomedical materials due to their biocompatibility. In recent years, many studies have shown their application in tissue engineering as a biocompatible and dissolvable scaffold. Designing scaffolds that contain functionality is desirable for optimizing interaction between cell and surface. Our group has worked out chemistry to synthesize functionalizable copolymers via bulk copolymerization of L-lactide and diallylglycolide. Through hydroboration/oxidation, we successfully converted the terminal double bond to terminal hydroxyl group and by carbodiimide coupling reactions, we attached biological substrates such as fatty acids to the copolymer covalently. These uniquely modified copolymers have also been evaluated for their potential as biocompatible surfaces to direct cell growth and differentiation.

As for tissue growth on surfaces, cell geometry has been shown to be a critical factor for death and growth. For functionalizing a biodegradable surface in a designed and well controllable fashion for further growth studies, we also worked on patterning polymer surfaces by photolabile protecting and deprotecting strategy. Anthraquinon-2-ylmethoxycarbonyl (Aqmoc) has been attached to our copolymer as the hydroxyl protecting group, and was removed by irradiating with UV light ($\lambda > 350\text{nm}$). The synthesis and characterization of the functionalized copolymers, initial physiological experiments results are reported.

To my family and parents

ACKNOWLEDGMENTS

I would like to acknowledge my advisor Mitch Smith for his guidance during my graduate study. I benefit tremendously from the training he has imparted to me, teaching me to creatively think and effectively execute scientific research. I especially appreciate his encouragement that made me realize my potentials and have the confidence in pursuing a career as a scientist. I would also like to thank him for his understanding and support in my life.

Secondly, I would like to thank Greg Baker for his guidance and help in my study and research. I would also like to thank my committee member, William Wulff for his helpful suggestions. I would also like to thank Professor Laura McCabe and her group members Moushumi Hossain and Katie Porter for their cooperation in the physiological studies on the polymer surfaces.

Also, I would like to thank Christopher Radano for teaching me the basic research skills, and other former group members Daniel Holmes, Jian-Yang Cho for their friendship profitable scientific discussion. I would like to thank Abbas, Mike and J.T. Lee for sharing lab duties and cooperation in everyday lab work. I would also like to collectively thank the MSU faculty and staff for catering to my needs for three years.

Finally and most importantly, I would like to thank my family and friends for their love, support and inspiration during my graduate study at Michigan State University.

TABLE OF CONTENTS

LIST OF FIGURES	vi
LIST OF TABLES	ix
LIST OF ABBREVIATIONS	x
CHAPTER ONE	1
1.1 Polylactide Applications as Biomedical Materials.....	1
1.1.1 Polylactide Application in Drug Delivery.....	1
1.1.2 Polylactide Application in Tissue Engineering.....	2
1.2 Processing and Modification of Polylactide for Tissue Engineering.....	5
1.2.1 Three Dimensional Structure Processing	5
1.2.2 Surface Modification of PLA-PGA Polymers	6
1.2.3 Synthesizing Novel PLA-PGA Based Polymers for Tissue Engineering ...	8
1.3 Cell Geometry Regulation on Material Surface	10
1.3.1 Cell Geometry Control over Cell Function	10
1.3.2 Micropatterning Material Surface for Cell Growth Studies.....	11
CHAPTER TWO.....	17
2 Functionalization of Polylactide Based Copolymer.....	17
2.1 Monomer Synthesis.....	18
2.2 Copolymer Synthesis and Characterization	20
2.3 Post-Polymerization Modification	22
2.3.1 Hydroboration-Oxidation	23
2.3.2 Side Chain Coupling Reactions.....	26
2.4 Cell Growth Studies on Fatty Acids Modified Poly(Lactic Acid) Surfaces	33
2.4.1 Copolymer Thin Films	33
2.4.2 Osteoblast Cell Shape.....	35
2.4.3 Osteoblast Proliferation.....	36
2.4.4 Osteoblast Differentiation	39
2.5 Conclusions	43
CHAPTER THREE.....	44
3 Photolabile Protection-Deprotection Strategy in Surface Patterning.....	44
3.1 Photolabile Protecting Group Selection.....	45
3.2 Synthesis of Aqmoc Protected PLLA-g-HP.....	47
3.3 Photolysis of Aqmoc Protected PLLA-g-HP	49
3.4 Conclusion.....	52
CHAPTER FOUR.....	54
4 Experimental Section.	54
4.1 General Considerations	54
4.2 Synthesis.....	58
CHAPTER FIVE.....	66
5 References	66
Appendix A	71
Appendix B	79

LIST OF FIGURES

Figure 1. Mechanism of delayed dissolution via biodegradable drug delivery system.	2
Figure 2. Schematic diagram of bone tissue regeneration via a cell-polymer biohybride device.	3
Figure 3. Surface modification by alkali hydrolysis treatment.	7
Figure 4. Copolymerization and modification of poly(lactic acid) using L-lysine and L-lactide cyclic comonomer.....	9
Figure 5. Amino acid containing cyclic comonomers.	10
Figure 6. Diagram of substrates used to vary cell shape independently of the cell-ECM contact area. Substrates were patterned with (A) a small single round island, (B) small closely spaced circular islands and (C) a large single round island.	11
Figure 7. Schematic Diagram of the Photoresist Surface Patterning Process.....	13
Figure 8. Schematic Diagram of the Microcontact Printing Process	14
Figure 9. Schematic Diagram of the Photografting Polymerization Process. (A) A polymer substrate containing photoiniferter is prepared on silicon surface, (B) additional monomer is added to the surface and exposed to UV light through a photomask, (C) covalently-bound polymer is grown from the substrate surface in the regions exposed to light.....	15
Figure 10. Synthetic route to 3,6-diallylglycolide.....	19
Figure 11. ^1H NMR (300 MHz, CDCl_3) spectrum of 3,6-diallylglycolide. H_c^* denotes the R,R and S,S isomers, H_c^{**} denotes the R,S isomer.	20
Figure 12. Synthetic route to poly(L-lactide- <i>co</i> -diallylglycolide).	21
Figure 13. ^1H NMR (300 MHz, CDCl_3) spectrum of poly(L-lactide- <i>co</i> -allylglycolide).	22
Figure 14. Mechanism of the hydroboration/oxidation reaction of terminal olefins.	23
Figure 15. Synthetic route to poly(lactide- <i>g</i> -hydroxypropane) <i>via</i> hydroboration-oxidation of poly(lactide- <i>co</i> -diallylglycolide).	24
Figure 16. ^1H NMR (300 MHz, CDCl_3) spectra of (A) PLLA- <i>g</i> -HP; poly(L-lactide- <i>g</i> -hydroxypropane) and (B) PLLA- <i>co</i> -AG; poly(L-lactide- <i>co</i> -diallylglycolide).	26
Figure 17. General synthetic route to polymer-bound esters using DCC coupling.	27
Figure 18. Structure of phospholipid and cell membrane phospholipids bilayer.....	28

Figure 19. Synthetic route to saturated and unsaturated fatty acid-modified PLLA using DCC coupling.....	29
Figure 20. ¹ H NMR (500 MHz, CDCl ₃) spectra of (a) PLLA-g-HP, (b) PLLA-g-MyPr, and (c) PLLA-g-StPr.	31
Figure 21. ¹ H NMR (300 MHz, CDCl ₃) spectra of (a) PLLA-g-OlPr; (b) PLLA-g-LnPr; and (c) PLLA-g-ArPr.	32
Figure 22. Microscope images of osteoblasts cultured for 48 hours on (a) silicon oxide and (b) PLLA-co-DAG (c) PLLA-g-HP (d) PLLA-g-MyPr (e) PLLA-g-StPr (f) PLLA-g-OlPr (g) PLLA-g-LnPr (h) PLLA-g-ArPr. The cells are stained red and the nuclei are stained blue.	36
Figure 23. Illustration of cell replication incorporating the BrdU fluorescent label.....	36
Figure 24. Digital photo images of fluorescent BrdU-labeled osteoblasts on (a) silicon oxide, (b) PLLA-co-DAG (c) PLLA-g-HP (d) PLLA-g-MyPr (e) PLLA-g-StPr (f) PLLA-g-OlPr (g) PLLA-g-LnPr (h) PLLA-g-ArPr.	38
Figure 25. Result of osteoblast cell proliferation on (a) silicon oxide, (b) PLLA-co-DAG (c) PLLA-g-HP (d) PLLA-g-MyPr (e) PLLA-g-StPr (f) PLLA-g-OlPr (g) PLLA-g-LnPr (h) PLLA-g-ArPr. Averages are expressed as an n-fold change compared to control, uncoated blank surfaces.	39
Figure 26. Gene expression levels of osteocalcin and alkaline phosphatase as a function of osteoblast culture time.	40
Figure 27. Result of osteoblast cell early and late stage differentiation on silicon oxide, PLLA-co-DAG, PLLA-g-HP, PLLA-g-MyPr, PLLA-g-StPr, PLLA-g-OlPr, PLLA-g-LnPr, and PLLA-g-ArPr. Averages are expressed as an n-fold change compared to control, uncoated blank surfaces.	41
Figure 28. Result of osteoblast cell early and late stage differentiation on silicon oxide, PLLA-co-DAG, PLLA-g-HP, PLLA-g-MyPr, PLLA-g-StPr, PLLA-g-OlPr, PLLA-g-LnPr, and PLLA-g-ArPr. Averages are expressed as a fold change compared to control, uncoated blank surfaces.	42
Figure 29. Photolabile protection-deprotection surface patterning for cell growth. (A) Polymer thin film with a functionalized side chain protected by photolabile protecting groups is exposed to UV light through a mask containing the desired pattern, (B) after irradiation, protecting groups are removed in the exposed region, (C) bioactive functional groups are incorporated in the deprotected region, (D) cells are seeded on the polymer surface with desired geometry.....	45
Figure 30. Photolabile polycyclic aromatic hydrocarbons bearing benzylic methylene groups.	46

Figure 31. Synthetic route of Aqmoc Protected PLLA-g-HP.	47
Figure 32. NMR spectrum PLLA-g-AqmocPr.....	48
Figure 33. DMAP Catalyzed PLA Depolymerization.	49
Figure 34. Photolysis of PLLA-g-AqmocPr.	49
Figure 35. UV-Vis spectra of PLLA-g-Aqmoc and PLLA-g-HP.	51
Figure 36. NMR spectra of PLLA-g-Aqmoc (<i>a</i>) before and (<i>b</i>) after photolysis.	52

LIST OF TABLES

Table 1. Copolymerization of <i>L</i> -Lactide and 3,6-diallylglycolide. ^a Molar composition of DAG determined by integration of the methylene resonance of the allyl repeat unit compared to the methine resonance of the lactide repeat unit. ^b Molecular weight determined by GPC. ^c PDI = Polydispersity index (M_w/M_n).	21
Table 2. Saturated and unsaturated fatty acid-modified PLLA copolymers containing 8 mol % fatty acid. ^a Molecular weight determined by GPC. ^b PDI = Polydispersity index. ^c From differential scanning calorimetry of 8 mol % fatty acid-modified copolymers. Data are from second heating scan at 10°C/min under helium. ^d Hydroxylated copolymer starting material used to couple fatty acids.	30
Table 3. Thin films of copolymers spin-coated on 1-inch diameter silicon wafers from a 1% (w/w) solution in toluene unless otherwise noted. Spin rate: 2500 rpm, spin time: 60 sec. ^a Mole percent loading determined by ¹ H NMR spectroscopy. ^b Determined by ellipsometry. ^c Samples were prepared by heating above the polymer melting point and quenching to room temperature to obtain amorphous samples. Static (θ_{st}), advancing (θ_{adv}) and receding (θ_{rec}) contact angles were measured at a rate of 3 μ L/s up to a total volume of 30 μ L using Milli-Q grade water.	34
Table 4. PDLLA stability under long and full range UV irradiation. ^a Molecular weight determined by GPC. ^b Polydispersity index (M_w/M_n).	46
Table 5. PDLL-g-AqmocPr deprotection under UV irradiation. ^a Conversion is determined by UV-vis spectroscopy. ^b Molecular weight determined by GPC. ^c Polydispersity index (M_w/M_n).	50

Images in this dissertation are presented in color.

LIST OF ABBREVIATIONS

Aqmoc	Anthraquinon-2-ylmethoxycarbonyl
BBA	4-tert-Butylbenzylalcohol
9-BBN	9-borabicyclononane
br	Broad
BrdU	Bromodeoxyuridine
d	Doublet
DAG	3,6-Diallylglycolide
DCC	Dicyclohexylcarbodiimide
dd	Doublet of Doublet
DMAP	N,N-Dimethyl-4-aminopyridine
DSC	Differential Scanning Calorimetry
ECM	Extracellular Matrix
GPC	Gel Permeation Chromatography
HA	Hydroxyapatite
HPA	2-Hydroxypent-4-enoic acid
J	Coupling Constant
m	Multiplet
M _n	Number Average Molecular Weight
NMR	Nuclear Magnetic Resonance
PDI	Polydispersity Index
PDLLA	Racemic Poly(lactide)
PDLLA- <i>co</i> -DAG	Poly(D,L-lactide- <i>co</i> -diallylglycolide)
PDMS	Polydimethylsiloxane

PEG	Poly(ethylene glycol)
PGA	Poly(glycolide)
PLLA	Poly(L-lactide)
PLLA-g-Aqmoc	Poly(L-lactide-g-Anthraquinon-2-ylmethyl propyl carbonate)
PLLA-g-ArPr	Poly(L-lactide-g-Arachidonic acid propyl ester)
PLLA-g-HP	Poly(L-lactide-g-Hydroxypropane)
PLLA-g-LnPr	Poly(L-lactide-g-Linoleic acid propyl ester)
PLLA-g-MyPr	Poly(L-lactide-g-Myristic acid propyl ester)
PLLA-g-OlPr	Poly(L-lactide-g-Oleic acid propyl ester)
PLLA-g-StPr	Poly(L-lactide-g-Stearic acid propyl ester)
PTSA	<i>p</i> -Toluenesulfonic acid
q	Quartet
RGD	Arginine-Glycine-Aspartic Acid
r.t.	Room Temperature
s	Singlet
SAM	Self-Assembled Monolayer
t	Triplet
T _c	Crystallization Temperature
TCP	Tricalcium Phosphate
T _g	Glass Transition Temperature
THF	Tetrahydrofuran
T _m	Melting Temperature
UV-Vis	Ultraviolet-Visible

CHAPTER ONE

1.1 Polylactide Applications as Biomedical Materials

Poly(lactide) was first used as absorbable suture material in the 1960s. Numerous *in vivo* and *in vitro* studies and its successful clinical use indicated satisfactory biocompatibility and the absence of significant toxicity, which opened the door to poly(lactide)'s application as a biomedical material in the fields of drug delivery and tissue engineering.¹

1.1.1 Polylactide Application in Drug Delivery

Drug delivery systems can improve drug efficacy by two mechanisms. The first is temporal control, where the effective drug concentration at the site of therapeutic action is controlled by the drug delivery system. The second mechanism involves targeting a specific therapeutic site. This maximizes drug concentration at the site of interest and minimizes side effects at nontherapeutic sites. Many kinds of biodegradable polymers have been investigated as drug carriers for controlled release. Ideal candidates allow for modification of the pharmacokinetics of the encapsulated drug through degradation/release kinetics and also should have good biocompatibility with the target site.

Poly(lactide) (PLA) (including Poly(L-lactide) (PLLA), Poly(D-lactide) (PDLA) and Poly(D,L-lactide (PDLLA)), poly(glycolide) (PGA), and their co-polymer, poly(lactide-*co*-glycolide) (PLGA) have proven to be an effective system for drug delivery, especially for prolonged delivery of peptides and proteins.² The delivery is usually achieved by a temporal release mechanism (Figure 1).³ The therapeutic reagent is

either coated with a biodegradable polymer or incorporated in the polymer matrix. The polymer degrades at a slower rate than the drug dissolution. Therefore the drug concentration is maintained at a constant and effective level through the dosage period.

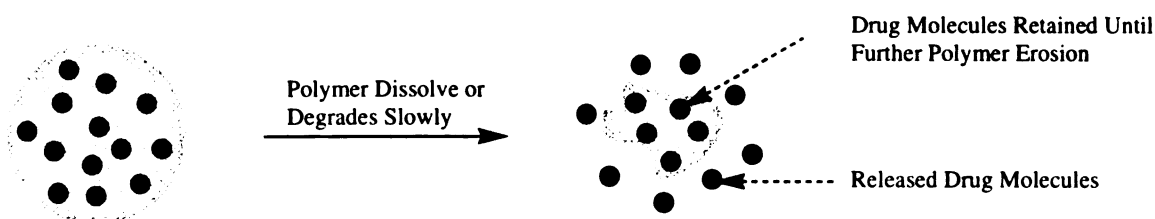


Figure 1. Mechanism of delayed dissolution via biodegradable drug delivery system.

The polymers are safe for *in vivo* use, because their degradation products are corresponding hydroxy acids, which are natural metabolism products of the body. Even though increased acidity during the polymer degradation might cause slight irritation at the site of polymer employment, this problem can be solved by introduction of basic salts to control the pH of the drug release environment.⁴ Moreover, since L-lactic acid is the naturally occurring enantiomer of lactic acid, PLLA is considered to be more biocompatible. It is widely applied as one of the major components of PLA based biodegradable copolymers.

1.1.2 Polylactide Application in Tissue Engineering

Several years ago, scientists believed that human tissue could only be replaced with direct transplants or fully artificial parts made of plastic. Although countless patients benefited from these therapies, they are still not the perfect solution for millions of patients suffering from tissue loss or organ failure. The number of organ donors is far from enough to supply the increasing numbers of patients. Even for patients lucky to

have organ transplantation, a large percent of them experienced multiple side effects due to rejection by the patients' immune system. Since fully artificial devices cannot perform all of the functions of single organ, they are currently far from a perfect tissue or organ substitute.^{5,6}

In recent years, biohybrid organs (a combination of living cells and natural or artificial polymers) have proven to be a feasible alternative to tissue or organ replacement. Cells from the patient or from a suitable donor are harvested and seeded into a three-dimensional scaffold of biodegradable polymers under appropriate *in vitro* culture conditions. After cell proliferation, differentiation and initial tissue development have taken place *in vitro*, the entire structure of cells and polymer scaffold is transplanted into the appropriate site in the patient. The cells will further replicate, reorganize and form new tissue. At the same time, the polymer scaffolds degrade into harmless small molecules, leaving only the newly generated tissue (Figure 2).⁷⁻⁹

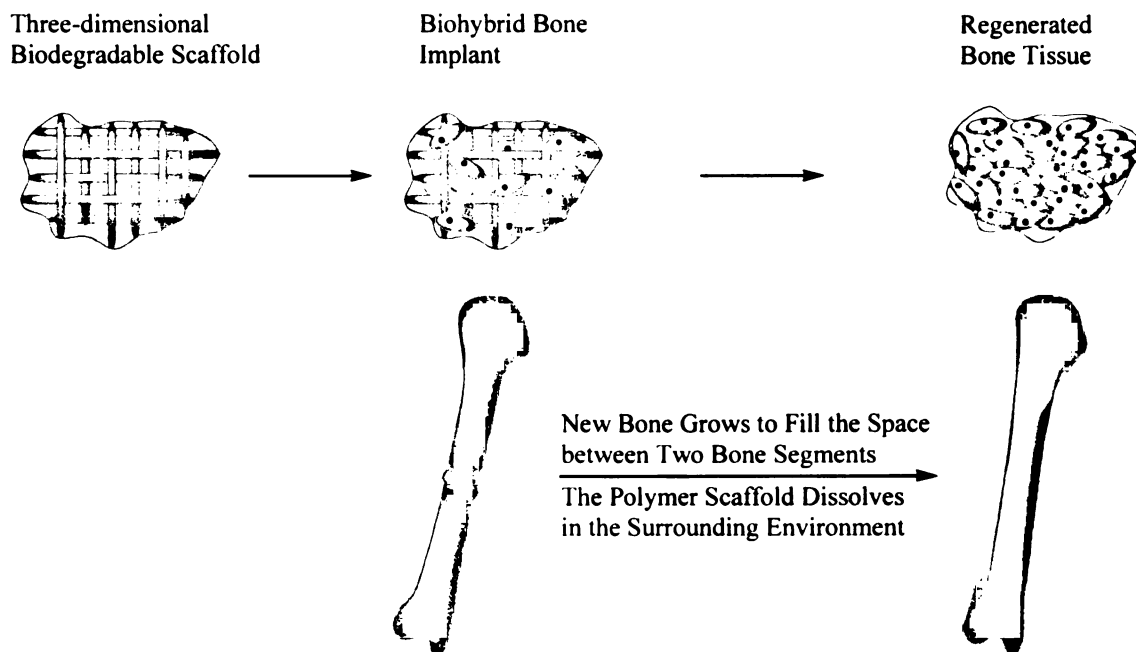


Figure 2. Schematic diagram of bone tissue regeneration via a cell-polymer biohybride device.

Designing biocompatible polymer scaffolds represents one of the major areas in tissue engineering research. Materials now being used as tissue engineering scaffolds fall into two major categories: natural materials such as collagen, and synthetic materials such as PLA, PGA and their copolymers. The advantage of natural materials is that they contain particular amino acid sequences that may facilitate cell attachment or guide cell differentiation at different stages.¹⁰ However, natural materials typically have poor physical properties, scale up difficulties, and show batch-to-batch variation. Synthetic materials, on the other hand, present good physical strength and processability as cell or tissue supports. Their molecular weights and degradation rates can be well controlled during large scale production.^{6,8,11}

The ideal synthetic polymers for tissue engineering should meet the following criteria: (1) The polymer surface should permit cell adhesion and growth, (2) both the polymer and its degradation products should have low toxicity for *in vivo* application, (3) the material should be processable into a three dimensional scaffold with high porosity to provide sufficient surface area for cell attachment and extracellular matrix (ECM, an insoluble aggregate of several large proteins and glycosaminoglycans, which provide a three dimensional environment to organize cells into tissue²⁸) regeneration, (4) the three dimensional scaffold must be strong enough to provide necessary support for the implant until the newly generated tissue is fully developed, (5) the material should be biodegradable, and the degradation rate should be adjustable to match the rate of tissue regeneration.²⁹

PLA, PGA and PLGA polymers are well characterized synthetic biomaterials. Numerous studies have demonstrated their sufficient biocompatibility with cells, such as

bone and cartilage cells.¹²⁻¹⁵ They present desirable physical properties to be processed into three dimensional structures with high porosity and desired shapes.^{13,16,17} By carefully manipulating monomer stereochemistry, comonomer ratio, molecular weight and polydispersity, the polymer degradation rate can be tuned to match the rate of tissue regeneration of different type of cells.¹⁸⁻²⁰

1.2 Processing and Modification of Polylactide for Tissue Engineering

1.2.1 Three Dimensional Structure Processing

To provide high surface area for high density cell seeding, nutrient supply, and ECM regeneration, the polymer scaffold must have high porosity (usually higher than 90%) and a large enough pore size.²¹ Many techniques have been successfully developed for making PLA-PGA polymers into three dimensional scaffolds for tissue engineering. Fiber bonding is one of the earliest techniques for developing PLA-PGA scaffolds. The three dimensional scaffold is developed by spraying PLLA or PLGA solution onto PGA fibers, followed by solvent evaporation.²² Particulate leaching is the most common method for creating porous polymer structures. A water soluble porogen, such as NaCl is mixed with a polymer solution. After the polymer solvent is removed, the polymer/salt composite is leached in water for two days to generate the porous structure.²³ The porosity of the resulting scaffold can be controlled by the amount of porogen added, and the pore size can be controlled by the size of the porogen. Similar to the particulate leaching methods, gas foaming techniques use gas as porogen to create porous scaffolds. The absence of the solvent leaching step shortens the preparation time, however the resulting pores are largely unconnected which might cause difficulties for cell seeding and migration.²⁴ Instead of using porogens, emulsification/freeze-drying and liquid-liquid

phase separation methods are based on the concepts of phase separation. In this method, a polymer emulsion or a polymer-rich and polymer-poor phase are created by either adding another immiscible solvent or cooling to a phase separation temperature. The polymer solution is quenched below the freezing point, and then solvent is freeze-dried to produce a porous structure. Due to the complexity of various thermodynamic and kinetic parameters applying in this method, various porous structures can be easily obtained.²⁵⁻²⁷

1.2.2 Surface Modification of PLA-PGA Polymers

Besides having a three dimensional macroporous structure that provides enough surface area for cell seeding, nutrient supply, and tissue growth, the cell affinity of biomaterials is a very important factor of successful tissue regeneration, because the surface properties of the material can regulate how cell responds to the material. Many studies have shown that cell attachment, growth, differentiation, and death is influenced by hydrophilicity/hydrophobicity³⁰, surface energy³¹, charge^{32,33} and roughness³⁴ of the material surface.

PLA-PGA polymers have many advantages as synthetic biocompatible materials being used in tissue engineering. However, the surface hydrophobicity, low surface energy and lack of functional sites for cell recognition are potential problems for further tissue engineering applications. To solve these problems and improve their surface interaction with cell cultures, much work has been done to improve the cell affinity of PLA-PGA polymers.

Plasma (a partially or fully ionized gas containing electrons, ions, and neutral atoms or molecules) treatment is one method used for improving cell affinity of PLA-PGA polymer surfaces. Wang and coworkers demonstrated that O-containing and N-

containing groups such as hydroxyl and amine were incorporated onto the surface of PDLLA films, improving the hydrophilicity of the surface and increasing the surface energy.³⁵

Surface alkali hydrolysis treatment is also a convenient method to modify PLA-PGA polymer surface. The polymer film or scaffolds were immersed into aqueous NaOH or a mixture of aqueous NaOH and ethanol. The ester bonds at the surface can be hydrolyzed, leaving carboxylic acid groups at the polymer surface. The resulting material can be used to conjugate other bioactive molecules, such as Arg-Gly-Asp (RGD) peptide, collagen, and biotin, which improve cell affiliation and reorganization (Figure 3).³⁶⁻³⁸

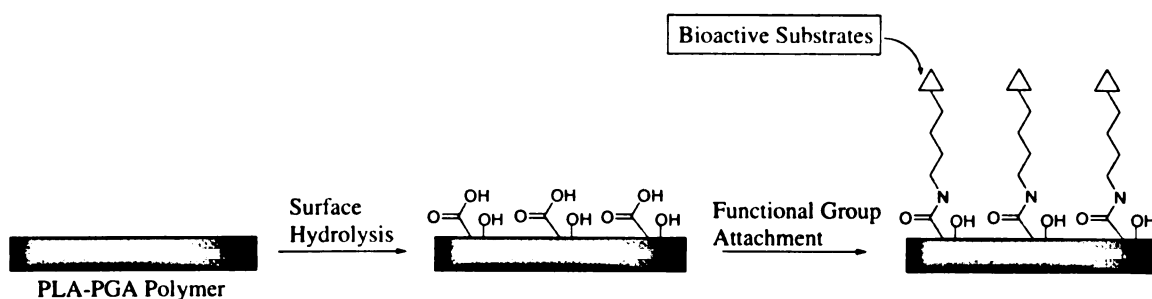


Figure 3. Surface modification by alkali hydrolysis treatment.

Hybridization is another method to overcome the hydrophobicity and chemical inertness of PLA-PGA polymers. PLA-PGA based polymers can be hybridized with natural polymers such as collagen or bioactive ceramics such as tricalcium phosphate (TCP), hydroxyapatite (HA), and selected compositions of commercially available Bioglass[®].³⁹⁻⁴³ By either coating or mixing, hybriide materials are developed with improved bioactivity and optimized physical properties result.

Other approaches have been developed to coat a layer of a bioactive substrate or another biocompatible polymer with functionalizable end groups on PLA-PGA polymer surfaced by techniques such as electrostatic self-assembly⁴⁴ and surface entrapment.^{45- 47}

ECM-like biomacromolecules were incorporated onto the polymer surface. *In vitro* cell growth study proved the incorporation of the bioactive substrates using the above methods has positive effects on cell attachment and growth.

1.2.3 Synthesizing Novel PLA-PGA Based Polymers for Tissue Engineering

Besides various techniques to modify PLA-PGA polymer surfaces, another approach is to covalently attach bioactive substrates such as certain amino acid sequences to the polymer chain. The hydroxyl end group on PLA-PGA polymer can be easily functionalized with bioactive substrates such as amino acids to provide some degree of functionality at the polymer surface. Langer and coworkers have developed a simple method to synthesize block copolymers of poly(lactide-*co*-glycolic acid) and polylysine by carbodiimide coupling reactions.⁴⁸ This simple method covalently attaches bioactive functionality to the polymer chain, however only the chain end is still limited to incorporate enough functional groups without sacrificing the bulk physical properties of the polymer.

Due to the limitation of end group functionalization, synthesizing novel PLA based biodegradable polymers with biologically significant groups covalently grafted onto the polymer back bone is a more desirable route for incorporating bioactive functionality. The immobilized bioactive side chain groups can improve cell adhesion on the polymer surface, and at the same time, it can also have specific interactions with cells to promote cell proliferation, differentiation, and tissue regeneration.

Langer and coworkers developed a synthetic route to the cyclic dimer of L-lactic acid and protected L-lysine. This cyclic dimer can be co-polymerized with L-lactide, yielding a copolymer of L-lactide with 1-5% of protected lysine units. After deprotection

of the lysine amino group, different bioactive substrates were attached to the polymer side chain through coupling reactions (Figure 4).^{49,50} Other groups designed similar routes to synthesize different amino acid containing copolymers that have different pendant groups for further functionalization. Ouchi and coworkers synthesized the cyclic dimers of glycolic acid with L-lysine, L-aspartic acid, and L-glutamic acid, and copolymerized them with L-lactide (Figure 5). The surface wettability, cell attachment and proliferation and material degradation during cell culture were analyzed. In general, the higher the mole fraction of the amino acid unit in the polymer, the more hydrophilic the surface becomes, and the higher degradation rate was observed. The amino acid containing copolymers showed higher cell attachment efficiency but lower cell growth rate compared with PLLA.^{51,52} The reason for the different results between cell attachment and cell growth still remains unclear. However, these copolymers can be further modified by coupling with other bioactive ligands such as the RGD cell adhesion peptide.

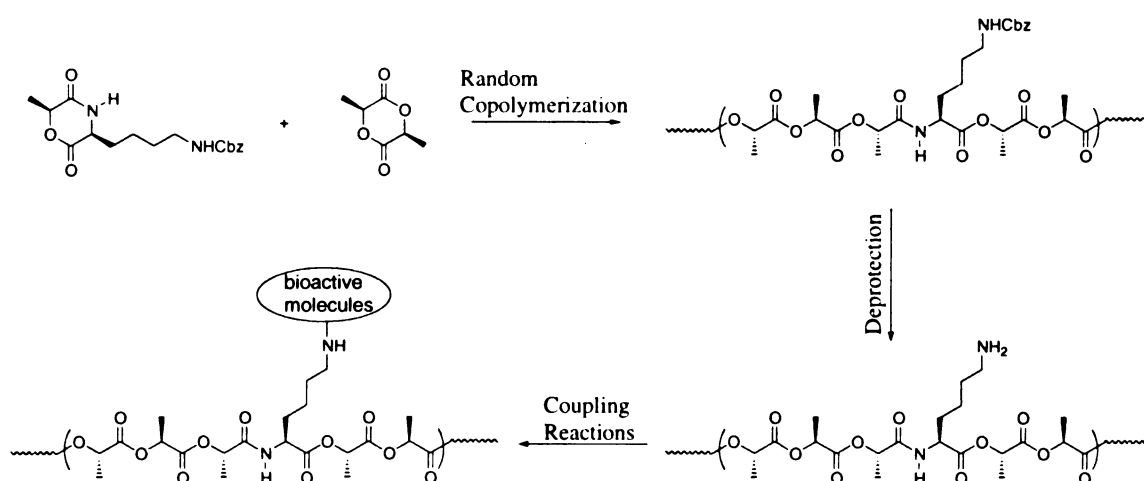


Figure 4. Copolymerization and modification of poly(lactic acid) using L-lysine and L-lactide cyclic comonomer.

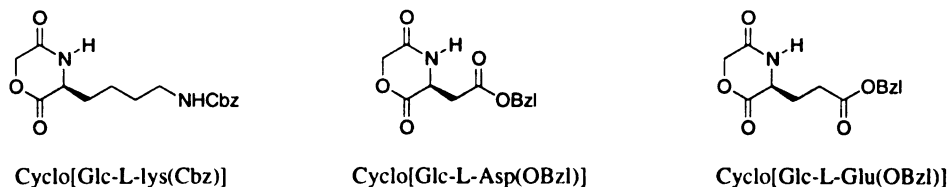


Figure 5. Amino acid containing cyclic comonomers.

Amino acid containing copolymers provide a certain amount of reactive sites on the polymer side chain for further functionalization. However the amino acid containing cyclic dimers usually have lower polymerization reactivity which often results in lower functional group density. The complex synthetic pathways often require protection and deprotection at the side chain functional group, which also might cause polymer molecular weight decrease and loss of functional groups.

1.3 Cell Geometry Regulation on Material Surface

1.3.1 Cell Geometry Control over Cell Function

Cell adhesion to surfaces plays a critical role in many cellular functions, such as proliferation, apoptosis (programmed cell death), migration and differentiation. Ingber and coworkers micropatterned planar surface to create cell adhesive islands that contained ECM and observed that human and bovine capillary endothelial cells were switched from growth to apoptosis by decreasing the cell attachment area (to about 400 μm^2 or smaller). To fully understand whether cell spreading or the total area of cell-ECM contact leads to cell survival and growth, they evaluated cell growth and apoptosis on multiple closely spaced adhesive islands. By changing the spacing between adhesive islands, cell spreading can be increased 10 fold without significantly altering the total cell-ECM contact area. They found that the extent of cell spreading, and not the area of

the adhesive contact, controlled cell life and apoptosis (Figure 6). These results showed that cell shape appears to be the critical determinant that switches cells between life and death and between proliferation and quiescence.⁵³ Further more, they also observed that intermediate cell spreading (area $\sim 1000 \mu\text{m}^2$) does not promote cell growth or death, but often exhibits differentiation behavior.⁵⁴

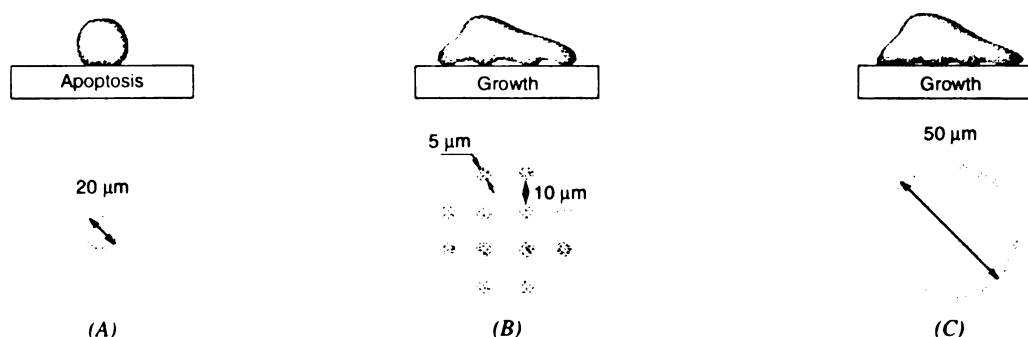


Figure 6. Diagram of substrates used to vary cell shape independently of the cell-ECM contact area. Substrates were patterned with (A) a small single round island, (B) small closely spaced circular islands and (C) a large single round island.

1.3.2 Micropatterning Material Surface for Cell Growth Studies

Based on the relationship between cell geometry and cell function, control of cell geometry on material surfaces has become an important topic in tissue engineering. However, the mechanisms of cell adhesion on specific material surfaces are still poorly understood. Therefore, it is beneficial to design methods for organizing cells on material surfaces, so cell-material and cell-cell interactions can be further studied. In recent several years, there have been many studies in cell biology that took advantage of patterned substrates. Healy and coworkers used patterned substrates to investigate gene expression in the differentiation of bone cells.¹⁰ Nelson and Chen used patterned substrates to confine pairs of contacting cells and demonstrated a novel proliferative

signal that stems from a direct cell-cell contact.⁵⁵ On the other hand, the cell biology studies on patterned surfaces can also be used to analyze a materials' ability to influence cell adhesion, proliferation, apoptosis, migration, orientation and differentiation, which leads to optimized biomaterial surface properties for tissue engineering applications.

Recent advances in patterning technology have generated a range of techniques to immobilize biomolecules on material surface with micron scale dimensions. Most of these different techniques begin with photolithography followed by another method such as laser ablation, photoresist lift-off, photoresist protection, photopolymerization and microcontact printing, etc. The micro scale pattern can be created by computer drawing software and printed on glass plates as the photolithographic mask. Then the pattern is transferred from the mask to the material surface.⁵⁶

The simplest technique is laser ablation. The substrate coated with chemical material is irradiated through a patterned mask. The material not protected by the pattern is degraded leaving the patterned area with chemical material on the surface. This method can be used to pattern protein materials such as polylysine.⁵⁷

Photoresists are commonly used to transfer patterns to substrates. A photodegradable material is first applied on the material surface, then placed in contact with the patterned mask and exposed to UV light. After removal of the degraded material, a photoresist copy of the pattern is produced. The area without photoresist pattern can be used to incorporate cell adhesive material. Finally the photoresist is "lifted off" of the material surface, leaving the cell adhesive material with designed pattern.^{58,59} Similarly, the photoresist can also be used to protect a material previously deposited on the

substrate. After patterning, the material at the unprotected area is removed from the substrate by chemical process (Figure 7).⁶⁰

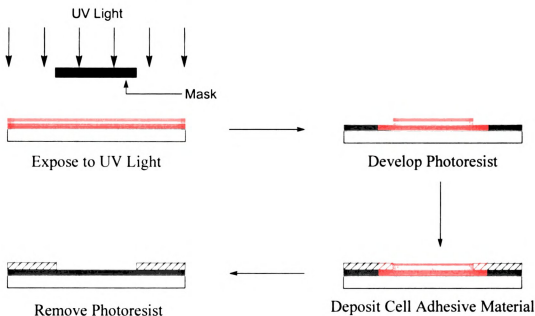


Figure 7. Schematic Diagram of the Photoresist Surface Patterning Process.

Microcontact printing is suitable for patterning fragile molecules.⁶¹ The method begins by using photolithography to mold a polydimethylsiloxane (PDMS) stamp. Different strategies have been developed to transfer patterns from the PDMS stamp to a substrate. A common example is to use alkanethiols, since the sulfur atoms in alkanethiols exhibits a strong affinity for gold atoms and alkanethiols are also readily absorbed into PDMS. Alkanethiols are stamped onto gold coated substrates with the alkane groups away from the substrate for further protein adsorption and cell attachment. The area without alkanethiol coating can be coated with polyethyleneglycol linked thiols which resist adsorption of protein (Figure 8).^{54,62}

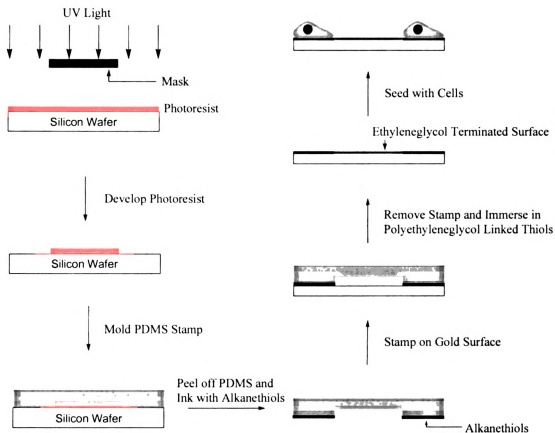


Figure 8. Schematic Diagram of the Microcontact Printing Process

The last example is the photografting polymerization technique, which usually uses a photoiniferter such as dithiocarbamate derivative to prepare micropatterned surface. Under UV irradiation, the photoiniferter can generate a reactive free radical that will initiate radical polymerization. When the photoiniferter is chemically bound to a surface with monomers deposited on it and irradiated through a photolithographic mask, a pattern of graft polymer chain can be created (Figure 9).⁶³

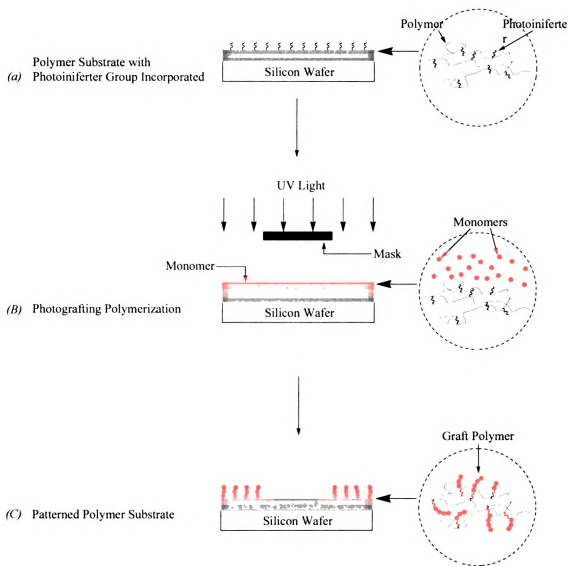


Figure 9. Schematic Diagram of the Photografting Polymerization Process. (A) A polymer substrate containing photoiniferter is prepared on silicon surface, (B) additional monomer is added to the surface and exposed to UV light through a photomask, (C) covalently-bound polymer is grown from the substrate surface in the regions exposed to light.

The surface micropatterning techniques being used still have some limitations, such as lengthy preparatory procedures and harsh chemical, photochemical and heating conditions during the process. The substrate and functional patterns being incorporated

are also limited. Thus new simple and moderate micropatterning techniques need to be designed for specific material surfaces and specific patterned functionalities.

CHAPTER TWO

2 Functionalization of Polylactide Based Copolymer

PLA and its copolymers have been proven to be suitable biomedical materials for drug delivery and tissue engineering applications. As synthetic biomaterials, they have good mechanical strength, are easy manipulated into desired shapes, and have optimal degradation kinetics. Through a variety of techniques, PLA copolymers can be made into unique three-dimensional scaffolds with high porosity. The highly porous material can provide enough surface area for cell seeding, nutrient supply, ECM regeneration and tissue growth. However, their hydrophobic nature, lack of cell recognition signals and poor surface chemistry for cell attachment, proliferation and differentiation could limit their applications as ideal three-dimensional matrices for cells. It will be beneficial to synthesize functionalized PLA based polymers that covalently incorporate bioactive moieties for cell attachment and cell-surface interaction. Many research groups have developed routes to synthesize lactide derivatives that have functionalizable side chains, and then copolymerized them with lactide.⁴⁹⁻⁵² The copolymers synthesized have a biodegradable ester backbone, and also present reactive side chain groups that can be further functionalized through chemical reactions. These methods provided opportunities to modify PLA polymer side chain for better cell surface interaction. However all of these methods require complicated synthetic pathways for each monomer. Further more, some reactive side chain functional groups are not compatible with the polymerization conditions. Protection and deprotection processes are required during the polymer synthesis, which might cause polymer molecular weight decrease or lose of functional groups.

An alternative copolymer synthesis pathway is to synthesize a common comonomer with a side group that is relatively inert under polymerization conditions, but can be converted into different reactive functional groups after polymerization. By applying this post polymerization modification strategy, protection-deprotection processes are minimized. Only one kind of comonomer needs to be synthesized, and a variety of functional groups can be attached to polymer side chain by a simple reaction protocol.

2.1 Monomer Synthesis

The allyl substituted lactide comonomer, 3,6-diallylglycolide (DAG), was synthesized using a general procedure for synthesizing lactide and a variety of alkyl substituted glycolides.⁶⁴ The metal-mediated allylation of glyoxylic acid monohydrate using allyl bromide as the allyl source, zinc powder and bismuth trichloride for *in situ* generation of the allylmethyl species, gave 2-hydroxypent-4-enoic acid (2-HPA) in 92% yield. The 2-HPA can be dimerized by acid catalyzed condensation in toluene at > 100 °C. The reaction usually takes 3 to 5 days, with the water produced from condensation being removed using a Dean-Stark trap. The crude product mixture contained both oligomers and the cyclic dimer. By distillation of the mixture over zinc oxide under reduced pressure, the oligomers can be converted to the cyclic dimer, 3,6-diallylglycolide (Figure 10).

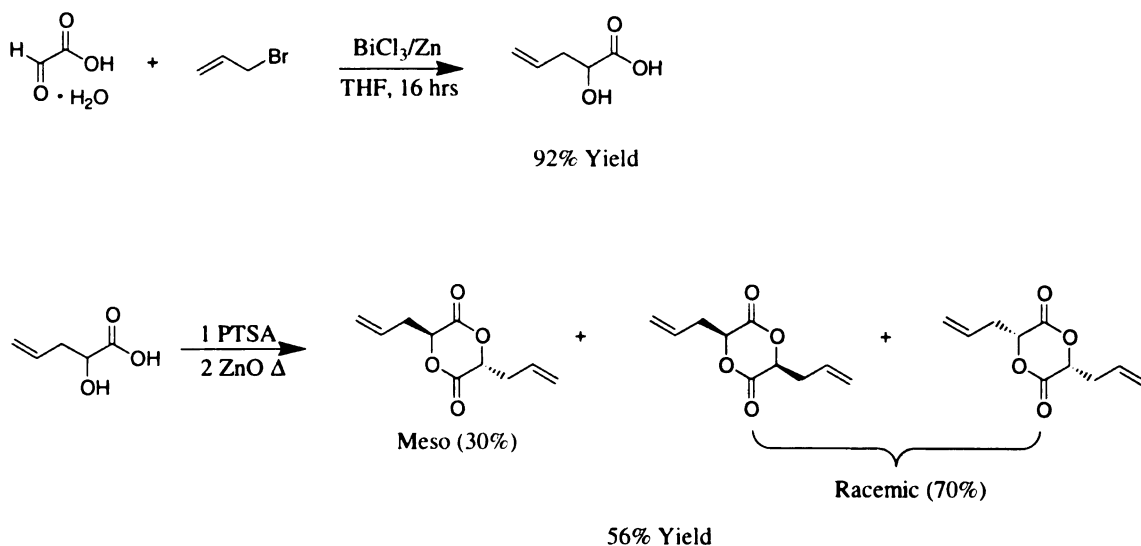


Figure 10. Synthetic route to 3,6-diallylglycolide.

The product contains 30% of the meso (RS) isomer and 70% of racemic (RR and SS) isomers. The RR, SS, and RS stereoisomers can be distinguished by NMR spectroscopy. This is mostly clearly seen in the methine region of the proton NMR spectrum. These protons both are observed as doublets of doublets at ~ 5.0 ppm (Figure 11).

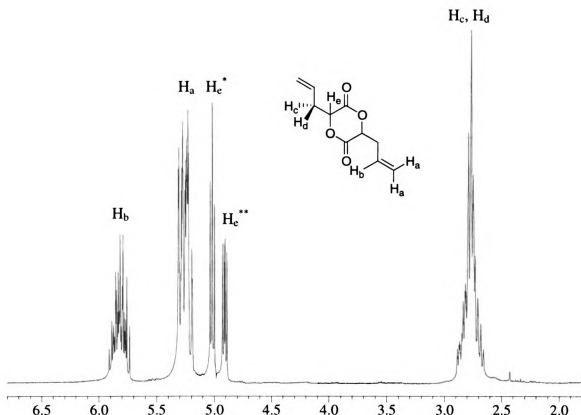


Figure 11. ^1H NMR (300 MHz, CDCl_3) spectrum of 3,6-diallylglycolide. H_c^* denotes the R,R and S,S isomers, H_c^{**} denotes the R,S isomer.

2.2 Copolymer Synthesis and Characterization

The copolymer poly(L-lactide-*co*-diallylglycolide), PLLA-*co*-DAG was synthesized by copolymerization of PLLA and DAG at 145 °C for 20 minutes, using tin(II)-2-ethylhexanoate as the catalyst and 4-*tert*-butylbenzylalcohol (BBA) as the initiators (Figure 12). The molecular weight can be controlled by varying the initiator and monomer ratio (M/I). Usually the copolymer is designed to contain 7-13% of DAG unit and have a M_n of 20,000-40,000 (Table 1).

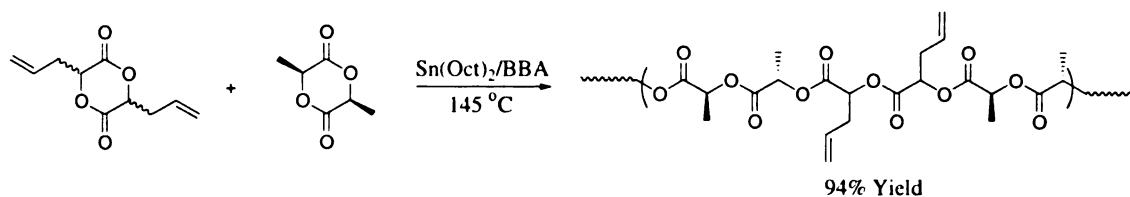


Figure 12. Synthetic route to poly(L-lactide-co-diallylglycolide).

<i>Monomer Feed Ratio (LLA:DAG)</i>	<i>Monomer/Initiator Ratio ([M]:[I])</i>	<i>Copolymer Composition^a (LLA:DAG)</i>	<i>M_n /gmol⁻¹ (PDI)^{b,c}</i>
90 : 10	300:1	92 : 8	33,900 (1.3)
85 : 15	300:1	86.5 : 13.5	20,800 (1.5)

Table 1. Copolymerization of *L*-Lactide and 3,6-diallylglycolide. ^a Molar composition of DAG determined by integration of the methylene resonance of the allyl repeat unit compared to the methine resonance of the lactide repeat unit. ^b Molecular weight determined by GPC. ^c PDI = Polydispersity index (M_w/M_n).

The copolymers were also characterized by ¹H NMR spectroscopy (Figure 13). The multiplet at 5.62- 5.81ppm indicates the presence of the internal olefin proton, while the resonance of the terminal olefin protons appears at 5.10-5.17, overlapping the methine proton resonance of both lactide and diallylglycolide units. Also, the methylene resonances of the pendant allyl group are observed between 2.5-2.8 ppm. The allyl monomer composition can be calculated by the integration of the methylene resonance vs. the integration of methyl resonance of the lactide unit. The molecular weights of the copolymers were determined by gel permeation chromatography (GPC). Based on the Fox equation, the thermal analysis previously done in our laboratory suggested the presence of a random copolymer.⁶⁵ The randomly distributed side chain olefins along the backbone are now ready to undergo functional group transformation.

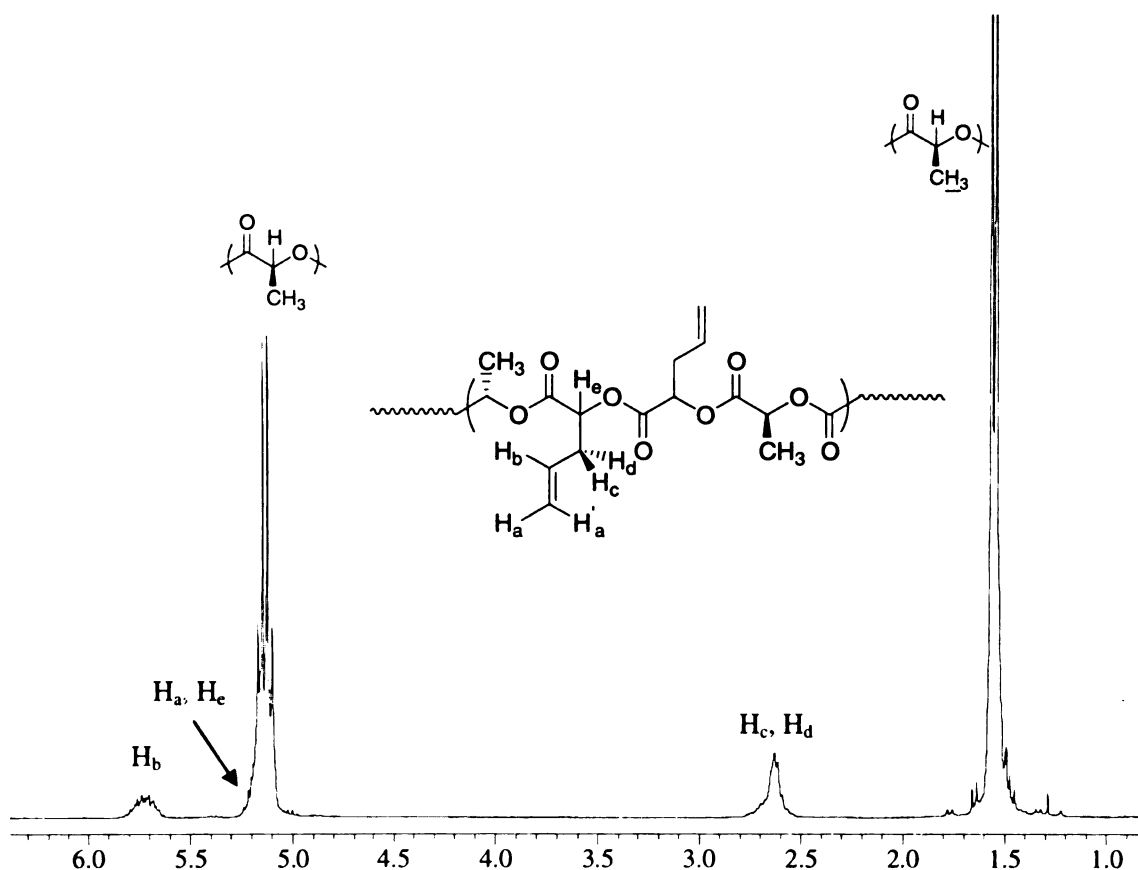


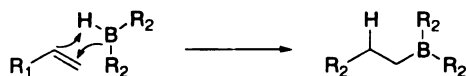
Figure 13. ¹H NMR (300 MHz, CDCl₃) spectrum of poly(L-lactide-*co*-allylglycolide).

2.3 Post-Polymerization Modification

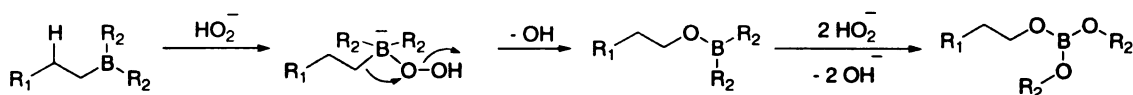
Our goal for the post polymerization modification is to link the polymer side chain with molecules with biological functions. The terminal olefin by itself doesn't provide enough available chemistry to achieve our desired transformation. However, the terminal olefin can be modified into other functional groups such as hydroxyl, carboxylic acid, etc, which would allow us to explore various types of coupling chemistry for attachment of bioactive substrates to the side chain. Alcohols are a particularly useful functional group for tethering substrates through reactions such as esterification or etherification, as well as carbonate and carbamate linkages. The best known transformation for converting olefins to alcohols is hydroboration followed by oxidation.

2.3.1 Hydroboration-Oxidation

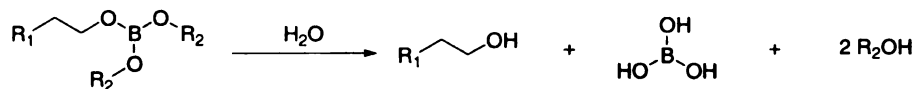
Hydroboration followed by oxidation is a very useful method to convert terminal olefins into primary alcohol groups. In a typical hydroboration-oxidation reaction, a borane molecule is added to the olefin double bond in an anti-Markovnikov fashion. The resulting organoborane is then treated with hydrogen peroxide under basic conditions to afford the primary alcohol (Figure 14). Similar to small molecule cases, hydroboration-oxidation reactions can also be applied on polymer substrates with an olefin group either in the polymer back bone or pendant from the polymer.^{66,67} The successful transformation provides a new method for synthesizing polymers with reactive side groups starting from simple, relatively inert monomers.



Step 1. Boron adds to the less substituted carbon of the double bond.



Step 2. Oxidation of the trialkylborate followed by migration of the alkyl group to the adjacent oxygen.



Step 3. Hydroxide attacks boron to give a primary alcohol and boronic acid.

Figure 14. Mechanism of the hydroboration/oxidation reaction of terminal olefins.

For our case, successful transformation of terminal olefin side group on the PLLA-*co*-DAG copolymer into a terminal hydroxyl side group provides us the opportunity to further incorporate biologically significant ligands onto our polymer side chain using simple organic methodology. This post-polymerization modification method

also avoids the synthesis of complex monomers, and subsequent protection and deprotection schemes before and after polymerization.

2.3.1.1 Synthesis and Characterization

The hydroxylated copolymer, poly(lactide-*g*-hydroxypropane) (PLLA-*g*-HP) was synthesized by the hydroboration of PLLA-*co*-DAG followed by oxidation using aqueous sodium acetate and hydrogen peroxide (Figure 1515).

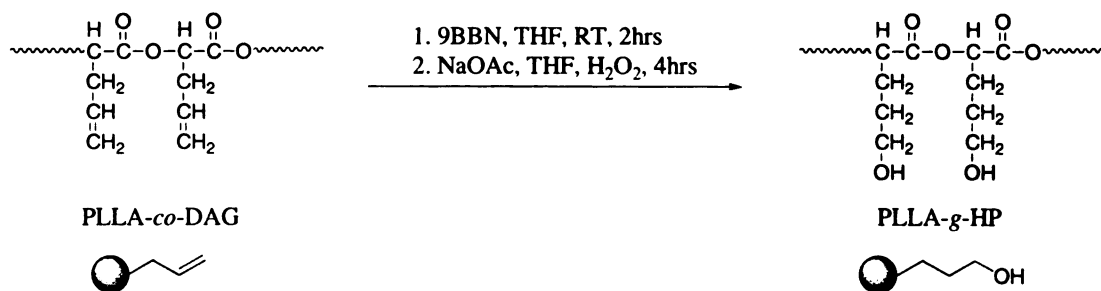


Figure 15. Synthetic route to poly(lactide-*g*-hydroxypropane) *via* hydroboration-oxidation of poly(lactide-*co*-diallylglycolide).

The first step of the hydroboration was carried out in the glove box. The polymer solution was stirred at room temperature for 2 hours using 9-borabicyclononane (9-BBN) as the borane source. The reaction can be followed by ^{11}B NMR, with a peak centered at 88 ppm indicating formation of the trialkyl-borane. In our first attempt, once the hydroboration was determined to be complete, the polymer was treated with 1.5 to 2.0 equivalents of aqueous sodium acetate and hydrogen peroxide. Boron was incompletely removed even when we increased the reaction time for the second step to 16 hours. A resonance at ~ 34 ppm in the ^{11}B NMR spectrum was observed indicating residual boronic acid on the polymer side chain. Repetition of the oxidation step was needed to fully remove the boron from the polymer. However, when we increased the amount of

H₂O₂ to three equivalents based on the 9-BBN added in the hydroboration step, the boron was removed completely after 4 hours and a second oxidation was not needed. After reprecipitation, no boron resonance can be observed in ¹¹B NMR spectrum and in ¹H NMR, a new peak at 3.62 ppm can be clearly seen indicating the successful hydroxylation of the olefin double bond.

After hydroxylation, the polymer molecular weight was unchanged ($M_n = 20,800$ gmol⁻¹ PDI = 1.50 for PLLA-*co*-AG vs. $M_n = 19,200$ gmol⁻¹ PDI = 1.55 for PLLA-*g*-HP) showing that no significant polymer degradation or crosslinking during the hydroboration-oxidation steps. The ¹H NMR spectrum of the copolymer shows the disappearance of the allyl methylene resonances and the appearance of the methylene next to the primary alcohol at 3.62 ppm. Also, the alkyl methylene resonances of the hydroxypropane group are seen between 1.65-2.04 ppm (Figure 16).

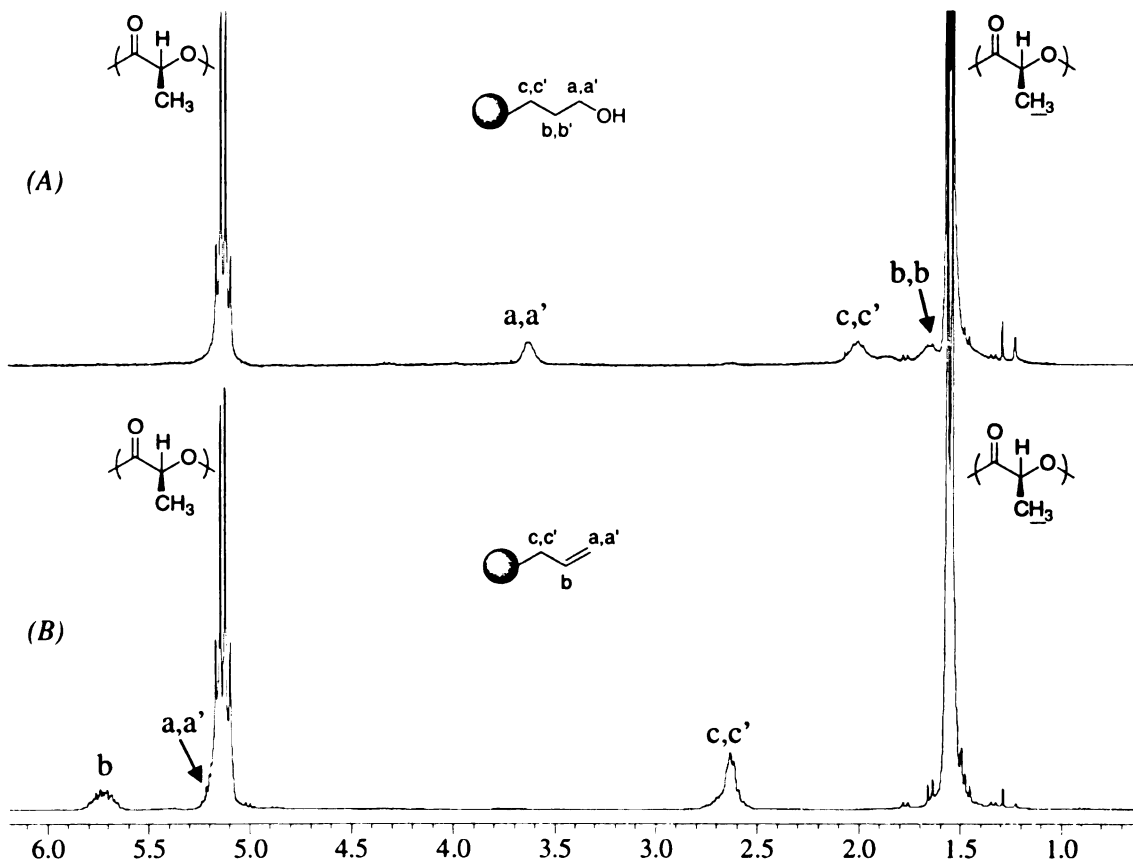


Figure 16. ^1H NMR (300 MHz, CDCl_3) spectra of (A) PLLA-g-HP; poly(L-lactide-g-hydroxypropane) and (B) PLLA-co-AG; poly(L-lactide-co-diallylglycolide).

The hydroxylated copolymer can be used directly as one kind of functional biomaterial for cell growth studies. On the other hand, the primary alcohol group on the polymer side chain can also be further functionalized with other bioactive molecules through simple transformations.

2.3.2 Side Chain Coupling Reactions

The primary alcohol group at the polymer side chain provides various methods for coupling the polymer side chain with other molecules through ester, carbonate or carbamate bonds. Since the polymer backbone contains ester bonds, harsh acidic or basic reaction conditions will cause polymer degradation. Therefore further side chain

modification reactions must be carried out under mild conditions. Many mild coupling reaction routes have been developed for coupling polymer chains or coupling a polymer chain with small molecules, such as dicyclohexyl carbodiimide (DCC) coupling^{48,74,75} and 1,1'-carbonyldiimidazole (CDI) coupling.^{68,69}

2.3.2.1 DCC Coupling

DCC coupling is a convenient synthetic route to connect alcohols with carboxylic acids by forming ester bonds. The reaction can be carried out at room temperature with a catalytic amount of N,N-dimethylaminopyridine (DMAP) as the catalyst. The insoluble dicyclohexyl urea byproduct can be removed by filtration. Due to the mild reaction conditions and easy product purification, DCC coupling is applied in peptide synthesis,^{70,71} dendrimer chemistry,^{72,73} and for coupling substrates to polymers.^{74,75} DCC coupling of our hydroxylated copolymer with a variety of carboxylic acids provides us a simple way to covalently attach bio-significant molecules that have carboxylic acid functional groups through an ester linkage (Figure 17). The newly modified copolymer might have improved biocompatibility as a material in tissue regeneration.

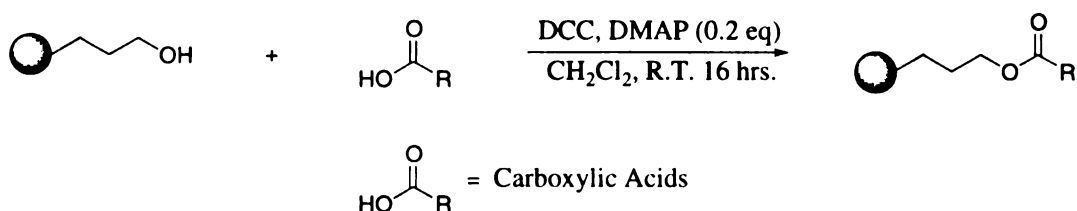


Figure 17. General synthetic route to polymer-bound esters using DCC coupling.

2.3.2.2 Side-Chain Esterification of Fatty Acids

Fatty acids are important biomolecules in cell biology. The basic structural unit of virtually all biomembranes is the phospholipid bilayer. In most common phospholipids,

glycerol forms the backbone of the molecules, with two hydroxyl groups linking to fatty acid residues to form the hydrophobic interior, and a third hydroxyl group linking to a bridging phosphate group to form the hydrophilic exterior (Figure 18). Besides being an important component of cell membrane, fatty acids have also been reported to influence the biology of bone tissue growth.^{76,77}

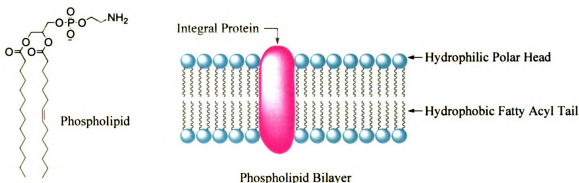


Figure 18. Structure of phospholipid and cell membrane phospholipids bilayer.

We chose myristic, stearic, oleic, linoleic and arachidonic acid to establish DCC coupling as a viable method for functionalizing PLLA-g-HP (Figure 19). Myristic acid and stearic acid are the most common saturated fatty acids, and cis unsaturated fatty acids are more common in cells than the trans form. The pendant hydroxyl groups reacted with the fatty acids in the presence of DCC and a catalytic amount of DMAP to incorporate fatty acids on our copolymer. Due to the biological significance of fatty acids in cell membrane structure and bone tissue growth, we expect that modified PLLA copolymers should show improved bone cell growth.

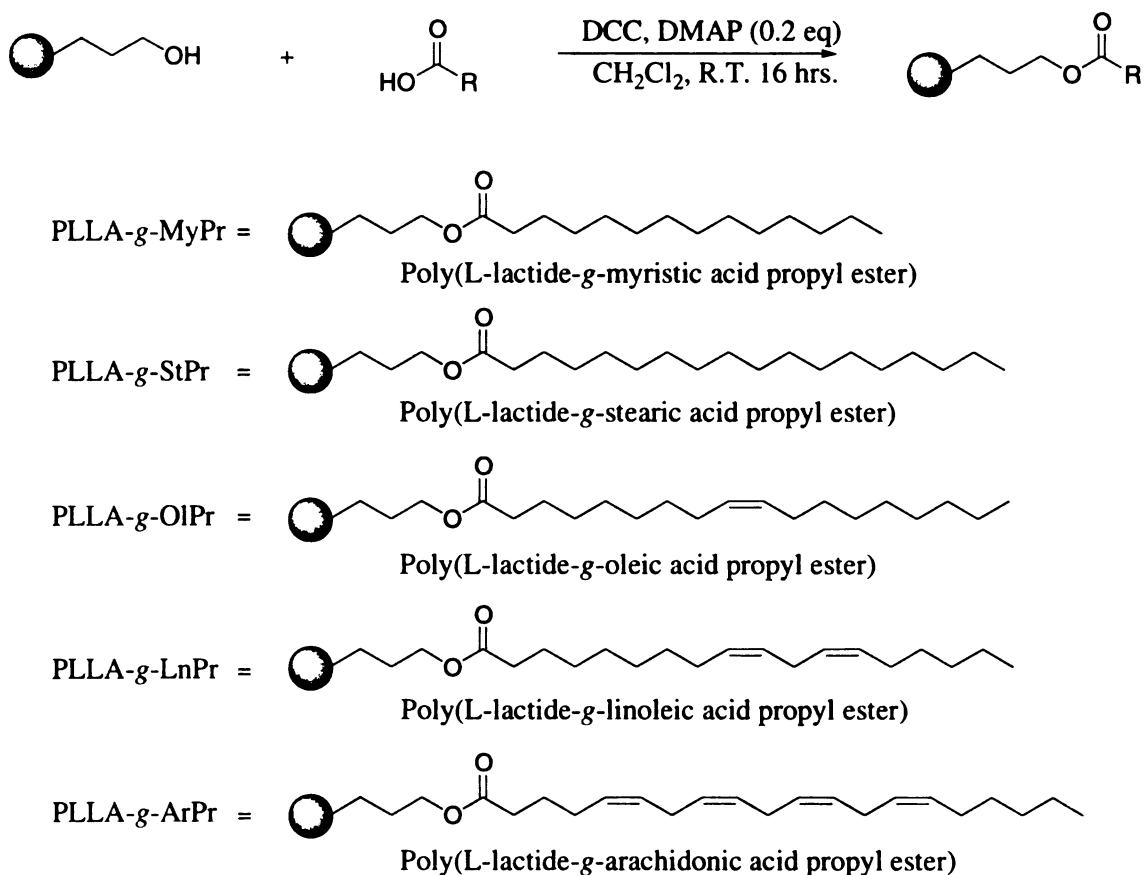


Figure 19. Synthetic route to saturated and unsaturated fatty acid-modified PLLA using DCC coupling.

The reactions were carried out at room temperature in CH_2Cl_2 for 20 hours. After the desired reaction time, the insoluble dicyclohexyl urea was removed by filtration, and the polymer solution was concentrated, and precipitated twice from methanol. Since no harsh acidic or basic conditions are required for DCC coupling reactions, high yield and full conversion were achieved with no molecular weight lost for all of the above fatty acid coupling reactions. Thermal analysis of the copolymers using DSC showed the T_g of the materials decreased from the original PLLA-g-HP (51°C) upon esterification of the fatty acids (Table 2). The DSC results of linoleic acid and the arachidonic acid-modified copolymers showed higher T_g s compares with saturated fatty acid and the oleic acid

modified copolymers we prepared, and no T_c and T_m were observed indicating oxidative and thermally-induced cross-linking occurred while the polymers were exposed to air.⁶⁵

<i>Fatty Acid</i>	$M_n / g mol^{-1} (PDI)^{a,b}$	$T_g / ^\circ C$	$T_c / ^\circ C$	$T_m / ^\circ C$	% Yield
PLLA-co-DAG	20,800 (1.50)	52	--	141	94
PLLA-g-HP ^d	24,900 (1.26)	51	122	147	85
Myristic	25,500 (1.29)	25	81	118	85
Stearic	28,900 (1.26)	37	112	141	86
Oleic	19,500 (1.35)	30	89	142	88
Linoleic	24,300 (1.40)	45	--	--	71
Arachidonic	25,600 (1.41)	45	--	--	78

Table 2. Saturated and unsaturated fatty acid-modified PLLA copolymers containing 8 mol % fatty acid. ^a Molecular weight determined by GPC. ^b PDI = Polydispersity index. ^c From differential scanning calorimetry of 8 mol % fatty acid-modified copolymers. Data are from second heating scan at 10°C/min under helium. ^dHydroxylated copolymer starting material used to couple fatty acids.

The products were also characterized by NMR. Quantitative incorporation was achieved for all coupling reaction with the above fatty acids. The methylene proton resonance at 3.62 ppm in PLLA-g-HP shifted to 4.04 ppm after CDD coupling indicating the complete conversion of fatty acids to their polymer-bound esters (Figure 20, 21). For the unsaturated fatty acid modified copolymers, olefinic proton resonances can be observed near 5.3 ppm. The olefinic proton integration increases with the increasing number of cis double bonds. PLLA-g-LnPr and PLLA-g-ArPr both have bisallylic methylene protons appearing at 2.7-2.8 ppm. The integration of the bisallylic methylene protons in PLLA-g-ArPr is about 3 times as much as in PLLA-g-LnPr.

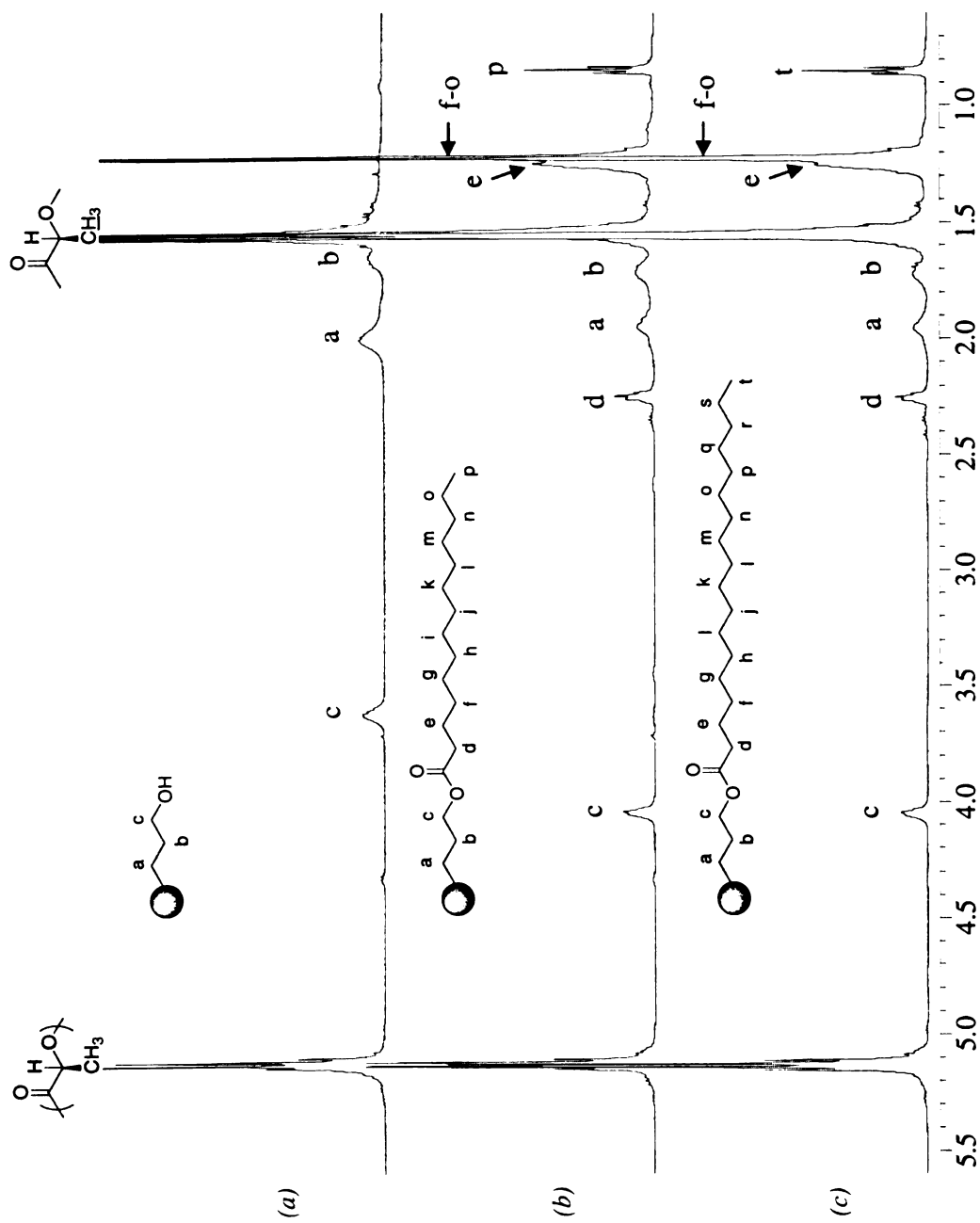


Figure 20. ^1H NMR (500 MHz, CDCl_3) spectra of (a) PLLA-g-HP, (b) PLLA-g-MyPr, and (c) PLLA-g-SPr.

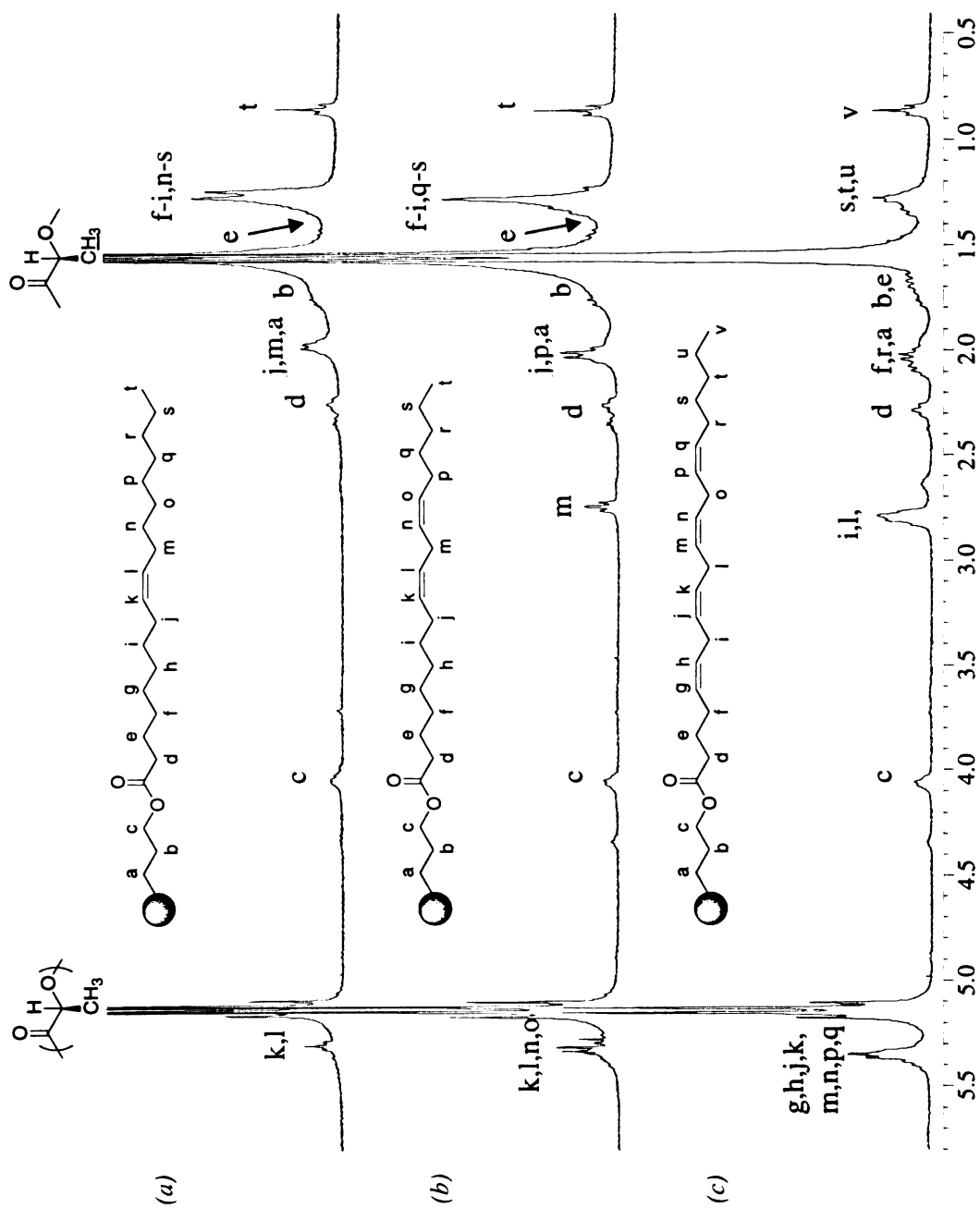


Figure 21. ^1H NMR (300 MHz, CDCl_3) spectra of (a) PLLA-g-OIPr; (b) PLLA-g-LnPr; and (c) PLLA-g-ArPr.

2.4 Cell Growth Studies on Fatty Acids Modified Poly(Lactic Acid) Surfaces

2.4.1 Copolymer Thin Films

In order to evaluate the properties of the modified materials for tissue engineering applications, thin films were prepared by spin coating the polymers on freshly cleaned silicon wafers. Osteoblasts were seeded on the polymer-coated wafers and their proliferation, differentiation, and shape during the culturing process were assessed.⁶⁵

Osteoblasts are important cells in bone physiology. They are responsible for the formation and organization of the extracellular matrix of bone and its subsequent mineralization. When seeded onto a surface, the osteoblasts first proliferate until the surface is covered completely by cells, then under the right conditions, they will undergo progressive differentiation and secrete a collagen rich substance essential for later mineralization of hydroxyapatite and other crystals.⁸⁴ We used osteoblast growth on our hydroxylated and fatty acids modified copolymer surfaces to evaluate the influence of our functional copolymer on cell attachment, shape, growth and differentiation.

To determine the polymer thin film thickness and whether or not our polymer surfaces possessed any functionalities, we characterized the surfaces of thin films using ellipsometry and contact angle measurements (Table 3). All of the films prepared were spin-coated from a 1% (w/w) solution of the polymer in toluene. The film thicknesses were measured using ellipsometry and had thicknesses generally around 30 ± 0.2 nm. The thicknesses of the films were uniform on a given substrate, but varied slightly between copolymers.

<i>Copolymer</i>	<i>Loading</i> ^a	<i>Thickness/nm</i> ^b	θ_{st} ^c	θ_{adv} ^c	θ_{rec} ^c
PDLLA	--	30 ± 0.3	74.1 ± 5.2	72.8 ± 3.3	65.3 ± 2.1
PLLA	--	19 ± 0.1	74.1 ± 3.1	77.4 ± 4.4	65.6 ± 4.8
PLLA- <i>co</i> -DAG	8%	27 ± 0.3	74.7 ± 2.2	79.2 ± 1.3	62.8 ± 1.8
PLLA- <i>g</i> -HP	8%	25 ± 0.1	62.0 ± 2.0	72.1 ± 4.2	56.1 ± 3.6
LLA- <i>g</i> -MyPr	8%	29 ± 0.3	87.8 ± 1.5	88.0 ± 1.2	75.2 ± 0.7
PLLA- <i>g</i> -StPr	8%	29 ± 0.3	86.1 ± 1.5	91.9 ± 1.8	77.1 ± 1.8
PLLA- <i>g</i> -OlPr	8%	30 ± 0.2	84.2 ± 2.2	89.0 ± 2.7	75.6 ± 1.1
PLLA- <i>g</i> -LnPr	8%	27 ± 0.2	73.6 ± 1.2	82.4 ± 1.2	68.9 ± 1.5
PLLA- <i>g</i> -ArPr	8%	29 ± 0.1	73.2 ± 1.8	80.7 ± 1.8	70.6 ± 1.9

Table 3. Thin films of copolymers spin-coated on 1-inch diameter silicon wafers from a 1% (w/w) solution in toluene unless otherwise noted. Spin rate: 2500 rpm, spin time: 60 sec. ^a Mole percent loading determined by ¹H NMR spectroscopy. ^b Determined by ellipsometry. ^c Samples were prepared by heating above the polymer melting point and quenching to room temperature to obtain amorphous samples. Static (θ_{st}), advancing (θ_{adv}) and receding (θ_{rec}) contact angles were measured at a rate of 3 μ L/s up to a total volume of 30 μ L using Milli-Q grade water.

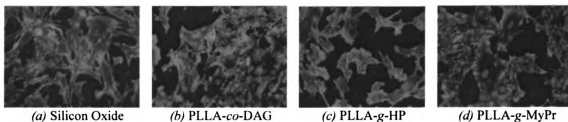
The wettability of the polymer surface was monitored by recording the static, advancing and receding contact angles of Milli-Q grade water. The polymer samples were all heated to 160°C under nitrogen, and then immediately cooled to room temperature and placed on a clean surface at room temperature in order to ensure a common sample history. Six separate contact angle measurements were taken on each polymer-coated silicon wafer, with the error set as one standard deviation from the mean. The surface wettability for PLLA, PDLLA and PLLA-*co*-DAG are similar. However, compared to PLLA, the contact angles for PLLA-*g*-HP is significantly smaller (by about 10 degrees), suggesting that the hydroxyl side groups are present near the surface of the film. Compared to PLLA, the contact angles for saturated fatty acid modified polymers are significantly higher (by about 12 degrees), indicating the highly hydrophobic alkyl

ester side chains are present near the surface of the film. The contact angles for unsaturated fatty acids modified copolymers are between those of saturated fatty acids modified copolymers and PLLA.

2.4.2 Osteoblast Cell Shape

Cell shape has been demonstrated to have important effect on cell growth, death or differentiation. Ingber and coworkers' research on cell geometry control over cell function showed that cells grow when spread, die when fully retracted, and differentiate if maintained at a moderate degree of extension.⁵³ By studying the osteoblast cell shape on different modified polymer surfaces we hope to obtain some information on biocompatibility of our polymers for bone tissue growth.

MC3T3-E1 osteoblasts were seeded at a concentration of 4400 cells/cm², cultured for 2 days in α -MEM (minimal essential medium) containing 2 mM β -glycerolphosphate and 25 μ g/mL ascorbic acid, after which they were stained and visualized in order to observe their appearance on different polymer surfaces. The differences in morphology of these sets of cells showed how the osteoblasts spread on each of the surfaces (Figure 22). Cells on different polymer surfaces showed different degrees of spreading, providing positive evidence that the different functionalized polymer surfaces influence the conformation of the cells and therefore, may be able to influence osteoblast proliferation and differentiation.



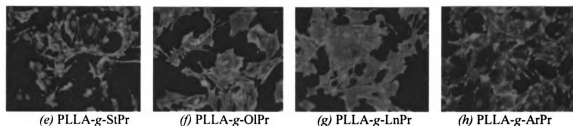


Figure 22. Microscope images of osteoblasts cultured for 48 hours on (a) silicon oxide and (b) PLLA-co-DAG (c) PLLA-g-HP (d) PLLA-g-MyPr (e) PLLA-g-StPr (f) PLLA-g-OIPr (g) PLLA-g-LnPr (h) PLLA-g-ArPr. The cells are stained red and the nuclei are stained blue.

2.4.3 Osteoblast Proliferation

Osteoblast proliferation was quantified by visualizing the DNA of dividing cells. This information was obtained by incubating the cultured osteoblast cells with the fluorescent label bromodeoxyuridine (BrdU). During the process of DNA replication, the BrdU label gets taken up by proliferating cells, and makes them visible as green fluorescent nuclei under UV light. The total number of nuclei is determined by propidium iodide staining which stains all nuclei red. The number of green nuclei was calculated as a percentage of the total nuclei to quantify osteoblast proliferation (Figure 23).

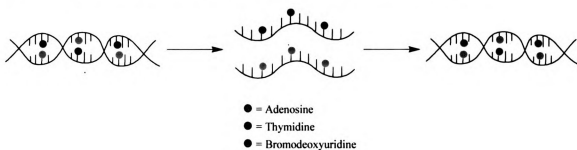
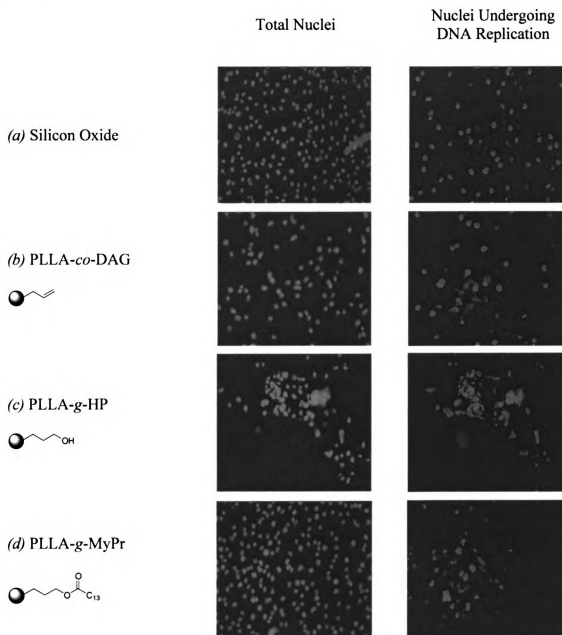


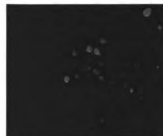
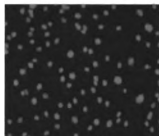
Figure 23. Illustration of cell replication incorporating the BrdU fluorescent label.

Osteoblasts were cultured on polymer-coated silicon discs. After 48 hours they were incubated for 2 hours with BrdU. Then, the cells were stained with propidium iodide. Digital pictures of cultured cells and cells under proliferation were taken and the

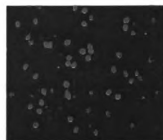
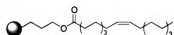
number of cells was counted respectively (Figure 24). The percentage of dividing cells on different surfaces was calculated and the numbers were normalized to the silicon oxide surface.



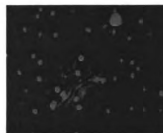
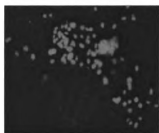
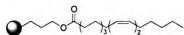
(e) PLLA-g-StPr



(f) PLLA-g-OlPr



(g) PLLA-g-LnPr



(h) PLLA-g-ArPr

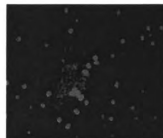
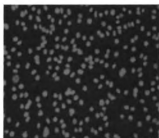
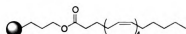


Figure 24. Digital photo images of fluorescent BrdU-labeled osteoblasts on (a) silicon oxide, (b) PLLA-co-DAG (c) PLLA-g-HP (d) PLLA-g-MyPr (e) PLLA-g-StPr (f) PLLA-g-OlPr (g) PLLA-g-LnPr (h) PLLA-g-ArPr.

Three sets of BrdU growth studies were carried out for each modified copolymer surface. The results indicated that osteoblasts placed on modified polymer surfaces showed different degrees of proliferation. Cells placed on PLLA-g-HP surfaces showed

the highest increase of growth by 3 fold which might be related to the hydrophilicity of the polymer surfaces (Figure 25).

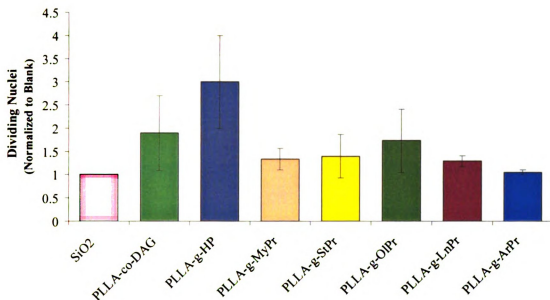


Figure 25. Result of osteoblast cell proliferation on (a) silicon oxide, (b) PLLA-co-DAG (c) PLLA-g-HP (d) PLLA-g-MyPr (e) PLLA-g-StPr (f) PLLA-g-OIPr (g) PLLA-g-LnPr (h) PLLA-g-ArPr. Averages are expressed as an n-fold change compared to control, uncoated blank surfaces.

2.4.4 Osteoblast Differentiation

After osteoblasts proliferate to a critical point, bone tissue formation can start through cell differentiation. To differentiate, cells must change the types of proteins they make. A hierarchy exists in the cell to control these changes. Genes/DNA provide the blueprint for mRNA which provides the blueprint for new proteins to be made. When studying osteoblast differentiation, levels of mRNA for alkaline phosphatase and osteocalcin are measured, which indicate levels of osteoblast differentiation in different stages (Figure 26). Elevated runx2 mRNA is another marker that indicates differentiation

since the runx2 protein goes into the nucleus and turns on genes associated with differentiation.⁸⁵⁻⁸⁷

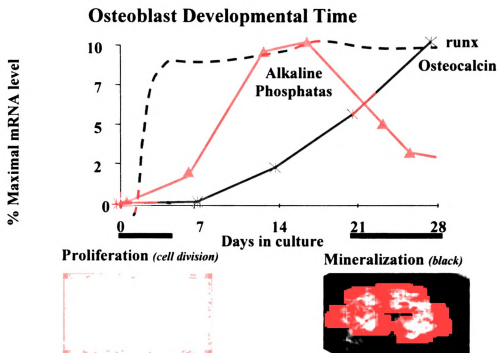


Figure 26. Gene expression levels of osteocalcin and alkaline phosphatase as a function of osteoblast culture time.

Osteoblasts were grown on the polymer surfaces for 14 days under conditions that enhance differentiation. RNA was extracted from the cells and levels of specific mRNAs were determined by standard quantitative RT-PCR. Elevated levels of alkaline phosphatase mRNA demonstrate that an osteoblast is in a early-middle stage of differentiation, while elevated levels of osteocalcin mRNA demonstrate that osteoblasts are more mature in late stage of differentiation. Data were collected from 6 sets of experiments and referenced to the result on a blank silicon oxide surface (Figure 27).

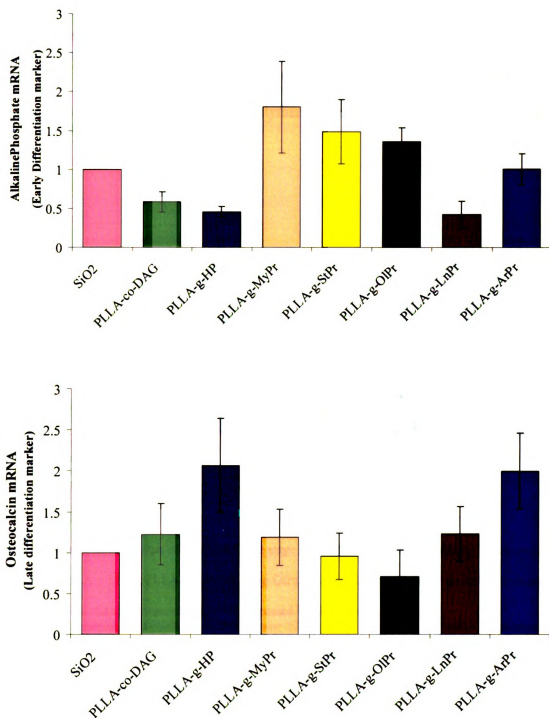


Figure 27. Result of osteoblast cell early and late stage differentiation on silicon oxide, PLLA-co-DAG, PLLA-g-HP, PLLA-g-MyPr, PLLA-g-StPr, PLLA-g-OIPr, PLLA-g-LnPr, and PLLA-g-ArPr. Averages are expressed as an n-fold change compared to control, uncoated blank surfaces.

Runx 2 is a transcription factor, which functions as a switch to turn on genes (and increase mRNA levels) associated with osteoblast differentiation. RNA of the cells was sampled and monitored for runx2 levels after 14 days of culturing. Data were collected from 6 sets of experiments on different polymer surfaces and referenced to the result on blank silicon oxide surface (Figure 28).

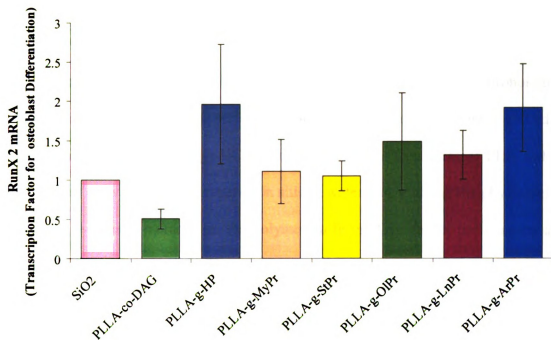


Figure 28. Result of osteoblast cell early and late stage differentiation on silicon oxide, PLLA-co-DAG, PLLA-g-HP, PLLA-g-MyPr, PLLA-g-StPr, PLLA-g-OIPr, PLLA-g-LnPr, and PLLA-g-ArPr. Averages are expressed as a fold change compared to control, uncoated blank surfaces.

The hydroxylated copolymer PLLA-g-HP increases osteocalcin mRNA levels while decreasing alkaline phosphatase mRNA levels. This suggests that PLLA-g-HP promotes late stage differentiation of osteoblasts. Other surface coatings promoted changes (increase or decrease) in early differentiation marker alkaline phosphatase mRNA levels. The significance of these effects is not yet understood.

The cell growth studies on our modified polymer surfaces indicate that PLLA-*g*-HP surface stimulates osteoblast proliferation and promotes late stage differentiation, which is consistent with the findings that hydrophilic surface could improve cell attachment and tissue growth.³⁰ PLLA-*g*-HP copolymer might be an interesting synthetic implant material for osteoblast growth and bone formation.

2.5 Conclusions

Copolymerization of L-lactide and diallylglycolide followed by hydroboration-oxidation have been successfully performed. Different fatty acids have been grafted to the copolymer side chain through DCC coupling reactions. Thin films of PLA and its functionalized derivatives were prepared on silicon wafers for studying the physiological response of osteoblast cultured on the polymer surfaces. Cell shape, proliferation and differentiation were analyzed. The distinct enhancement of cell proliferation and differentiation on PLLA-*g*-HP surface proved that surface hydrophilicity is an important factor for cell attachment and growth. The different responses of osteoblast to the modified copolymer surfaces provide us a direction of screening biopolymer substrate for improved tissue engineering applications.

The post polymerization modification has proven to be an effective way to graft functional or biosignificant side chain units on biodegradable polymers such as PLLA. The mild synthetic conditions, high yield and conversion, and the commercial availability and diversity of the functional side chains make this route widely applicable for biopolymer modifications.

CHAPTER THREE

3 Photolabile Protection-Deprotection Strategy in Surface Patterning.

As for tissue growth on surfaces, cell geometry has been shown to be a critical factor for death and growth.^{53,78} In order to control cell geometry on surfaces, strategies are needed for patterning surfaces with biosignificant functionalities. Many methods have been developed for patterning surfaces for cell growth studies, such as photolithographic laser ablation, photopolymerization and microcontact printing, etc. To functionalize our biodegradable polymer surface in a designed and well controllable fashion for further cell growth studies, we attempted to use a photolabile protection and deprotection strategy to pattern our modified PLA copolymer substrates.

Photolabile protecting groups have great potential in both synthetic and biological chemistry. The importance of this type of protection has been growing because of recent advances in solid phase synthesis in combinatorial chemistry and the need to photochemically removable probe molecules in cell biology.^{79,80} These photolabile groups can be cleaved photochemically without harsh acidic or basic conditions. We think that photolabile protecting groups can also be applied to patterning polymer surfaces with functional groups which will be beneficial to control cell geometry on polymer surfaces. A polymer that has functionalized side chains protected by photolabile groups is spin coated on a silicon wafer. Then, the surface is exposed to UV light through a mask containing the desired pattern. After irradiation, the protecting groups are removed at the exposed region, and therefore the surface is patterned with functional groups for further biosignificant molecule incorporation. Cells can then be placed on polymer surfaces with certain geometries to optimize cell surface interaction (Figure 29).

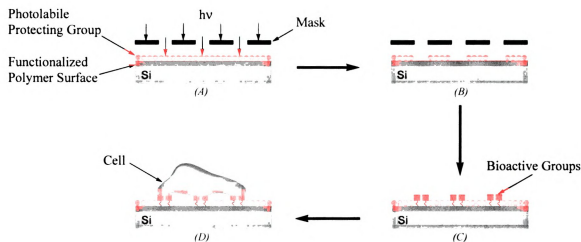


Figure 29. Photolabile protection-deprotection surface patterning for cell growth. (A) Polymer thin film with a functionalized side chain protected by photolabile protecting groups is exposed to UV light through a mask containing the desired pattern, (B) after irradiation, protecting groups are removed in the exposed region, (C) bioactive functional groups are incorporated in the deprotected region, (D) cells are seeded on the polymer surface with desired geometry.

3.1 Photolabile Protecting Group Selection

To choose a suitable photolabile protecting group for our copolymer substrates, the PDLLA was tested for stability under short and long wavelength UV light. The polymer was dissolved in dioxane, and then the same volume of H_2O was added into the solution. The polymer suspension was transferred into quartz and Pyrex tubes respectively. After degassing, the samples were irradiated under UV light. The quartz tube allowed the full range of UV light to pass through while the Pyrex tube cut off UV light with wavelengths shorter than 290 nm. After irradiation, the polymers were recovered and the molecular weight was measured by GPC. The PDLLA in the quartz tube had a large molecular weight decrease after being irradiated for 22 hours. The

molecular weight of the PDLLA in the Pyrex tube did not decrease even after irradiation for 6 days, and instead increased (Table 4).

<i>Polymer</i>	<i>λ (nm)</i>	<i>Time (hrs)</i>	<i>Solvent</i>	<i>M_n /gmol⁻¹ (PDI)^{a,b} Before Irradiation</i>	<i>M_n /gmol⁻¹ (PDI)^{a,b} After Irradiation</i>
PDLLA	Full range	22	1:1 Dioxane/H ₂ O	33,300 (1.48)	4,900 (1.24)
PDLLA	> 290	144	1:1 Dioxane/H ₂ O	41,600 (1.16)	64,700 (1.13)

Table 4. PDLLA stability under long and full range UV irradiation. ^a Molecular weight determined by GPC. ^b Polydispersity index (M_w/M_n).

The above results showed that the PLA based polyester degraded when irradiated at shorter wavelength, but no polymer degradation when irradiated at $\lambda > 290$ nm. Therefore, an appropriate photolabile protecting group should be cleaved by irradiation at $\lambda > 290$ nm with a high quantum yield. Polycyclic aromatic hydrocarbons bearing benzylic methylene groups are of good photolabile protecting groups for alcohols.⁸¹ Recently the anthraquinon-2-ylmethoxycarbonyl (Aqmoc), Pyren-1-ylmethoxycarbonyl (Pmoc), and 7-methoxycoumarin-4-ylmethoxycarbonyl (Mcmoc) groups have been synthesized and tested (Figure 30). They showed high reactivity at 350 nm, which is within the wavelength safe for our polymer substrates.

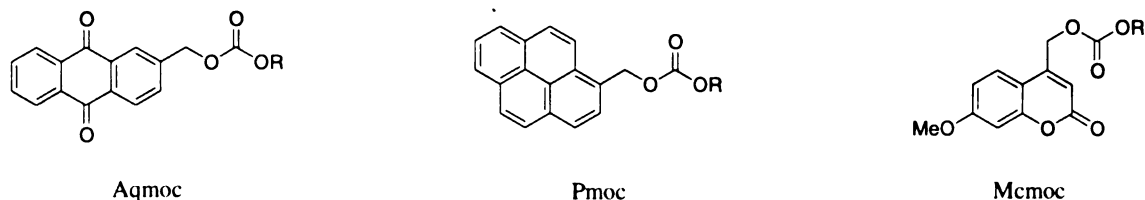


Figure 30. Photolabile polycyclic aromatic hydrocarbons bearing benzylic methylene groups.

3.2 Synthesis of Aqmoc Protected PLLA-g-HP

Aqmoc was linked to the hydroxyl group on PLLA-g-HP through a carbonate bond. The synthesis was based on a literature procedure.⁸² A solution of PLLA-g-HP in CH_2Cl_2 was added dropwise into a CH_2Cl_2 solution of 4-nitrophenyl chloroformate and DMAP. After stirring at room temperature for 6 hours, the polymer intermediate was isolated by precipitation in methanol, and then redissolved in CH_2Cl_2 for the next step. One equivalent of DMAP and 2-hydroxymethyl anthraquinone was added into the polymer solution and the solution was stirred at room temperature for another 6 hours. The final product PLLA-g-AqmocPr was precipitated in methanol for two times. The two step reaction gives a 73% overall yield (Figure 31).

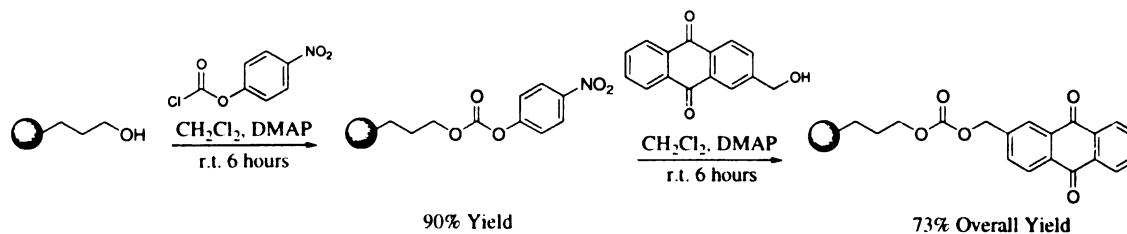


Figure 31. Synthetic route of Aqmoc Protected PLLA-g-HP.

The protected polymer, PLLA-g-AqmocPr, was characterized by ^1H NMR spectroscopy. Nearly complete conversion of the side chain alcohol to the carbonate was indicated by the disappearance of the methylene resonance at 3.62 ppm and the appearance of a methylene resonance at 4.18 ppm (Figure 32). The polymer is stable in solid form at room temperature under visible light.

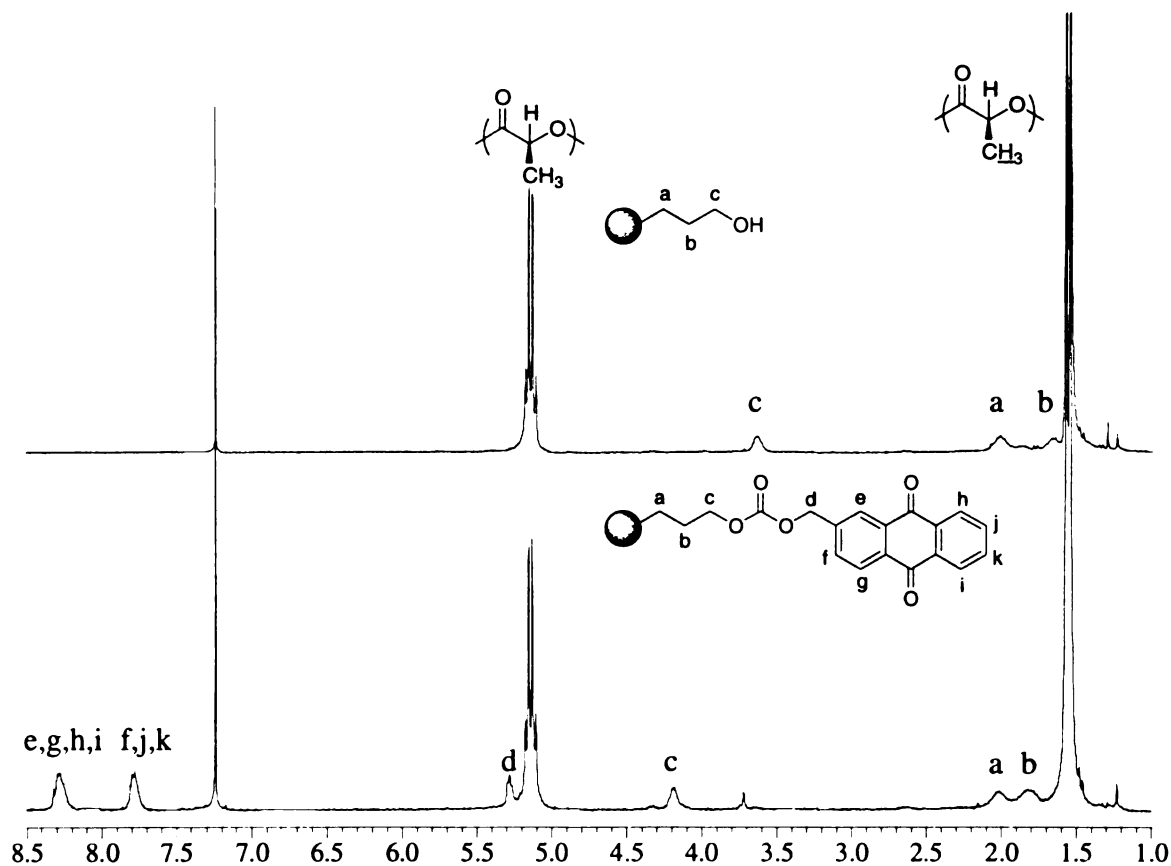


Figure 32. NMR spectrum PLLA-g-AqmocPr.

The molecular weights of the polymers before and after the protecting reactions were measured by GPC. The M_n for the starting PLLA-g-HP was 19,200 and the PDI was 1.55. After the protecting reaction, The M_n of the resulting PLLA-g-AqmocPr dropped to 11,000 and the PDI increased to 1.90. The molecular weight decrease indicates chain scission occurred during the coupling reactions in the presence of DMAP. Similar base catalyzed transesterification of PLA has been previously reported by Hedrick and coworkers (Figure 33).⁸³

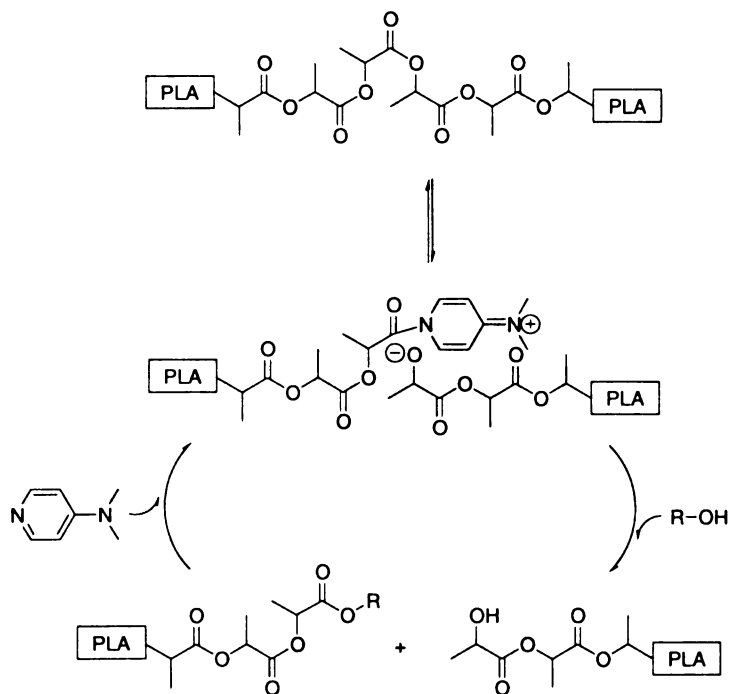


Figure 33. DMAP Catalyzed PLA Depolymerization.

3.3 Photolysis of Aqmoc Protected PLLA-*g*-HP

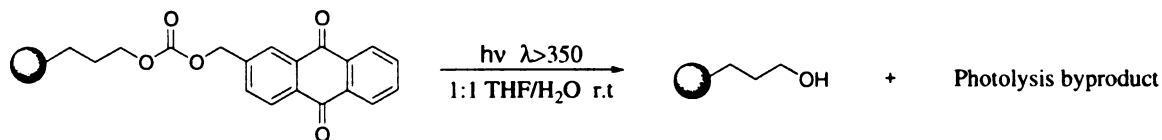


Figure 34. Photolysis of PLLA-*g*-AqmocPr.

The photolysis of PLLA-*g*-AqmocPr was carried out in 1:1 THF/H₂O solution. After degassing, the sample was irradiated with a high pressure mercury arc lamp (Figure 34). Initially, we used a Pyrex reaction vessel to limit the wavelength to above 290 nm. However after 6 hours, polymer gelation indicating that the deprotected PLLA-*g*-HP might be crosslinked under the photolysis conditions. To solve this problem, we filtered out UV light < 350 nm, and carried out the photolysis under the same conditions. After 6 hours, the sample was immediately worked up and reprecipitated with cold methanol. No

gelation was observed and the polymer molecular weight remained constant after irradiation (Table 5).

λ (nm)	Time (hrs)	Solvent	Conversion (%) ^a	Mn /gmol-1 (PDI) ^{b,c} Before Irradiation	Mn /gmol-1 (PDI) ^{b,c} After Irradiation
> 290	6	1:1 THF/H ₂ O	--	11,000 (1.90)	13,000(1.91)
> 350	2.5	1:1 THF/H ₂ O	60.7	8,900 (1.50)	9,950 (1.75)
> 350	6	1:1 THF/H ₂ O	83.6	8,900 (1.50)	9,688 (1.84)

Table 5. PDLL-g-AqmocPr deprotection under UV irradiation. ^a Conversion is determined by UV-vis spectroscopy. ^b Molecular weight determined by GPC. ^c Polydispersity index (M_w/M_n).

Quantification of the photochemical conversion of PLLA-g-AqmocPr to PLLA-g-HP was carried out by UV-Vis and ¹H NMR spectroscopy. GPC was used not only for measuring the polymer molecular weight before and after the photolysis reaction, but also to quantitate the photochemical deprotection conversion using ultraviolet-visible spectroscopy. Since GPC is a chromatographic separation technique, we measured the absorbance of the polymer using the UV-Vis detector and correlated it to the concentration of the chromophore using a calibration curve. The prerequisite for reliable UV-Vis quantification is that the side chain chromophore strongly absorbs at a wavelength where the polymer backbone is transparent. In our case, λ_{max} is 234 nm for PLLA-g-HP, while the λ_{max} for the Aqmoc moiety is 327 nm (Figure 35). Therefore, we were able to quantify the amount of conversion using UV-Visible spectroscopy. The model compound anthraquinon-2-ylmethyl butylcarbonate was synthesized and solutions of different concentrations were injected into GPC. By plotting absorbance at 325 nm vs. sample concentration, a calibration curve was generated. The chromophore concentrations on our polymer substrates before and after photolysis were compared to

determine the percent conversion of the photolysis reactions. When the sample was irradiated for 2.5 hours, 61% deprotection of the Aqmoc group was observed. When the irradiation time was increased to 6 hours under the same condition, deprotection increased to 84%.

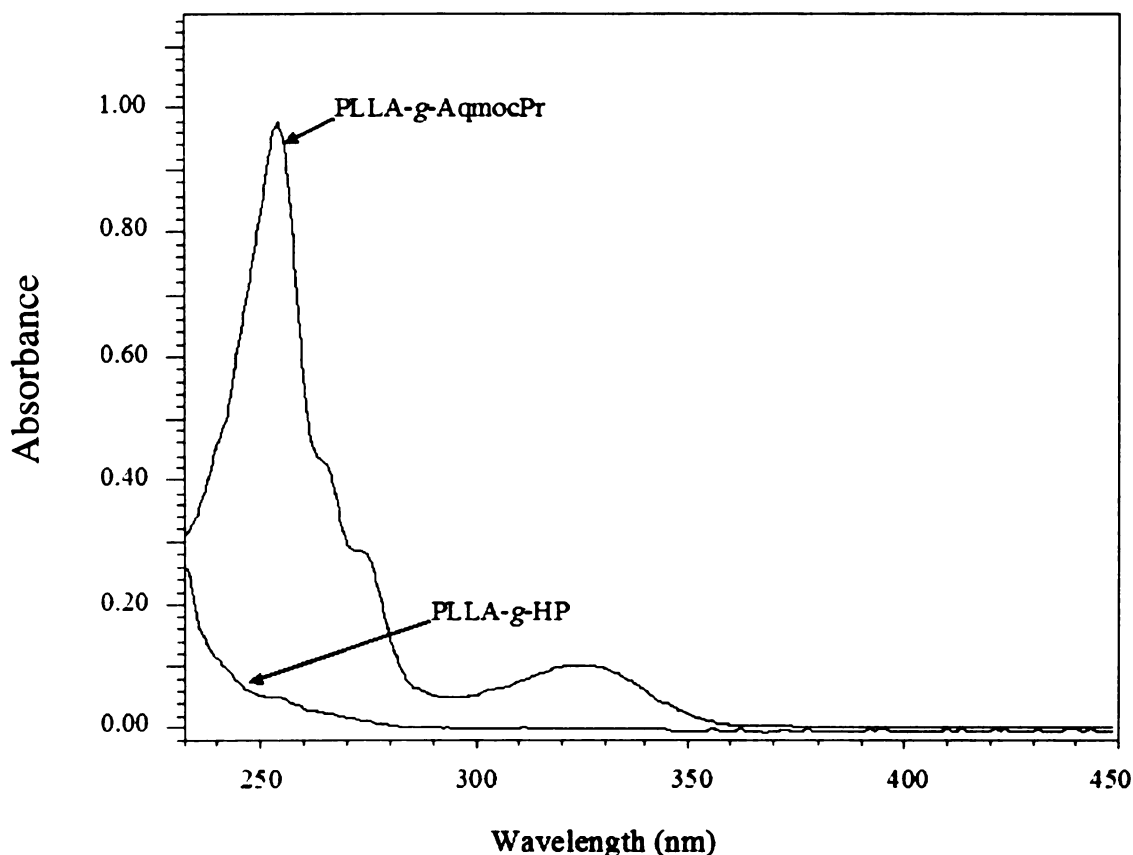


Figure 35. UV-Vis spectra of PLLA-g-Aqmoc and PLLA-g-HP.

^1H NMR analysis was performed by comparing the integration of the resonances between photochemically deprotected polymer and the unreacted polymer (Figure 36). After photolysis, the aromatic proton resonances at 8.29 ppm and 7.78 ppm, and the methylene proton resonance at 5.15 ppm decreased indicating the cleavage of Aqmoc group. A peak that appeared at 3.63 indicated the recovery of PLLA-g-HP. The percent

conversion determined by ^1H NMR integration compared well with result obtained from UV-Vis analysis.

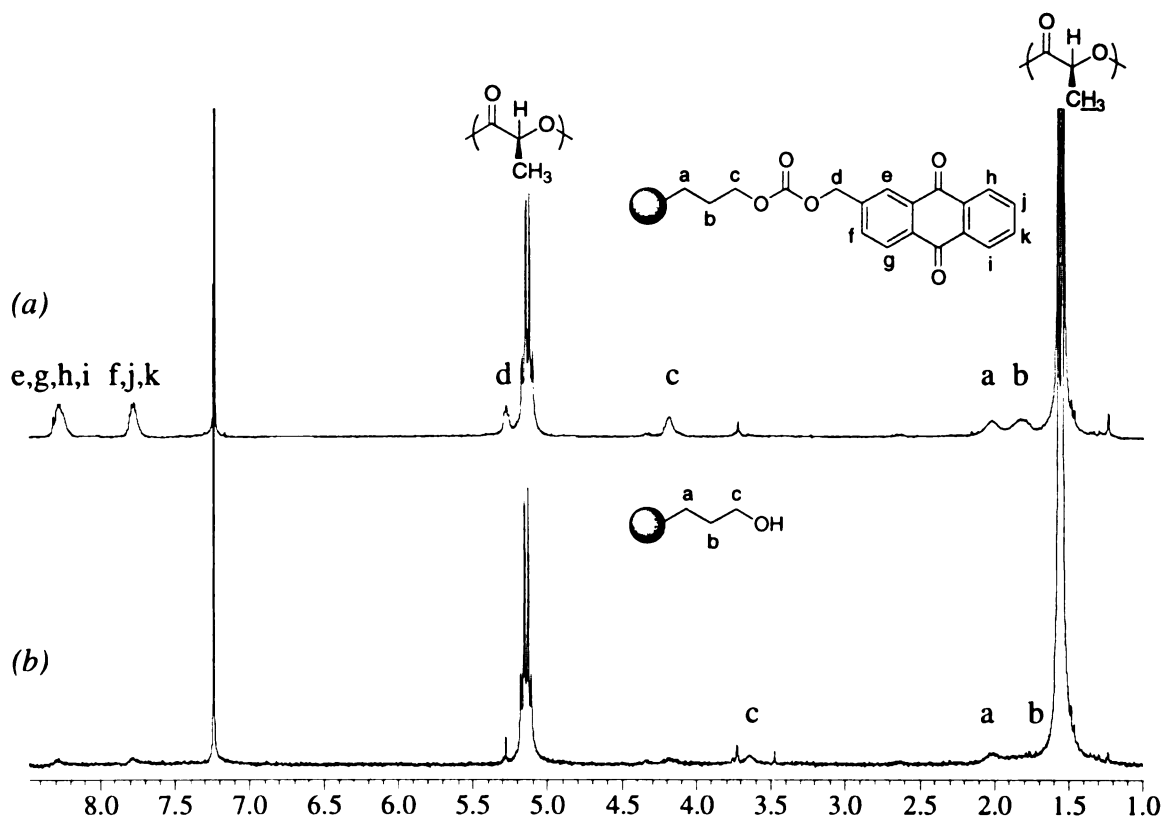


Figure 36. NMR spectra of PLLA-g-Aqmoc (a) before and (b) after photolysis.

3.4 Conclusion

The Aqmoc group is a good photolabile protecting group for the side chain hydroxyl group of PLLA-g-HP. It has been successfully linked to PLLA-g-HP through a carbonate bond by using 4-nitrophenyl chloroformate as coupling reagent. Transesterification side reaction occurred in the presence of DMAP, which decreased the polymer molecular weight. However, by increasing the molecular weight of the starting PLLA-g-HP, one can still expect to synthesize PLLA-g-AqmocPr with reasonable molecular weights. Photolysis of PLLA-g-AqmocPr was carried out with UV light ($\lambda >$

350 nm). The hydroxyl group is successfully deprotected with high conversion. And the polymer molecular weight remained constant before and after irradiation. The above experiment suggests that Aqmoc group can be an efficient photolabile group for protecting the side chain hydroxyl group of PLLA-g-HP during chemical reactions, and it can also be applied in PLLA-g-HP coated surface photolithographic patterning.

CHAPTER FOUR

4 Experimental Section.

4.1 General Considerations

^1H NMR spectra were recorded on Varian Gemini-300 and Inova-300 (299.9 MHz) and Varian Unity-500 (499.9 MHz) spectrometers and referenced to residual proton solvent signals. ^{13}C NMR spectra were recorded on Varian Gemini-300 and Inova-300 (75.4 MHz) and Varian Unity-500 (125.7 MHz) spectrometers and referenced to residual solvent signals. ^{11}B NMR spectra were recorded on a Varian VXR-300 (160.6 MHz) and referenced using $\text{BF}_3\cdot\text{OEt}_2$ as the external standard. Differential Scanning Calorimetry (DSC) analyses of the polymers were performed under a helium atmosphere at a heating rate of $10^\circ\text{C}/\text{min}$ on a Perkin-Elmer DSC 7, with the temperature calibrated using an indium standard. The reported DSC curves are second heating scans, taken after an initial heating scan to erase thermal history, and a slow cooling scan to -50°C . Molecular weights of the polymers were determined by gel permeation chromatography (GPC) Waters instrument, equipped with a Waters 410 differential refractometer detector and a Waters 960 photodiode array detector. Measurements were obtained in THF with two PLgel 5 μ Mix columns (Polymer Laboratories) at a flow rate of $1.0\text{ mL}/\text{min}$ at 35°C . Results were calibrated with monodisperse polystyrene standards. Polished silicon wafers purchased from WaferWorldTM were cleaned by immersion in a 70:30 volume ratio solution of concentrated H_2SO_4 (98% by mass) and H_2O_2 (30% by mass) and rinsed in deionized water. Polymers were dissolved in toluene (1% w/w), filtered two times through $0.2\text{ }\mu\text{m}$ PTFE filters and spin-coated onto polished silicon wafers (1" diameter) at a spin rate of 2500 rpm for 60 s. Ellipsometric

measurements were obtained with a rotating analyzer ellipsometer (model M-44, J.A. Woollam) using WVASE32 software. The angle of incidence was 75° for all measurements. A film refractive index of 1.50 was used for the calculation of the film thickness.

Contact Angle Measurements. After spin-coating the polymers onto silicon wafers, the wafers were held under vacuum at 40°C for 12 hours to ensure that all solvent was removed from the wafers. The polymer-coated wafers were kept at room temperature for 1 hour under a constant purge of nitrogen. Samples were heated under a nitrogen atmosphere at a rate of 10°C/min to 160°C (15°C above the melting point of the all polymer samples) and held for 1 minute. The samples were immediately removed from the oven and placed on a clean surface at room temperature. Advancing and receding contact angles were measured by dispensing a droplet of Milli-Q grade water (18 MΩ cm) at a rate of 3 μL/s to a total volume of 30 μL on the surface of polymer-coated silicon wafers. Contact angles were measured by capturing the image as a movie with a Sanyo® B/W CCD camera (model VC8 3512). The angles were measured using the FTA200 software.

Cell Growth Study. The osteoblast growth studies were done at the department of physiology by Dr. Laura McCabe group members.

Cell Culture. MC3T3-E1 osteoblasts (OBS) were plated on silicon discs (WaferWorld™) at a concentration of 4,400 cells/cm². These were either cultured for 2 days for the proliferation studies or 14 days for the differentiation studies, where at this stage OBS exhibit maximal levels of alkaline phosphatase and mineralization. Cells were

fed every two days with α -MEM containing 2mM β -glycerolphosphate (Sigma, St. Louis, MO) and 25 μ g/ml ascorbic acid (Sigma).

Cell Growth and Shape. After plating for 48 hours, osteoblasts were incubated with 10 μ M BrdU (5-Bromo-2'Deoxyuridine) (Sigma, St. Louis, MO) for two hours. Subsequently, cells were fixed with 70% ethanol. The cell culture plates were then spun at 1500 rpm for 5 minutes to ensure that all cells remained at the bottom of the plate, followed by a quick rinse with 1Xphosphate buffered solution (1XPBS). Cells were permealized with 4 N HCl in 1XPBS, and subsequently washed gently with 1 mL of 1XPBS until the PBS in the wells reached pH=7. Osteoblasts were further incubated in 20% anti-BrdU (BD Biosciences, San Jose, CA) antibody solution, in 1XPBS, 0.5% BSA, 0.1% Tween-20, for 45 minutes at 37°C under humid conditions. Brdu antibodies were removed and cells further introduced to propidium iodide stain at 200 μ g/mL PBS (BD Biosciences, San Jose, CA) immediately after which nuclei of the cells were visualized by fluorescence microscopy and recorded with a digital camera. BrdU stains the nuclei at the S phase of cell cycle, i.e. when cells are dividing, and therefore, was used to determine cell growth. Propidium iodide stains all nuclei.

Actin and Hoechst Stain. Osteoblasts were fixed with 3.7% formaldehyde for 10 minutes at room temperature, 2 days after seeding, and subsequently permealized for 5 minutes with 0.1% Triton X-100 in 1XPBS. Cells were blocked with 1% bovine serum albumin for 30 minutes and subsequently incubated for 20 minutes with rhodamine-pahlloidin (Molecular Probes Inc. Eugene, OR) and further incubated with at 10 μ M stain in deionized H₂O, for 30 minutes. Actin localization and Hoechst stained

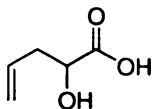
(Molecular Probes Inc. Eugene, OR) nuclei were visualized by fluorescence microscopy and recorded with a digital camera.

RNA Analysis. RNA was extracted, on day 14, using TRI Reagent RNA isolation reagent (Molecular Research Center, Inc., Cincinnati, OH). Integrity of the RNA was verified by formaldehyde-agarose gel electrophoresis. Two-step quantitative RT-PCR was performed to verify gene expression. First strand cDNA was synthesized by reverse transcription of 2 μ g RNA, using the Superscript II Kit and oligo d(T12-18) primers (Invitrogen Life Technologies, Carlsbad, CA). 1 μ l of cDNA was amplified by Real Time PCR, by using the SYBR Green Core Reagents (PE Biosystems, Warrington, UK) and Taq DNA polymerase (Invitrogen Life Technologies, Carlsbad, CA) with a final volume of 25 μ l. Genes associated with osteoblast differentiation, alkaline phosphatase, osteocalcin, and runx2, were analyzed using cyclophilin as the internal control. Real time PCR was carried out and analyzed for 40 cycles, using iCycler software (Biorad, Hercules, CA). Gel electrophoresis and melting curves were used to verify the integrity of a single PCR product (amplicon).

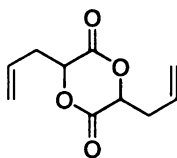
Photolysis. The photolysis samples were prepared in 1:1 THF/H₂O solution in Pyrex tubs, and degassed by purging with N₂. The irradiation was carried out by using high pressure mercury arc lamp with a 350 nm uranium glass filter.

Solvents. Toluene, tetrahydrofuran, diethyl ether, and pentane were pre-dried over sodium and distilled from sodium/benzophenone ketyl. Dichloromethane was distilled from calcium hydride (CaH₂). All other reagents were used as received unless otherwise noted.

4.2 Synthesis

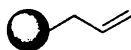


2-Hydroxypent-4-enoic acid (2-HPA).²⁴⁰ Glyoxylic acid monohydrate (9.60g, 0.104mol) and freshly distilled allyl bromide (18.8g, 0.156mol) were added to a stirred suspension of zinc powder (14.2g, 0.217mol), and BiCl₃ (49.2g, 0.156mol) in 120mL tetrahydrofuran. The reaction was initially kept at 0°C and allowed to warm to room temperature while stirring under N₂ for 16h. After 16h, the reaction was quenched with 80mL of 1M HCl, and the product was extracted with diethyl ether (3x150mL). The organic phases were decanted from the solid, combined, and washed with saturated NaCl_(aq) until the ether solution became colorless (5x20mL). The ether layer was then dried over MgSO₄, and the solvent removed to give a colorless oil which crystallized under vacuum. Yield: 11.1g (92%). ¹H NMR (300 MHz, CDCl₃, δ): 5.74-5.85 (m, 1H, -CHCH₂CH=CH₂), 5.16-5.28 (m, 2H, -CHCH₂CH=CH₂), 4.24 (dd, 1H, HO₂CCH(OH)CH₂CH=CH₂), 2.42-2.66 (m, 2H, -CHCH₂CH=CH₂). ¹³C NMR (75.0 MHz, CDCl₃, δ): 178.5, 131.9, 119.3, 69.8, 38.3.



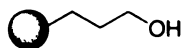
3,6-Diallylglycolide (DAG). 2-HPA (7.8g, 0.0672mol) was dissolved in 672mL toluene (0.1M), and a catalytic amount (0.895g, 0.0047mol) of *p*-toluenesulfonic acid (pTsOH) was added into the solution. The mixture was refluxed for 3 days with the water removed by Dean-Stark trap. After 3 days the mixture was cooled, washed 3 times with 20mL of saturated aqueous NaHCO₃ and the resultant oil distilled over ZnO under high

vacuum at 80°C/0.01mmHg. Gas chromatography data indicates a statistical mixture of S/S, R/S, and R/R isomers of the diallylglycolide. Yield: 3.68g (56%). ¹H NMR (300MHz, CDCl₃, δ): 5.70-5.83 (m, 1H, -CHCH₂CH=CH₂), 5.18-5.27 (m, 2H, -CHCH₂CH=CH₂), 5.00 (dd, 1H, -CHCH₂CH=CH₂, *J* = 6.3 Hz), 4.93 (dd, 2H, *-CHCH₂CH=CH₂, *J* = 7.2 Hz), 2.68-2.79 (m, 4H, -CHCH₂CH=CH₂). ¹³C NMR (75 MHz, CDCl₃, δ): *166.2, 164.8, *130.6, 129.8, 121.3, *120.0, 75.8, *75.0, 36.3, *34.0. LRMS (EI, *m/z*): 197 (MH⁺), 98, 81, 54, 41. Anal. Calcd for C₁₀H₁₂O₄: C, 61.21; H, 6.18. Found: C, 61.29; H, 6.17. *Indicates RR/SS isomer. (Note: Using a combination of L-lactic acid and 2-HPA in the desired ratio under identical reaction conditions and workup results in a statistical mixture of L-lactide, 3-allyl-6-methylglycolide, and 3,6-diallylglycolide and appropriate stereoisomers.)

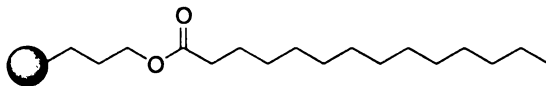


Poly(L-lactide-*co*-diallylglycolide) (PLLA-*co*-DAG). In a typical synthesis of PLLA-*co*-AG, freshly sublimed L-lactide (4.16g, 28.9mmol) and distilled diallylglycolide (DAG) (1.0g, 5.10mmol) were combined in a glass tube with tin(II)-2-ethylhexanoate (0.068mmol) and 4-*tert*-butylbenzylalcohol (BBA) (0.068mmol) as the coinitiators. The reaction tube was flame-sealed under vacuum and placed in an oil bath at 145°C. After 20 minutes, the sample was removed from the oil bath, cooled, and monitored for conversion. ¹H NMR of the crude product revealed nearly complete conversion (>90%). Polymers were dissolved in a minimal amount of CH₂Cl₂, and precipitated into cold methanol two times. The copolymer has 13.1% diallylglycolide units (percentage can vary according to percentage of diallylglycolide co-monomer) Yield: 94%. ¹H NMR (300 MHz, CDCl₃, δ): 5.62- 5.81 (m, 1H, -CHCH₂CH=CH₂),

5.10-5.17 (q, $^*\text{-CH}(\text{CH}_3)$, $\text{-CHCH}_2\text{CH=CH}_2$), 2.5-2.8 (m, 2H, $\text{-CH}_2\text{CH=CH}_2$), 1.5-1.7 (d, $^*\text{-CH}(\text{CH}_3)$). ^{13}C NMR (75 MHz, CDCl_3 , δ): *169.6, 168.2, 131.4, 119.2, 72.0, *69.0, 35.1, *16.6. *PLLA.

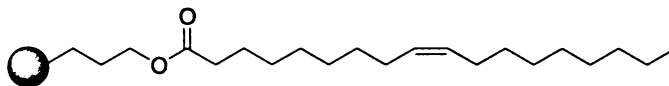


PLLA-g-HP (HP = Hydroxypropane) In a round bottom flask, PLLA-*co*-AG (1.5 g, 1.0 mmol g^{-1} , 1.49 mmol) was dissolved in 50 mL of dry THF. 9-BBN solution in THF (4.16 mL, 0.50 M, 2.08 mmol) was slowly added to the polymer solution *via* syringe and stirred at room temperature for 2 h. The reaction was then cooled to 0°C and a 1 M aqueous solution of sodium acetate (6.24 mL, 6.24 mmol) and a 30% solution of H_2O_2 (0.71 g, 6.24 mmol) were added. The mixture was stirred for 4 h. The reaction was quenched with 2 M HCl (3.12 mL, 6.24 mmol) and the solvent were reduced by rotary evaporation. The polymer was then precipitated from methanol. The polymer was filtered and dried under vacuum. Yield: 85%. ^1H NMR (300 MHz, CDCl_3 , δ): 5.08-5.20 (q, $^*\text{-CH}(\text{CH}_3)$, $\text{-CHCH}_2\text{CH}_2\text{CH}_2\text{OH}$), 3.62 (m, 2H, $\text{-(CH}_2)_2\text{CH}_2\text{OH}$), 2.04 (m, 2H, $\text{-CH}_2(\text{CH}_2)_2\text{OH}$), 1.65 (m, 2H, $\text{-CH}_2\text{CH}_2\text{CH}_2\text{OH}$), 1.54-1.62 (d, $^*\text{-CH}(\text{CH}_3)$). ^{13}C NMR (75 MHz, CDCl_3 , δ): *169.6, 168.7, 72.5, *69.0, 61.8, 27.7, 27.5, *16.6. * PLLA. Note: the base catalyzed oxidation can be monitored by ^{11}B NMR, the disappearance of peak at 34 ppm indicates complete conversion. Repetition of the oxidation step can fully remove the boronic acid residue if the first oxidation does not achieve 100% conversion.

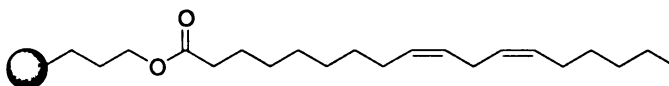


PLLA-g-MyPr (MyPr = Myristic acid propyl ester). PLLA-g-HP (0.352 g, $0.950 \text{ mmol g}^{-1}$, 0.333 mmol), myristic acid (0.114 g, 0.50 mmol), and DMAP (8.0 mg,

(75 MHz, CDCl₃, δ): 173.7, *169.6, 72.1, *69.0, 63.2, 34.2, 33.9, 31.9, 29.7, 29.5, 29.3, 29.2, 29.1, 27.6, 24.9, 24.7, 24.2, 22.7, *16.6, 14.1. * PLLA.

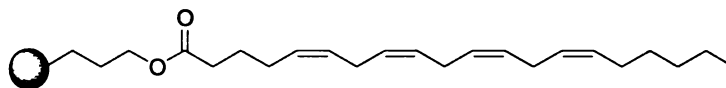


PLLA-g-OlPr (OlPr = Oleic acid propyl ester). The polymer-bound DCC coupling procedure was identical to that for PLLA-g-MyPr. Yield: 88%. ¹H NMR (300 MHz, CDCl₃, δ): 5.32 (m, 2H, -CH=CH), 5.18-5.10 (q, *-CH(CH₃), -CH(CH₂)₃CO₂C₁₇H₃₃), 4.05 (m, 2H, -CH₂CO₂C₁₇H₃₃), 2.26 (m, 2H, -CO₂CH₂C₁₆H₃₁), 1.99 (m, 6H, -CH₂CH₂CH₂CO₂C₁₇H₃₃, -(CH₂)(CH=CH)(CH₂)), 1.76 (m, 2H, -CH₂CH₂CH₂CO₂C₁₇H₃₃), 1.60-1.52 (d, *-CH(CH₃)), 1.45 (m, 2H, -CO₂CH₂CH₂C₁₅H₂₉), 1.28-1.25 (m, 20H, -(CH₂)₄(CH₂)(CH=CH)(CH₂)(CH₂)₆CH₃), 0.86 (t, 3H, -(CH₂)₆CH₃). ¹³C NMR (75 MHz, CDCl₃, δ): 173.8, *169.6, 130.0, 129.7, 72.2, *69.0, 63.2, 34.2, 31.9, 29.7, 29.6, 29.5, 29.3, 29.2, 29.1, 27.2, 27.1, 24.9, 22.6, *16.6, 14.1. * PLLA.

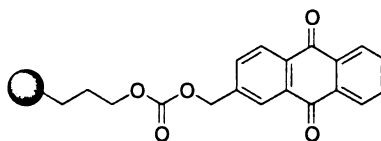


PLLA-g-LnPr (LnPr = Linoleic acid propyl ester). The polymer-bound DCC coupling procedure was similar to that used to prepare PLLA-g-MyPr. This polymer has been reported to be sensitive to oxygen.⁶⁵ Therefore the reaction was carried out in a glove box under nitrogen, and then worked up quickly in air. The product was kept under nitrogen. Yield: 71%. ¹H NMR (300 MHz, CDCl₃, δ): 5.32 (m, 4H, -CH=CH-(CH₂)-CH=CH), 5.18-5.10 (q, *-CH(CH₃), -CH(CH₂)₃CO₂C₁₇H₃₁), 4.05 (m, 2H, -CH₂CO₂C₁₇H₃₁), 2.78 (t, 2H, =CH-(CH₂)-CH), 2.4-2.2 (m, 2H, -CO₂CH₂C₁₆H₂₉), 2.03 (m, 6H, -CH₂CH₂CH₂CO₂C₁₇H₃₁, -CH₂(C₅H₆)CH₂), 1.76 (m, 2H, -CH₂CH₂CH₂CO₂C₁₇H₃₁), 1.60-1.52 (d, *-CH(CH₃)), 1.45 (m, 2H, -CO₂CH₂CH₂C₁₅H₂₇),

1.27 (m, 14H, $-(CH_2)_4(CH_2)(C_5H_6)(CH_2)(CH_2)_3CH_3$), 0.86 (t, 3H, $-(CH_2)_6CH_3$). ^{13}C NMR (75 MHz, $CDCl_3$, δ): 173.7, *169.6, 130.2, 130.0, 128.0, 127.8, 72.2, *69.0, 63.2, 34.1, 33.8, 31.5, 29.7, 29.6, 29.3, 29.5, 29.3, 29.1, 29.0, 27.6, 27.2, 25.6, 24.9, 24.7, 24.2, 22.5, *16.6, 14.1. * PLLA.



PLLA-g-ArPr (ArPr = Arachidonic acid propyl ester). The polymer-bound DCC coupling procedure was similar to that used to prepare PLLA-g-LnPr. This polymer has been reported to be sensitive to oxygen.⁶⁵ Therefore the reaction was carried out in a glove box under nitrogen, and then worked up quickly in air. The product was kept under nitrogen. Yield: 78%. 1H NMR (300 MHz, $CDCl_3$, δ): 5.34 (m, 8H, $-(CH=CH-CH_2)_3CH=CH-$), 5.18-5.10 (q, $^*-CH(CH_3)$, $-CH((CH_2)_3CO_2C_{19}H_{31})$), 4.05 (m, 2H, $-CH_2CO_2C_{19}H_{31}$), 2.79 (m, 6H, $-(CH=CH-CH_2)_3$), 2.4-2.2 (m, 2H, $-CO_2CH_2C_{18}H_{29}$), 2.10-1.90 (m, 6H, $-CH_2CH_2CH_2CO_2C_{19}H_{31}$, $-CH_2(CH=CH-CH_2)_3(CH=CH)CH_2$), 1.8-1.6 (m, 4H, $-CO_2CH_2CH_2C_{17}H_{27}$, $-CH_2CH_2CH_2CO_2C_{19}H_{31}$), 1.60-1.52 (d, $^*-CH(CH_3)$), 1.26 (m, 6H, $-(CH_2)_3CH_3$), 0.86 (t, 3H, $-(CH_2)_4CH_3$). ^{13}C NMR (75 MHz, $CDCl_3$, δ): 173.8, *169.6, 130.45, 128.85, 128.55, 128.18, 128.17, 128.12, 127.80, 127.48, 72.1, *69.0, 63.3, 33.8, 33.51, 31.47, 29.28, 27.63, 27.17, 26.49, 25.56, 24.70, 24.17, 22.54, *16.6, 14.0. * PLLA.

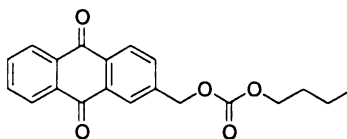


PLLA-g-pNpPr (pNpPr = p-nitro-phenyl propyl carbonate). To a stirred a solution of 4-dimethylaminopyridine (0.0914g, 0.748mmol) and 4-nitrophenyl

chloroformate (0.172g, 0.855mmol) in CH_2Cl_2 (6mL), a 5mL solution of PLLA-g-HP (0.4109g, 0.713mmol) was added dropwise. The reaction mixture was stirred for 5 hours at room temperature. The solution was then concentrated, and the polymer was precipitated in cold methanol. Yield: 90%. ^1H NMR (300 MHz, CDCl_3 , δ): 8.25 (d, 2H, -H_{Ar}), 7.36 (d, 2H, H_{Ar}), 5.15 (q, 11 H, $\text{*CHCO}_2\text{-}$), 4.30 (br, 2H, $\text{-CH}_2\text{CH}_2\text{CH}_2\text{CO}_2\text{-}$), 2.17 – 2.0 (br, 2H, $\text{-CH}_2\text{CH}_2\text{CH}_2\text{CO}_2\text{-}$), 1.82-1.98 (br, 2H, $\text{-CH}_2\text{CH}_2\text{CH}_2\text{CO}_2\text{-}$), 1.56 (d, 33H, $\text{*CH}_3\text{CH-}$)

PLLA-g-AqmocPr (AqmocPr = Anthraquinon-2-ylmethyl propyl carbonate)

The isolated polymer, PLLA-g-pNpPr was dissolved in CH_2Cl_2 , and one equivalent of 4-dimethylaminopyridine (0.078g, 0.642mmol) and 2-hydroxymethyl anthraquinone (0.168g, 0.71mmol) were added. After stirring for 12 hours the solution was concentrated and the polymer was precipitated in methanol. Yield: 81%. ^1H NMR (300 MHz, CDCl_3 , δ): 8.29 (br, 4H, H_{Ar}), 7.78 (br, 3H, H_{Ar}), 5.15 (br, 2H, $\text{H}_{\text{Ar}}\text{CH}_2\text{OCO}_2\text{-}$), 5.14 (q, 12H, $\text{*CHCO}_2\text{-}$), 4.18 (br, 2H, $\text{-CO}_2\text{OCH}_2\text{CH}_2\text{CH}_2\text{-}$), 2.02 (br, 2H, $\text{-CO}_2\text{OCCH}_2\text{CH}_2\text{CH}_2\text{-}$) 1.83 (br, 2H, $\text{-CO}_2\text{OCH}_2\text{CH}_2\text{CH}_2\text{-}$) 1.56 (d, 33H, $\text{*CH}_3\text{CH-}$). ^{13}C NMR (75 MHz, CDCl_3 , δ): 182.53, *169.46 , *169.25 , 154.71, 141.72, 134.11, 133.53, 133.29, 133.10, 132.82, 127.65, 127.14, 126.05, *72.09 , *68.88 , 68.14, 67.35, 66.57, 27.37, 24.07, *16.52 . Note: * From Polymer backbone.



Anthraquinon-2-ylmethyl butyl carbonate. To a stirred a solution of 4-dimethylaminopyridine (0.134g, 1.1mmol) and 4-nitrophenyl chloroformate (0.222g,

1.1mmol) in CH_2Cl_2 (6mL), 1-butanol (0.148g, 0.18mL) was added dropwise. The reaction mixture was stirred for 5 hrs at room temperature. Thin layer chromatography indicated the formation of intermediate 4-nitrophenyl carbonate was complete. Then, one equivalent of 2-hydroxymethyl anthraquinone (0.238g, 1mmol) and an additional equivalent of 4-dimethylaminopyridine were added in the reaction mixture. After 12 hours, the mixture was diluted with CHCl_3 , washed with sat. NaHCO_3 , 1M HCl , and dried over MgSO_4 . The product was purified by column chromatography. Yield: 72%. ^1H NMR (300 MHz, CDCl_3 , δ): 8.31-8.28 (m, 4H, $-\text{H}_{Ar}$), 7.80-7.77 (m, 3H, H_{Ar}), 5.29 (s, 2H, $-\text{CH}_2\text{OCOOCH}_2-$), 4.17 (t, 2H, $-\text{CH}_2\text{OCOOCH}_2-$, $J = 6.6$ Hz), 1.69-1.66 (m, 2H, $-\text{OCH}_2\text{CH}_2\text{CH}_2\text{CH}_3$), 1.41-1.38 (m, 2H, $-\text{OCH}_2\text{CH}_2\text{CH}_2\text{CH}_3$), 0.92 (t, 3H, $-\text{OCH}_2\text{CH}_2\text{CH}_2\text{CH}_3$, $J = 7.2$ Hz). ^{13}C NMR (75 MHz, CDCl_3 , δ): 182.72, 182.64, 155.00, 142.03, 134.18, 134.14, 133.38, 133.17, 132.88, 127.72, 127.24, 127.22, 126.23, 68.42, 68.07, 30.58, 18.86, 13.59.

Photolysis of PLLA-g-AqmocPr. In a Pyrex tube, PLLA-g-AqmocPr (0.107g, 0.938mmol g^{-1} , 0.1mmol Aqmoc) was dissolved in 25ml THF (no stabilizer included). Then, 25mL deionized water was added dropwise to the polymer solution (the polymer solution became cloudy after adding water). After the mixture was degassed by purging with N_2 for 15 minutes, the sealed sample tube was irradiated at >350 nm using a high pressure mercury lamp for 5 hours. After irradiation, the solvent was immediately removed by rotovap and the polymer was isolated by centrifugation followed by reprecipitation in cold methanol. Yield: 79%. Conversion: 76% (by NMR), 83.6% (By UV-Vis).

CHAPTER FIVE

5 References

- (1) Athanasiou, K. A.; Niederauer, G. G.; Agrawal, C. M. *Biomaterials* 1996, 17, 93-102.
- (2) Li, Y. X.; Volland, C.; Kissel, T. *Polymer* 1998, 39, 3087-3097.
- (3) Uhrich, K. E.; Cannizzaro, S. M.; Langer, R. S.; Shakesheff, K. M. *Chemical Reviews* 1999, 99, 3181-3198.
- (4) Agrawal, C. M.; Athanasiou, K. A. *Journal of Biomedical Materials Research* 1997, 38, 105-114.
- (5) Langer, R.; Vacanti, J. P. *Science* 1993, 260, 920-926.
- (6) Langer, R. S.; Vacanti, J. P. *Scientific American* 1999, 280, 86-89.
- (7) Mooney, D. J.; Mikos, A. G. *Scientific American* 1999, 280, 60-65.
- (8) Langer, R. *Journal of Controlled Release* 1999, 62, 7-11.
- (9) Hubbell, J. A.; Langer, R. *Chemical & Engineering News* 1995, 73, 42-54.
- (10) Mrksich, M. *Current Opinion in Chemical Biology* 2002, 6, 794-797.
- (11) Langer, R. *Pharmaceutical Research* 1997, 14, 840-841.
- (12) Freed, L. E.; Marquis, J. C.; Vunjaknovakovic, G.; Emmanuel, J.; Langer, R. *Biotechnology and Bioengineering* 1994, 43, 605-614.
- (13) Freed, L. E.; Marquis, J. C.; Nohria, A.; Emmanuel, J.; Mikos, A. G.; Langer, R. *Journal of Biomedical Materials Research* 1993, 27, 11-23.
- (14) Matsusue, Y.; Yamamuro, T.; Oka, M.; Shikinami, Y.; Hyon, S. H.; Ikada, Y. *Journal of Biomedical Materials Research* 1992, 26, 1553-1567.
- (15) Hollinger, J. O. *Journal of Biomedical Materials Research* 1983, 17, 71-82.
- (16) Vacanti, J. P.; Morse, M. A.; Saltzman, W. M.; Domb, A. J.; Perezatayde, A.; Langer, R. *Journal of Pediatric Surgery* 1988, 23, 3-9.
- (17) Cima, L. G.; Vacanti, J. P.; Vacanti, C.; Ingber, D.; Mooney, D.; Langer, R. *Journal of Biomechanical Engineering-Transactions of the Asme* 1991, 113, 143-151.
- (18) Gilding, D. K.; Reed, A. M. *Polymer* 1979, 20, 1459-1464.

- (19) Schaefer, D.; Martin, I.; Shastri, P.; Padera, R. F.; Langer, R.; Freed, L. E.; Vunjak-Novakovic, G. *Biomaterials* 2000, 21, 2599-2606.
- (20) Vert, M.; Li, S. M.; Garreau, H. *Journal of Biomaterials Science-Polymer Edition* 1994, 6, 639-649.
- (21) Freed, L. E.; Vunjaknovakovic, G.; Biron, R. J.; Eagles, D. B.; Lesnoy, D. C.; Barlow, S. K.; Langer, R. *Bio-Technology* 1994, 12, 689-693.
- (22) Mooney, D. T.; Mazzoni, C. L.; Breuer, C.; McNamara, K.; Hern, D.; Vacanti, J. P.; Langer, R. *Biomaterials* 1996, 17, 115-124.
- (23) Mikos, A. G.; Thorsen, A. J.; Czerwonka, L. A.; Bao, Y.; Langer, R.; Winslow, D. N.; Vacanti, J. P. *Polymer* 1994, 35, 1068-1077.
- (24) Mooney, D. J.; Baldwin, D. F.; Suh, N. P.; Vacanti, L. P.; Langer, R. *Biomaterials* 1996, 17, 1417-1422.
- (25) Whang, K.; Thomas, C. H.; Healy, K. E.; Nuber, G. *Polymer* 1995, 36, 837-842.
- (26) Schugens, C.; Maquet, V.; Grandfils, C.; Jerome, R.; Teyssie, P. *Journal of Biomedical Materials Research* 1996, 30, 449-461.
- (27) Nam, Y. S.; Park, T. G. *Journal of Biomedical Materials Research* 1999, 47, 8-17.
- (28) Hohenester, E.; Engel, J. *Matrix Biology* 2002, 21, 115-128.
- (29) Hutmacher, D. W. *Biomaterials* 2000, 21, 2529-2543.
- (30) Webb, K.; Hlady, V.; Tresco, P. A. *Journal of Biomedical Materials Research* 1998, 41, 422-430.
- (31) Daw, R.; Candan, S.; Beck, A. J.; Devlin, A. J.; Brook, I. M.; MacNeil, S.; Dawson, R. A.; Short, R. D. *Biomaterials* 1998, 19, 1717-1725.
- (32) Shelton, R. M.; Rasmussen, A. C.; Davies, J. E. *Biomaterials* 1988, 9, 24-29.
- (33) Vanwachem, P. B.; Hogt, A. H.; Beugeling, T.; Feijen, J.; Bantjes, A.; Detmers, J. P.; Vanaken, W. G. *Biomaterials* 1987, 8, 323-328.
- (34) Chehroudi, B.; Gould, T. R. L.; Brunette, D. M. *Journal of Biomedical Materials Research* 1990, 24, 1203-1219.
- (35) Yang, J.; Bei, J. Z.; Wang, S. G. *Polymers for Advanced Technologies* 2002, 13, 220-226.
- (36) Yang, J.; Wan, Y. Q.; Tu, C. F.; Cai, Q.; Bei, J. Z.; Wang, S. G. *Polymer International* 2003, 52, 1892-1899.

- (37) Lee, K. B.; Yoon, K. R.; Woo, S. I.; Choi, I. S. *Journal of Pharmaceutical Sciences* 2003, 92, 933-937.
- (38) Gao, J. M.; Niklason, L.; Langer, R. *Journal of Biomedical Materials Research* 1998, 42, 417-424.
- (39) Dunn, M. G.; Bellincampi, L. D.; Tria, A. J.; Zawadsky, J. P. *Journal of Applied Polymer Science* 1997, 63, 1423-1428.
- (40) Chen, G. P.; Ushida, T.; Tateishi, T. *Chemistry Letters* 1999, 561-562.
- (41) Lu, H. H.; El-Amin, S. F.; Scott, K. D.; Laurencin, C. T. *Journal of Biomedical Materials Research Part A* 2003, 64A, 465-474.
- (42) Roether, J. A.; Gough, J. E.; Boccaccini, A. R.; Hench, L. L.; Maquet, V.; Jerome, R. *Journal of Materials Science-Materials in Medicine* 2002, 13, 1207-1214.
- (43) Blaker, J. J.; Gough, J. E.; Maquet, V.; Notingher, I.; Boccaccini, A. R. *Journal of Biomedical Materials Research Part A* 2003, 67A, 1401-1411.
- (44) Zhu, H. G.; Ji, J.; Tan, Q. G.; Barbosa, M. A.; Shen, J. C. *Biomacromolecules* 2003, 4, 378-386.
- (45) Zhu, H. U.; Ji, J.; Lin, R. G.; Gao, C. G.; Feng, L. X.; Shen, J. C. *Journal of Biomedical Materials Research* 2002, 62, 532-539.
- (46) Zhu, H. G.; Ji, J.; Lin, R. Y.; Gao, C. Y.; Feng, L. X.; Shen, J. C. *Biomaterials* 2002, 23, 3141-3148.
- (47) Otsuka, H.; Nagasaki, Y.; Kataoka, K. *Biomacromolecules* 2000, 1, 39-48.
- (48) Lavik, E. B.; Hrkach, J. S.; Lotan, N.; Nazarov, R.; Langer, R. *Journal of Biomedical Materials Research* 2001, 58, 291-294.
- (49) Barrera, D. A.; Zylstra, E.; Lansbury, P. T.; Langer, R. *Journal of the American Chemical Society* 1993, 115, 11010-11011.
- (50) Barrera, D. A.; Zylstra, E.; Lansbury, P. T.; Langer, R. *Macromolecules* 1995, 28, 425-432.
- (51) Ouchi, T.; Nozaki, T.; Okamoto, Y.; Shiratani, M.; Ohya, Y. *Macromolecular Chemistry and Physics* 1996, 197, 1823-1833.
- (52) Ohya, Y.; Matsunami, H.; Yamabe, E.; Ouchi, T. *Journal of Biomedical Materials Research Part A* 2003, 65A, 79-88.
- (53) Chen, C. S.; Mrksich, M.; Huang, S.; Whitesides, G. M.; Ingber, D. E. *Science* 1997, 276, 1425-1428.

- (54) Tien, J.; Chen, C. S. *Ieee Engineering in Medicine and Biology Magazine* 2002, 21, 95-98.
- (55) Nelson, C. M.; Chen, C. S. *Febs Letters* 2002, 514, 238-242.
- (56) Corey, J. M.; Feldman, E. L. *Experimental Neurology* 2003, 184, S89-S96.
- (57) Corey, J. M.; Wheeler, B. C.; Brewer, G. J. *Journal of Neuroscience Research* 1991, 30, 300-307.
- (58) Corey, J. M.; Brunette, A. L.; Chen, M. S.; Weyhenmeyer, J. A.; Brewer, G. J.; Wheeler, B. C. *Journal of Neuroscience Methods* 1997, 75, 91-97.
- (59) Irimia, D.; Karlsson, J. O. M. *Biophysical Journal* 2002, 82, 1858-1868.
- (60) Corey, J. M.; Wheeler, B. C.; Brewer, G. J. *Ieee Transactions on Biomedical Engineering* 1996, 43, 944-955.
- (61) Kumar, A.; Biebuyck, H. A.; Whitesides, G. M. *Langmuir* 1994, 10, 1498-1511.
- (62) Gallant, N. D.; Capadona, J. R.; Frazier, A. B.; Collard, D. M.; Garcia, A. J. *Langmuir* 2002, 18, 5579-5584.
- (63) Luo, N.; Metters, A. T.; Hutchison, J. B.; Bowman, C. N.; Anseth, K. S. *Macromolecules* 2003, 36, 6739-6745.
- (64) Yin, M.; Baker, G. L. *Macromolecules* 1999, 32, 7711-7718.
- (65) Radano, C. P. Ph.D. Dissertation 2003.
- (66) Chung, T. C.; Janvikul, W.; Bernard, R.; Hu, R.; Li, C. L.; Liu, S. L.; Jiang, G. J. *Polymer* 1995, 36, 3565-3574.
- (67) Ruckenstein, E.; Zhang, H. M. *Journal of Polymer Science Part a-Polymer Chemistry* 2000, 38, 1195-1202.
- (68) Huang, W. X.; Kim, J. B.; Bruening, M. L.; Baker, G. L. *Macromolecules* 2002, 35, 1175-1179.
- (69) Houlihan, F. M.; Bouchard, F.; Frechet, J. M. J.; Willson, C. G. *Macromolecules* 1986, 19, 13-19.
- (70) Chinchilla, R.; Dodsworth, D. J.; Najera, C.; Soriano, J. M. *Tetrahedron Letters* 2001, 42, 4487-4489.
- (71) Ball, H. L.; King, D. S.; Cohen, F. E.; Prusiner, S. B.; Baldwin, M. A. *Journal of Peptide Research* 2001, 58, 357-374.

- (72) Carnahan, M. A.; Grinstaff, M. W. *Journal of the American Chemical Society* 2001, 123, 2905-2906.
- (73) Ihre, H.; Hult, A.; Frechet, J. M. J.; Gitsov, I. *Macromolecules* 1998, 31, 4061-4068.
- (74) Park, Y. J.; Hwang, K. S.; Song, J. E.; Ong, J. L.; Rawls, H. R. *Biomaterials* 2002, 23, 3859-3864.
- (75) Padmaja, T.; Lele, B. S.; Deshpande, M. C.; Kulkarni, M. G. *Journal of Applied Polymer Science* 2002, 85, 2108-2118.
- (76) Watkins, B. A.; Lippman, H. E.; Le Bouteiller, L.; Li, Y.; Seifert, M. F. *Progress in Lipid Research* 2001, 40, 125-148.
- (77) Watkins, B. A.; Li, Y.; Lippman, H. E.; Feng, S. *Prostaglandins Leukotrienes and Essential Fatty Acids* 2003, 68, 387-398.
- (78) Ingber, D. *Faseb Journal* 1999, 13, S3-S15.
- (89) Akerblom, E. B. *Molecular Diversity* 1998, 4, 53-69.
- (80) Dorman, G.; Prestwich, G. D. *Trends in Biotechnology* 2000, 18, 64-77.
- (81) Bochet, C. G. *Journal of the Chemical Society-Perkin Transactions 1* 2002, 125-142.
- (82) Furuta, T.; Hirayama, Y.; Iwamura, M. *Organic Letters* 2001, 3, 1809-1812.
- (83) Nederberg, F.; Connor, E. F.; Glausser, T.; Hedrick, J. L. *Chemical Communications* 2001, 2066-2067.
- (84) Ng, K. W.; Romas, E.; Donnan, L.; Findlay, D. M. *Baillieres Clinical Endocrinology and Metabolism* 1997, 11, 1-22.
- (85) Marie, P. J. *Gene* 2003, 316, 23-32.
- (86) Karsenty, G.; Wagner, E. F. *Developmental Cell* 2002, 2, 389-406.
- (87) Nakashima, K.; Zhou, X.; Kunkel, G.; Zhang, Z. P.; Deng, J. M.; Behringer, R. R.; de Crombrughe, B. *Cell* 2002, 108, 17-29.

Appendix A

DSC Data for:

PLLA-*co*-DAG

PLLA-*g*-HP

PLLA-*g*-MyPr

PLLA-*g*-StPr

PLLA-*g*-OlPr

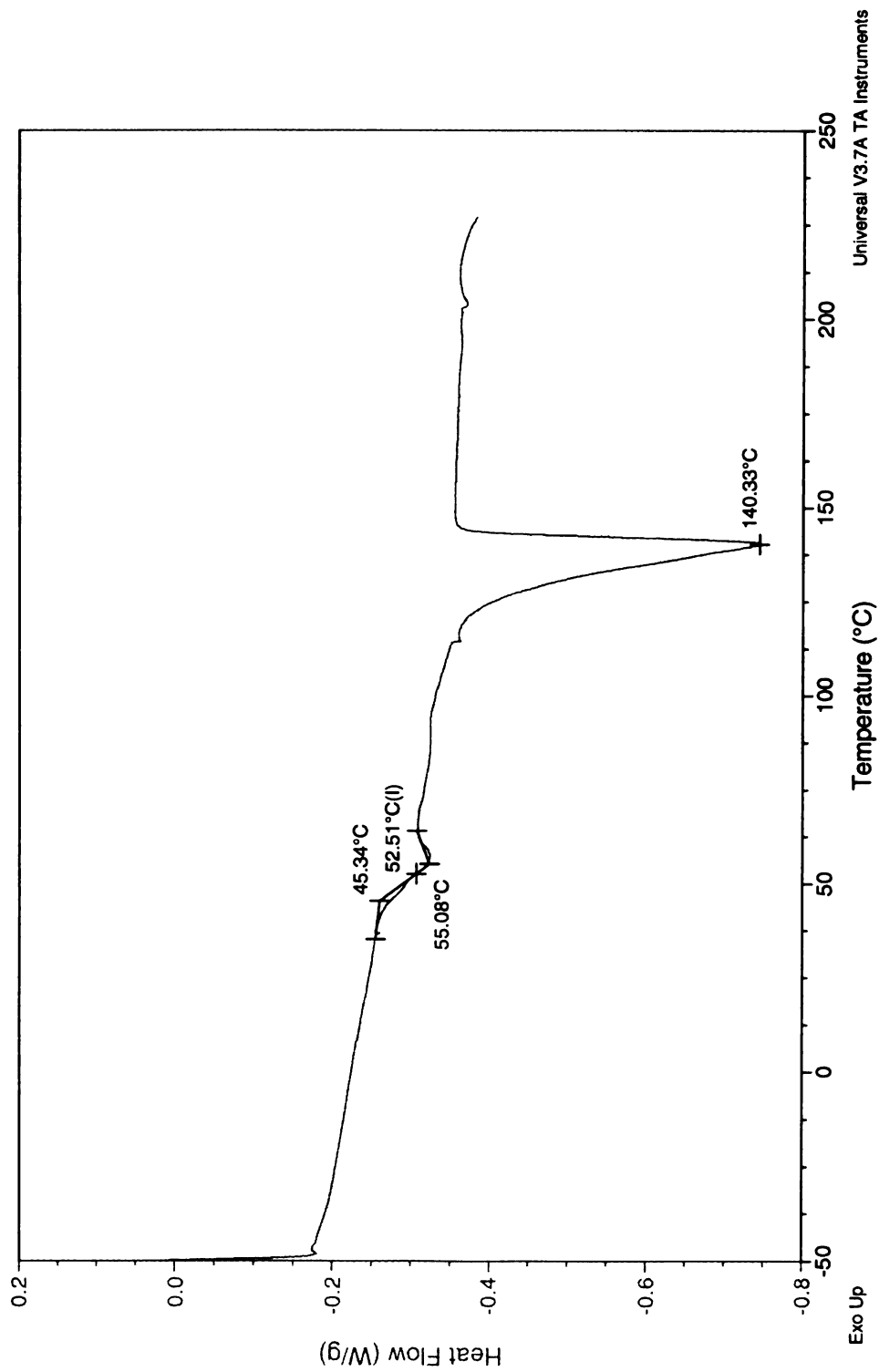
PLLA-*g*-LnPr

PLLA-*g*-ArPr

Sample: PLLA-co-DAG
Size: 5.3000 mg
Method: Conventional DSC

DSC

File: C:\TA\Data\DSC\Mei\PLLA-co-DAG1
Operator: Mei
Run Date: 04-May-04 19:25
Instrument: DSC Q1000 V7.0 Build 244

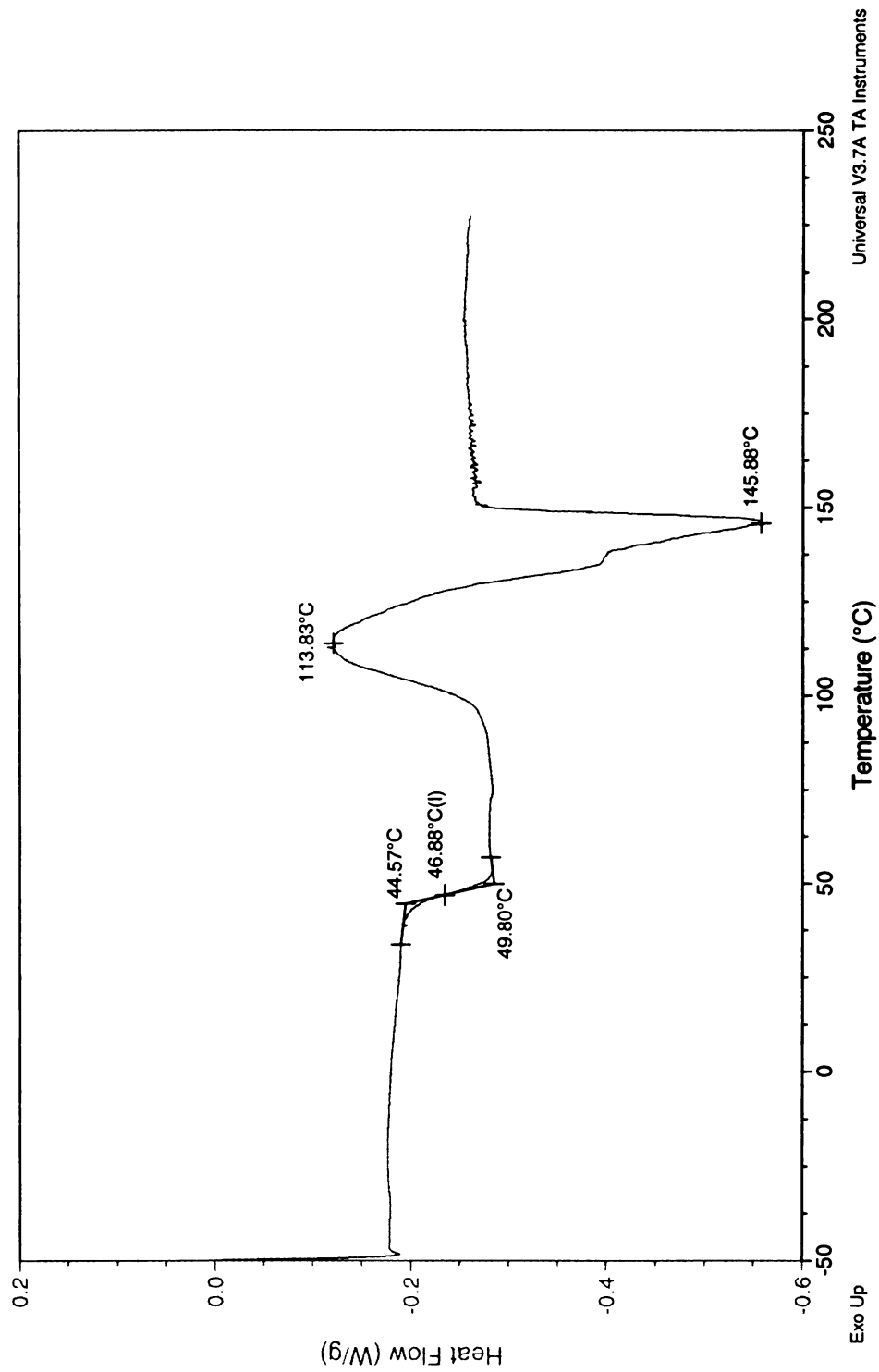


Universal V3.7A TA Instruments

Sample: PLLA-g-HP
Size: 3.7000 mg
Method: Conventional DSC

DSC

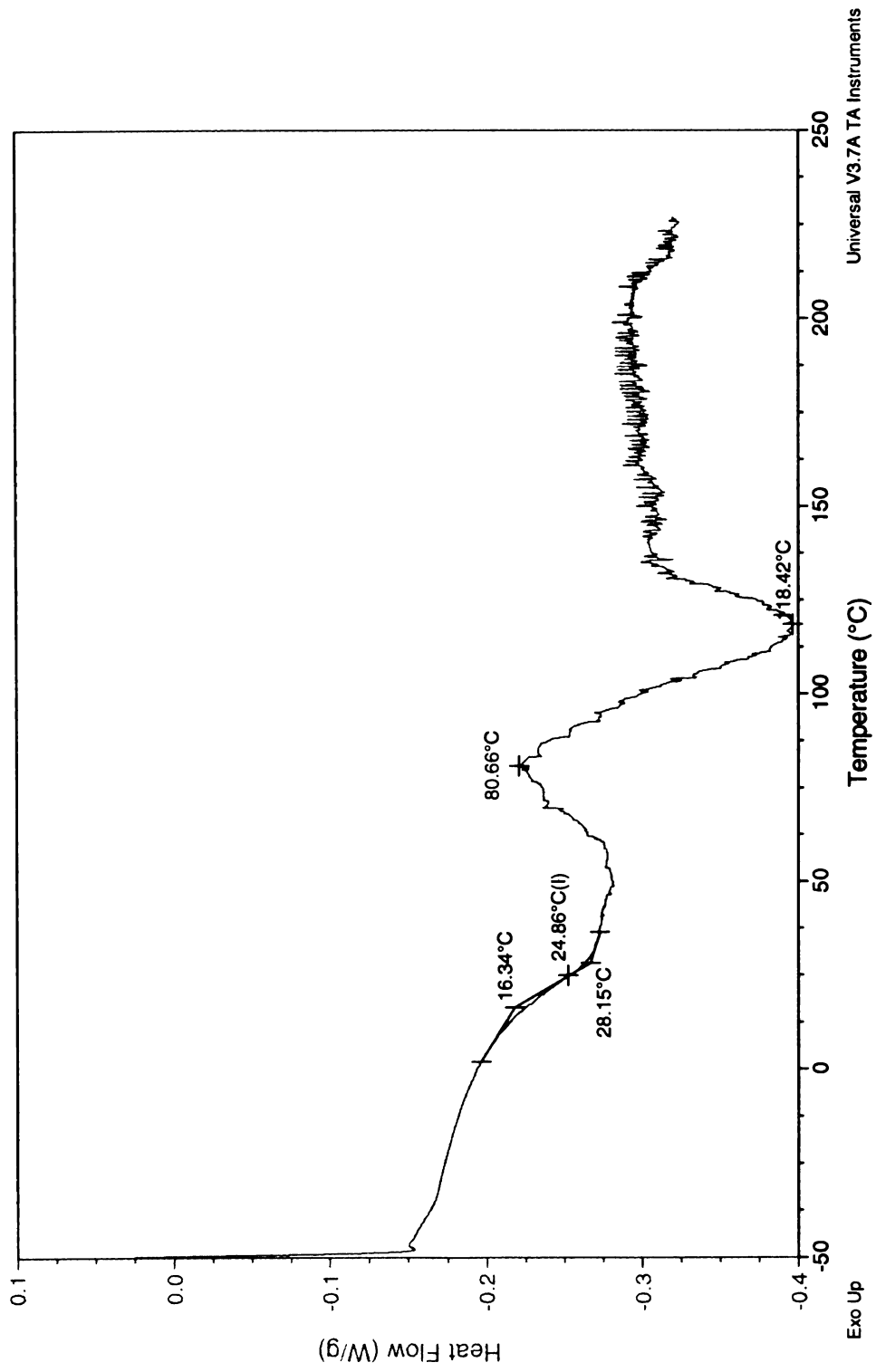
File: C:\TA\Data\DSC\Mei\PLLA-g-HP1
Operator: Mei
Run Date: 04-May-04 17:40
Instrument: DSC Q1000 V7.0 Build 244



Sample: PLLA-g-Mypr
Size: 4.5000 mg
Method: Conventional DSC

DSC

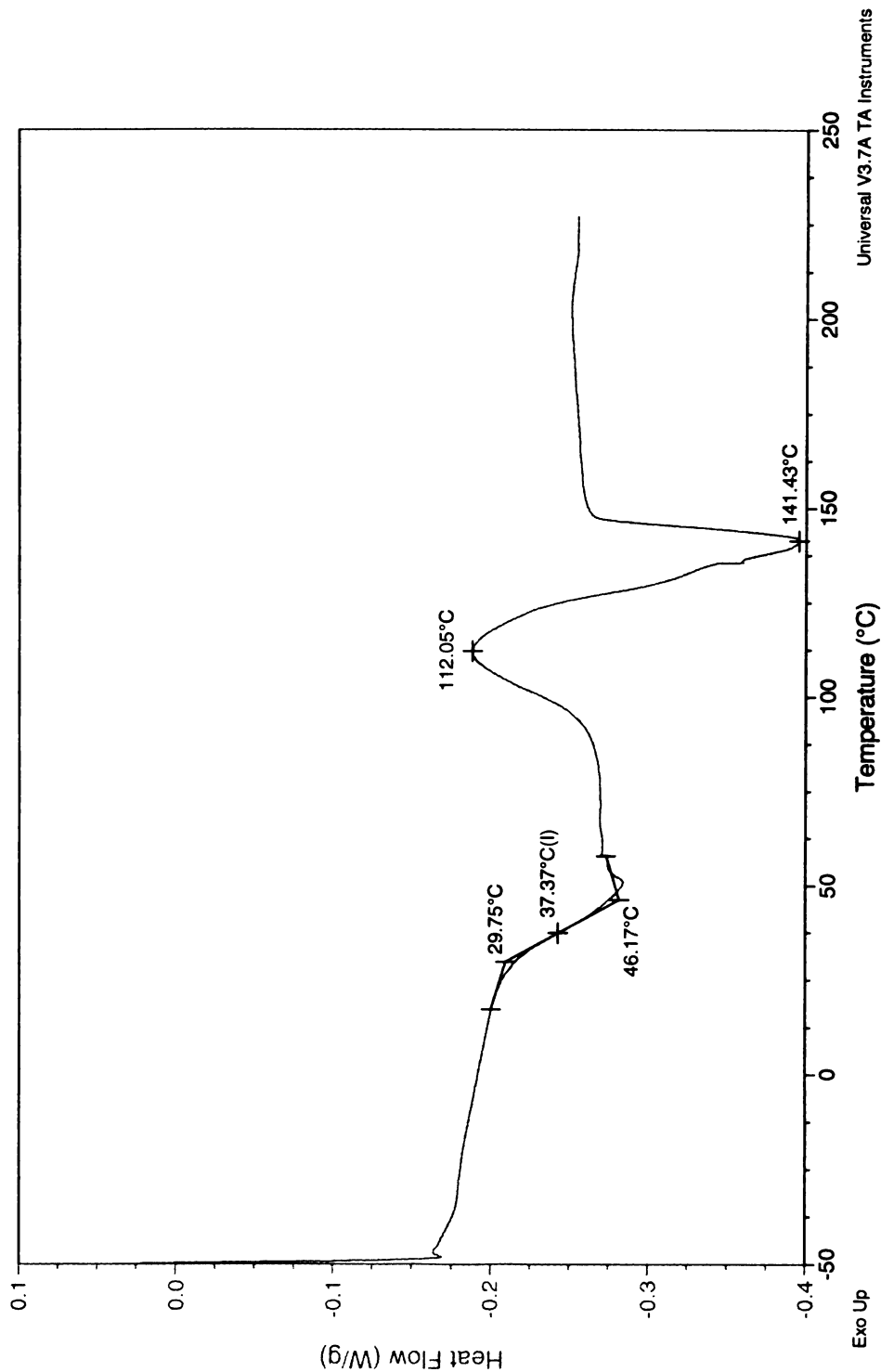
File: C:\TA\Data\DSC\Mei\PLLA-g-Mypr2
Operator: Mei
Run Date: 03-May-04 17:50
Instrument: DSC Q1000 V7.0 Build 244



Sample: PLLA-g-stpr
Size: 4.1000 mg
Method: Conventional DSC

DSC

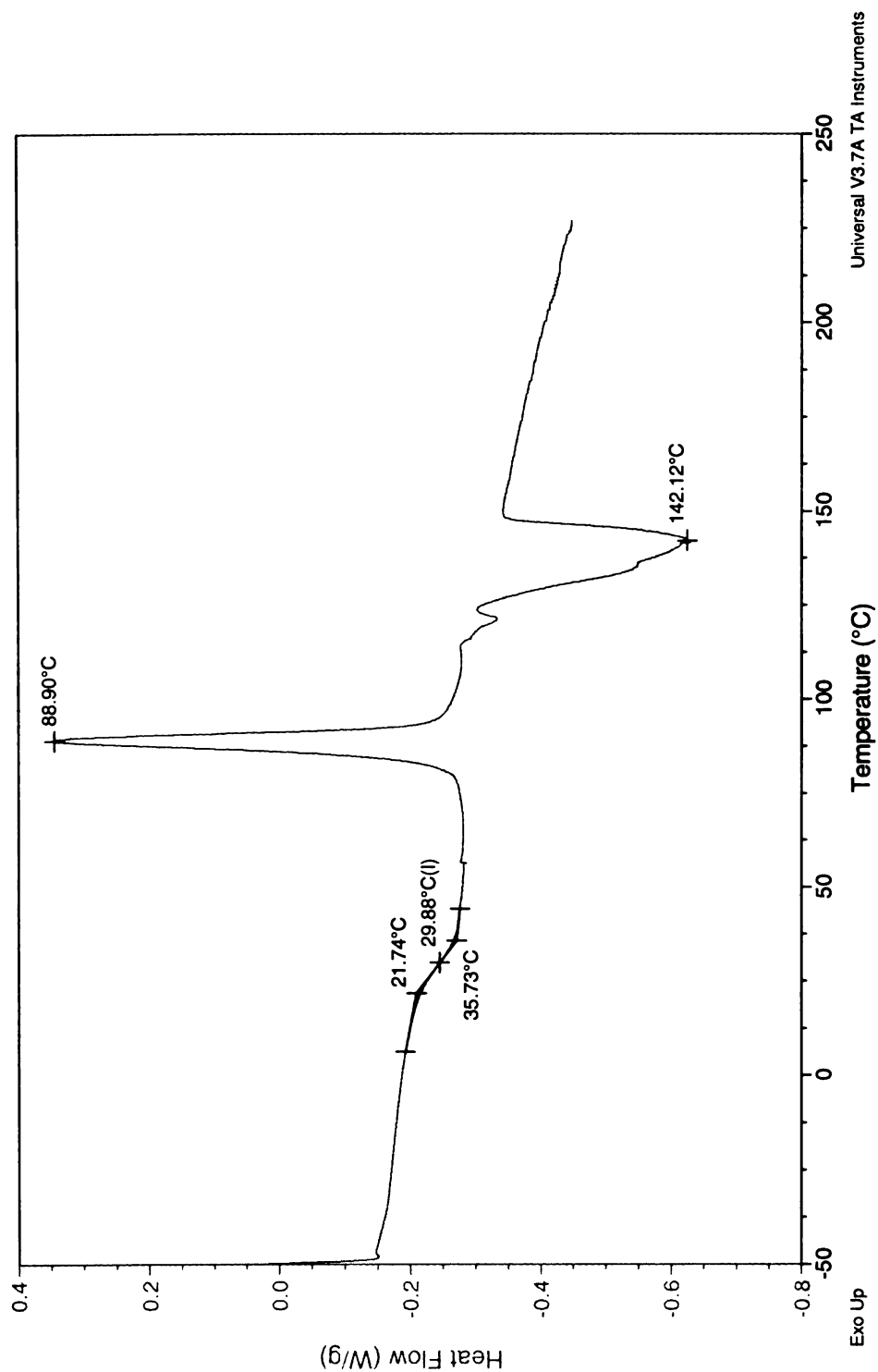
File: C:\TA\Data\DSC\Mei\PLLA-g-stpr1
Operator: Mei
Run Date: 03-May-04 19:33
Instrument: DSC Q1000 V7.0 Build 244



File: C:\TA\Data\DSC\Mei\PLLA-g-olpr 1
Operator: Mei
Run Date: 03-May-04 21:17
Instrument: DSC Q1000 V7.0 Build 244

DSC

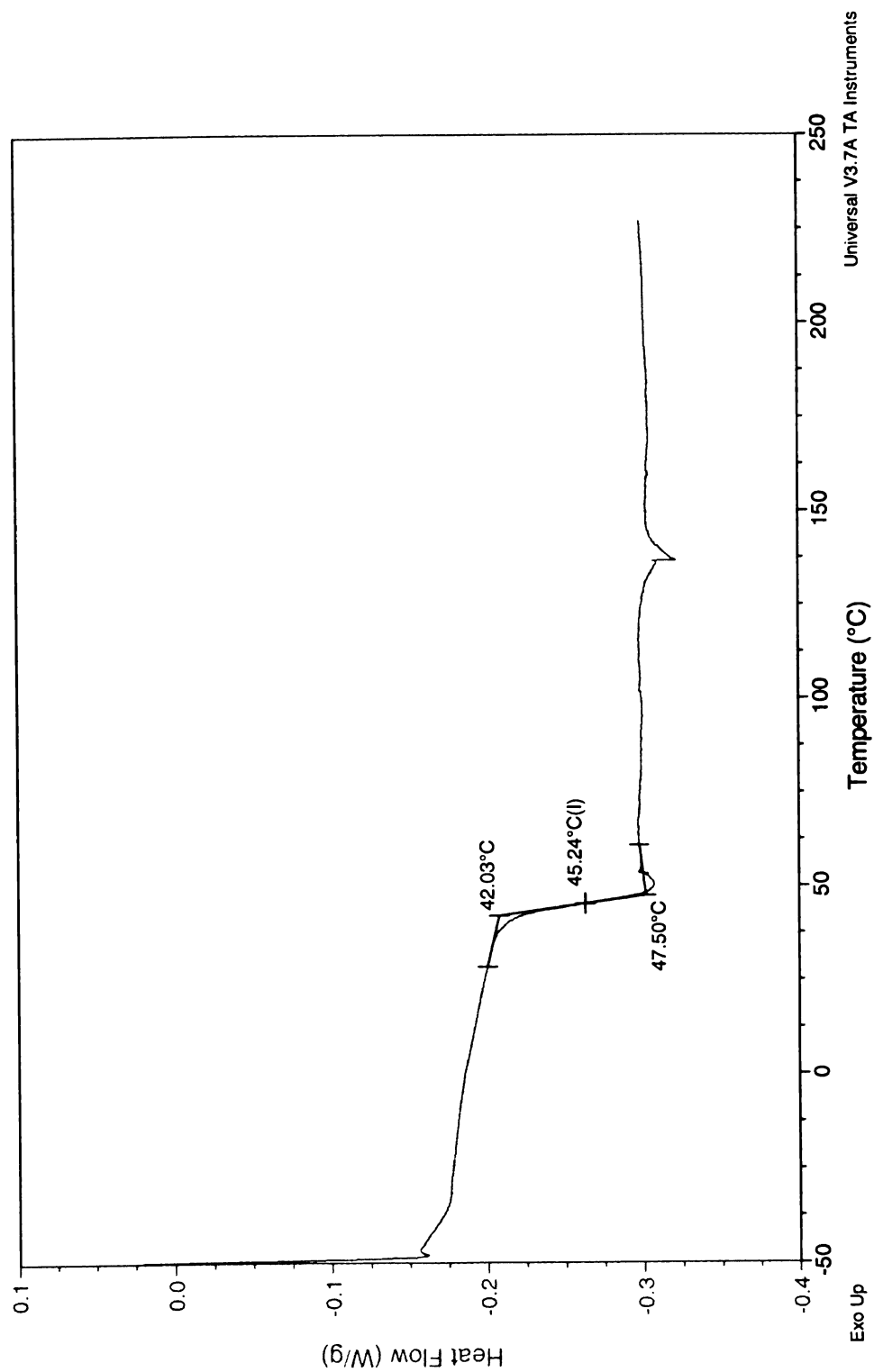
Sample: PLLA-g-olpr
Size: 4.9000 mg
Method: Conventional DSC



File: C:\TA\Data\DSC\Mei\PLLA-g-LnPr1
Operator: Mei
Run Date: 04-May-04 00:44
Instrument: DSC Q1000 V7.0 Build 244

DSC

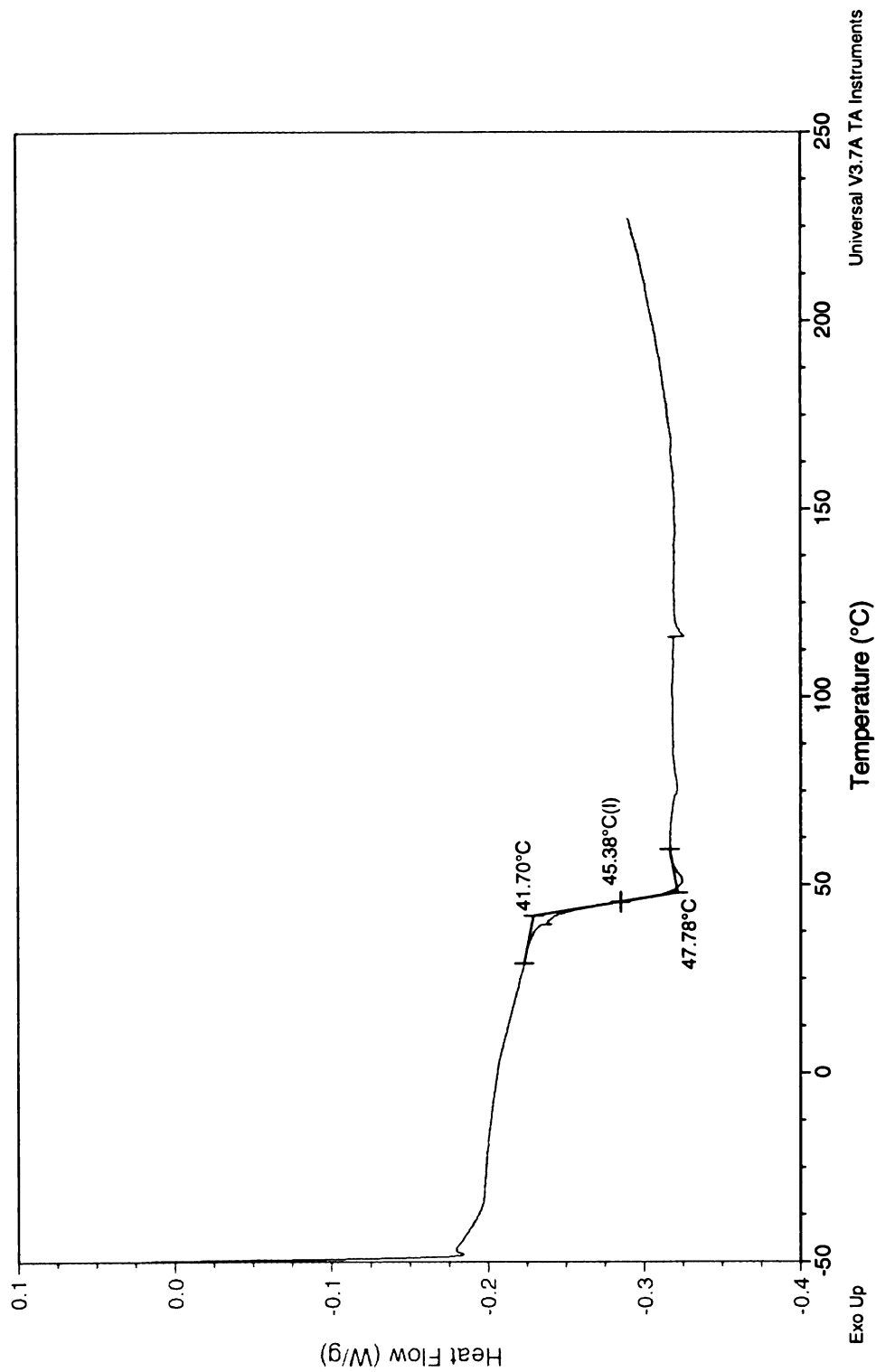
Sample: PLLA-g-LnPr
Size: 3.5000 mg
Method: Conventional DSC



Sample: PLLA-g-ArPr
Size: 3.9000 mg
Method: Conventional DSC

DSC

File: C:\TA\Data\DSC\Mei\PLLA-g-ArPr1
Operator: Mei
Run Date: 04-May-04 22:09
Instrument: DSC Q1000 V7.0 Build 244



Appendix B

TGA Data for:

PLLA-*co*-DAG

PLLA-*g*-HP

PLLA-*g*-MyPr

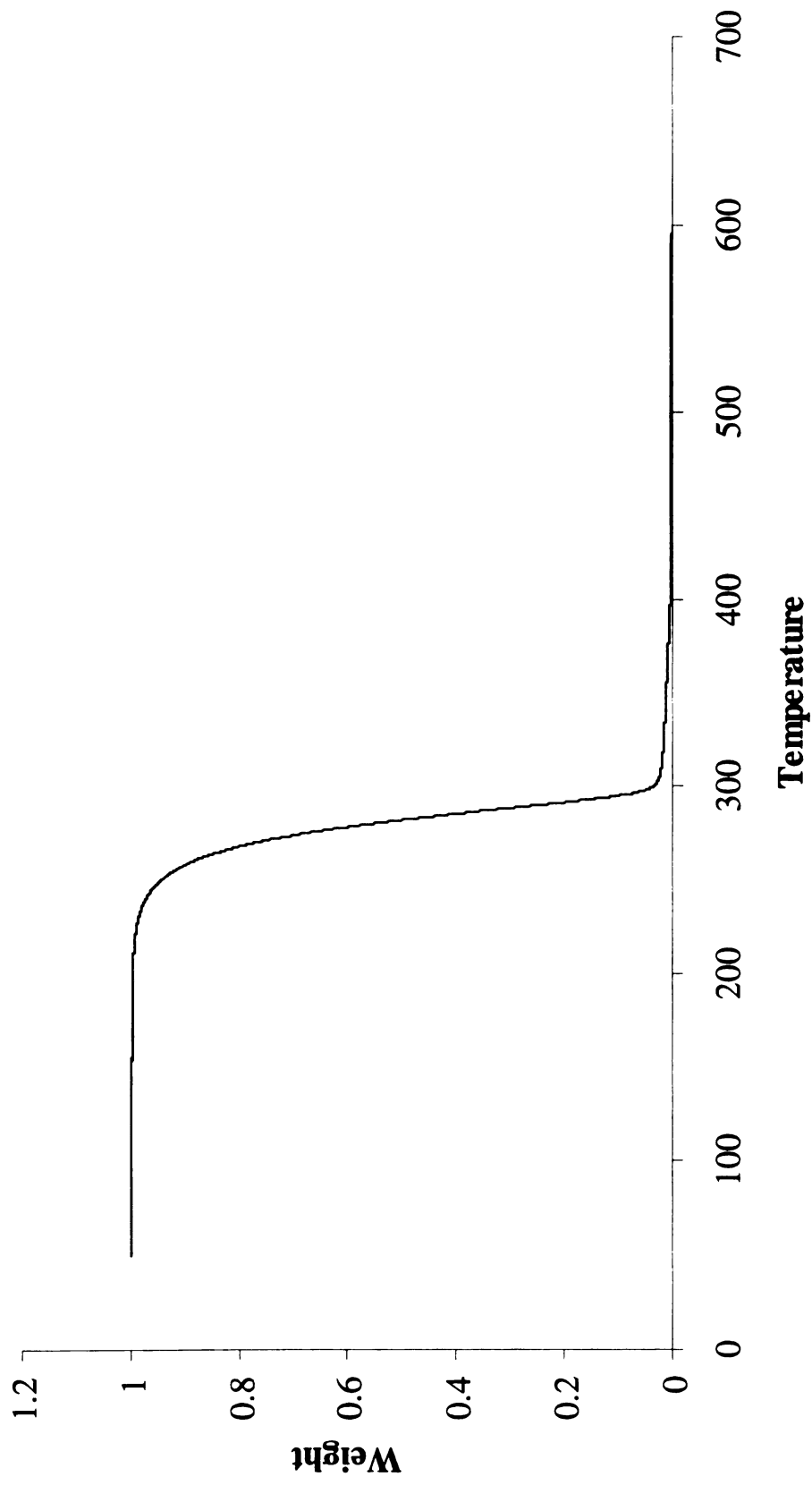
PLLA-*g*-StPr

PLLA-*g*-OlPr

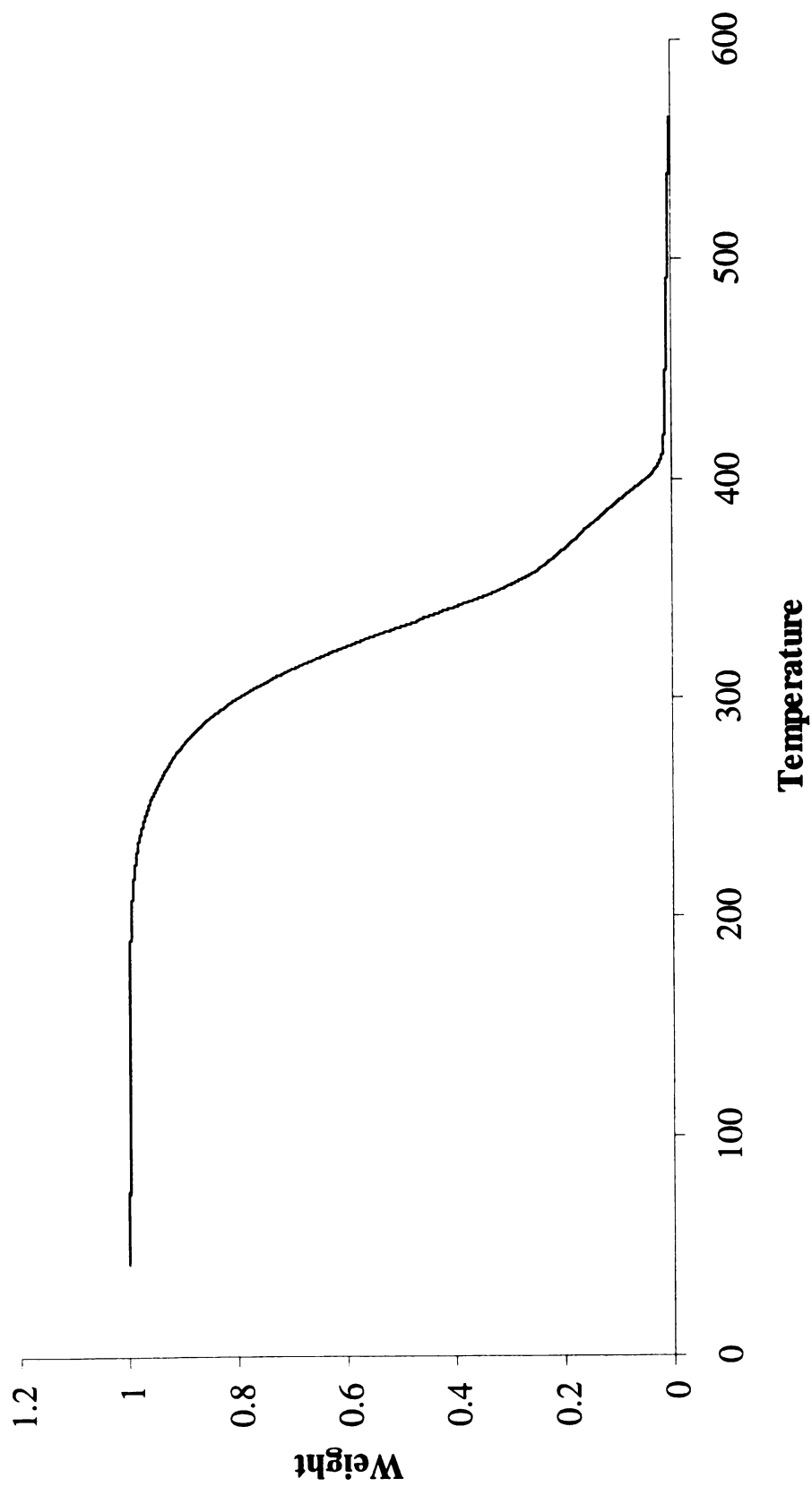
PLLA-*g*-LnPr

PLLA-*g*-ArPr

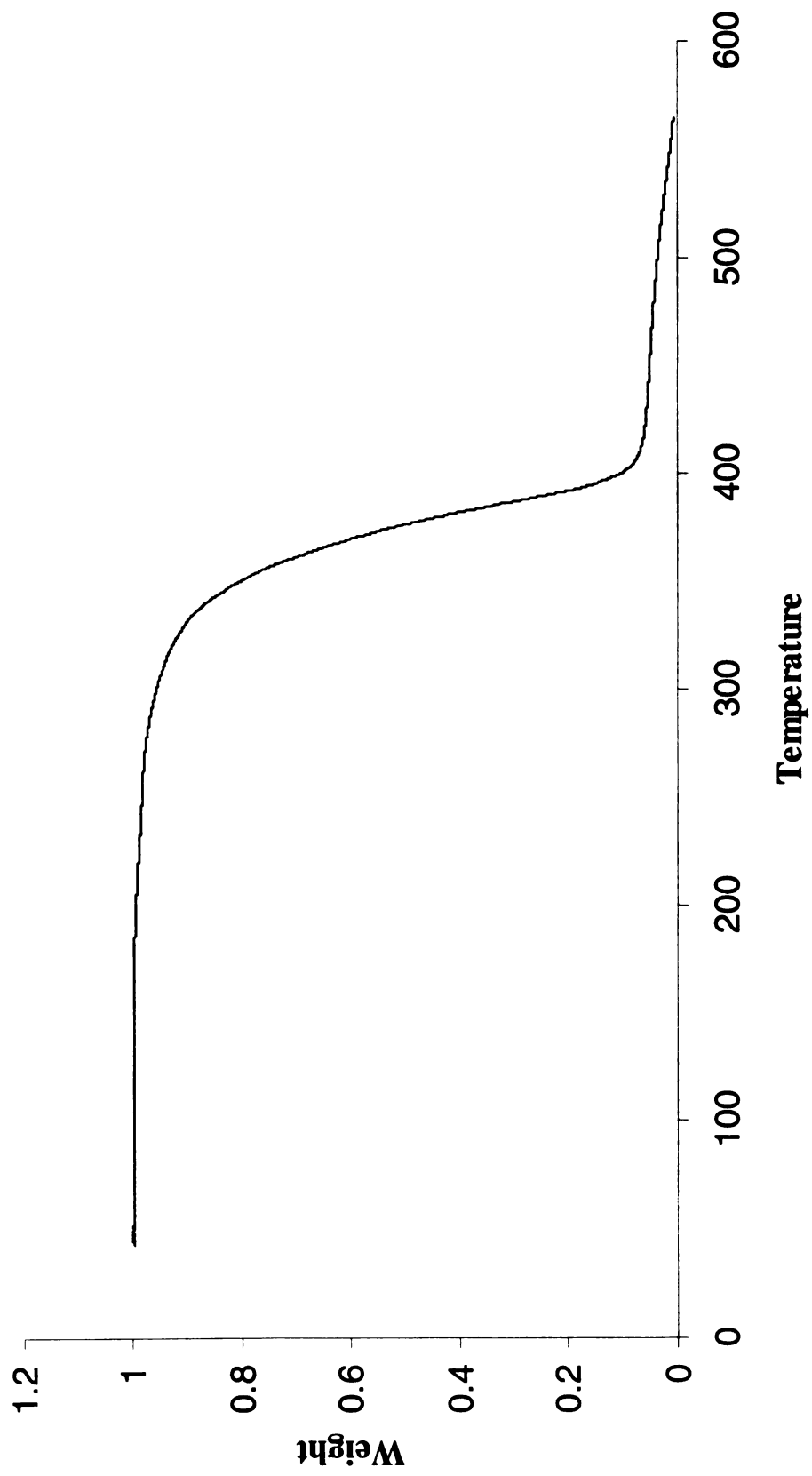
PLLA-co-DAG



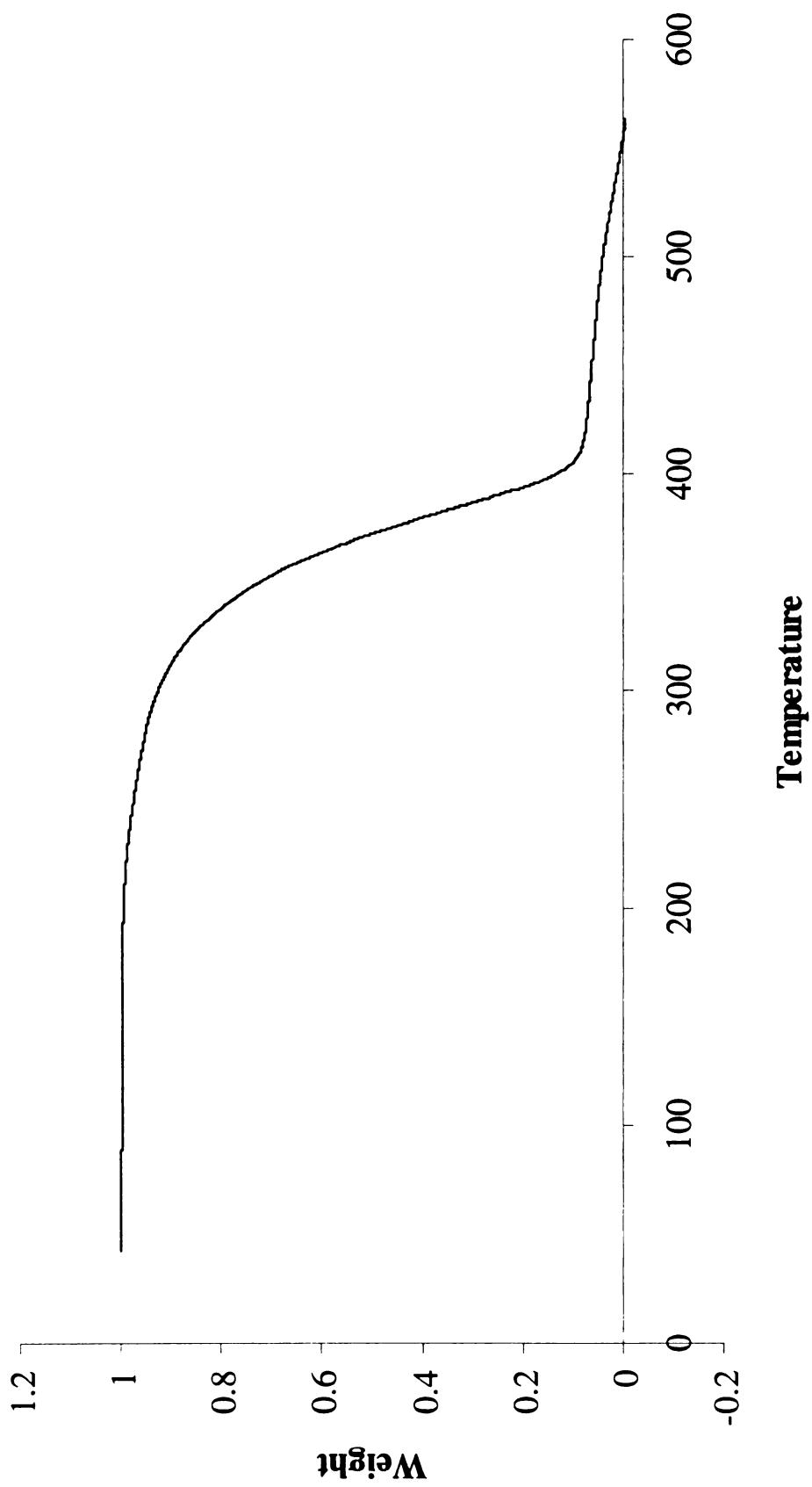
PLLA-g-HP



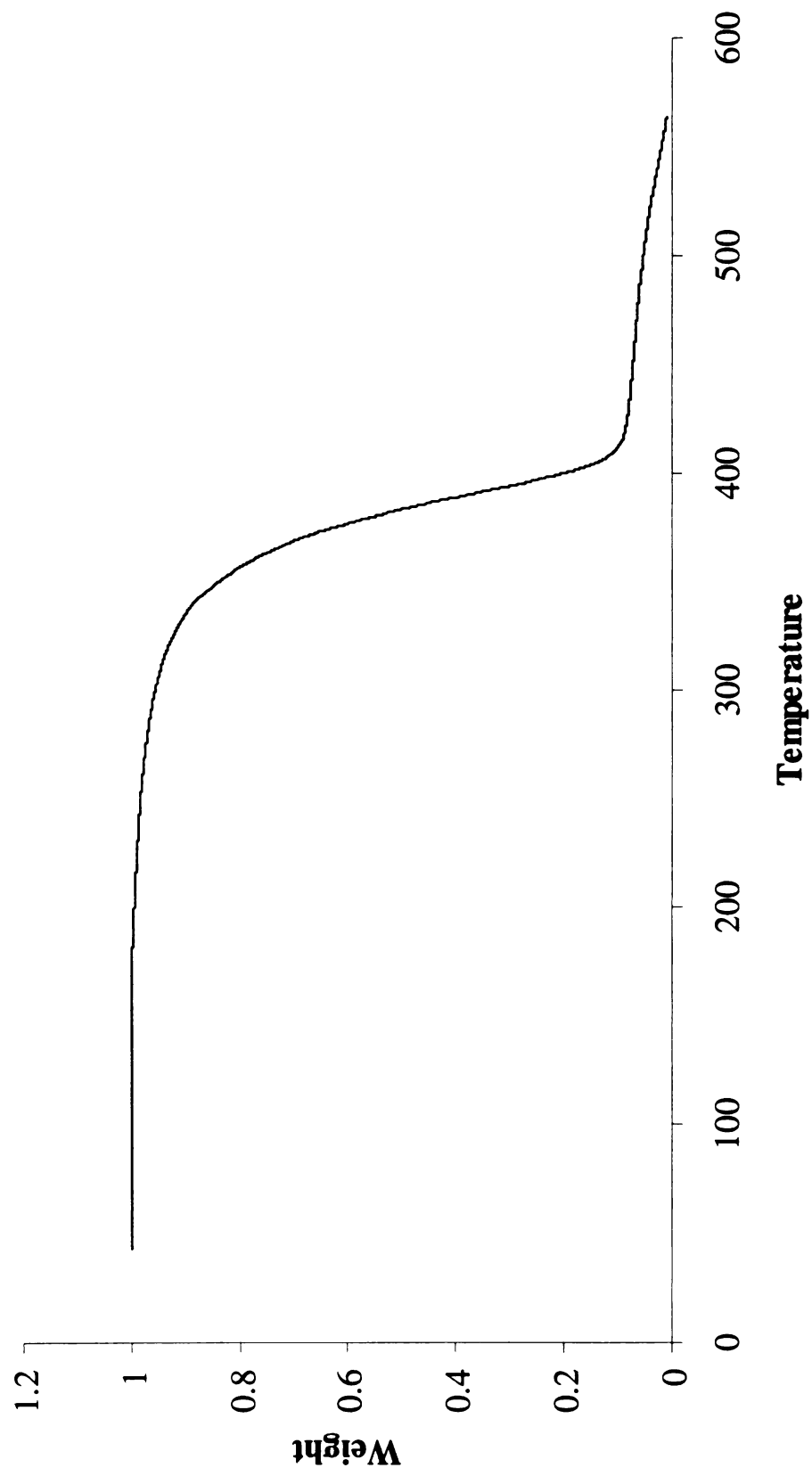
PLLA-g-MyPr



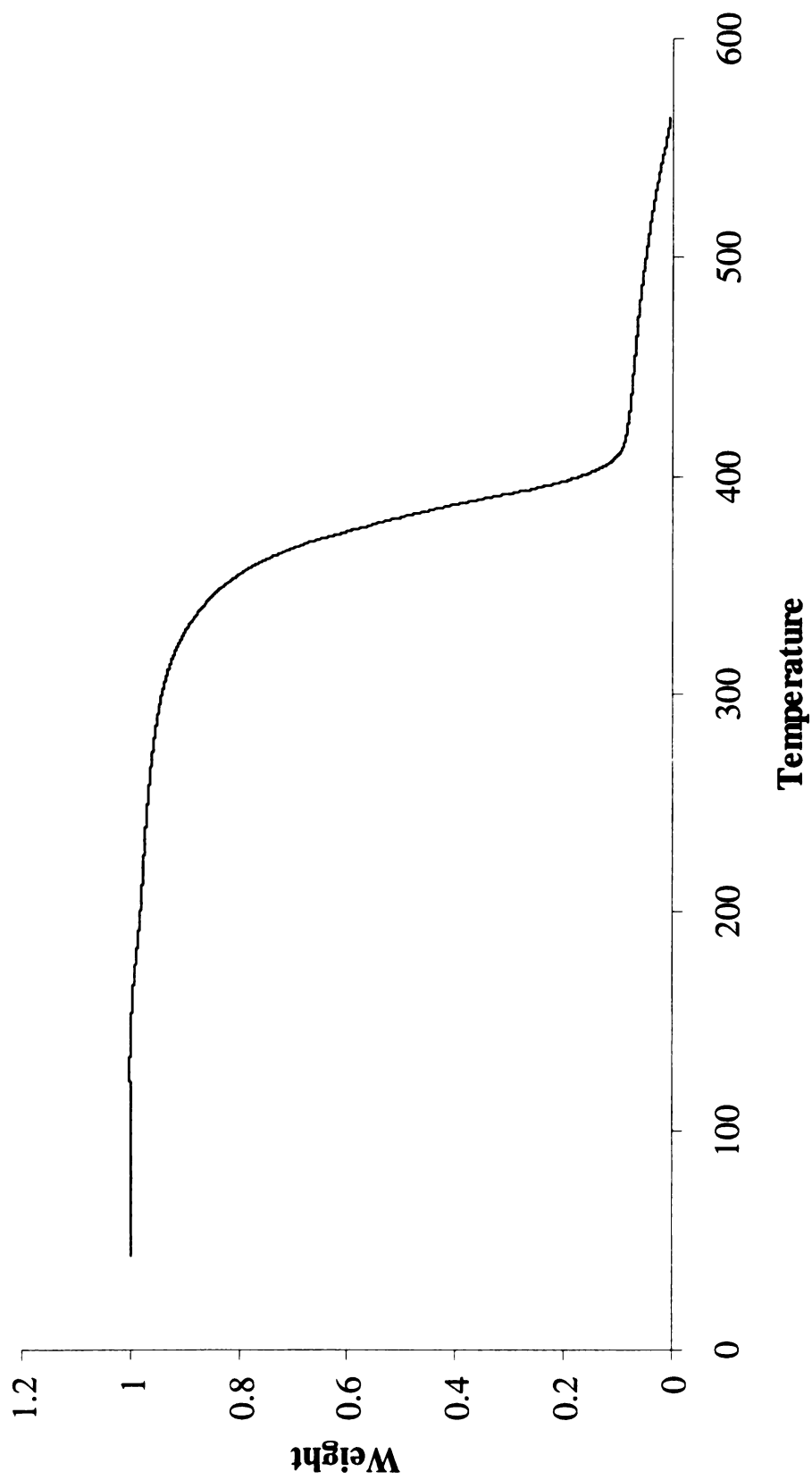
PLLA-g-StPr



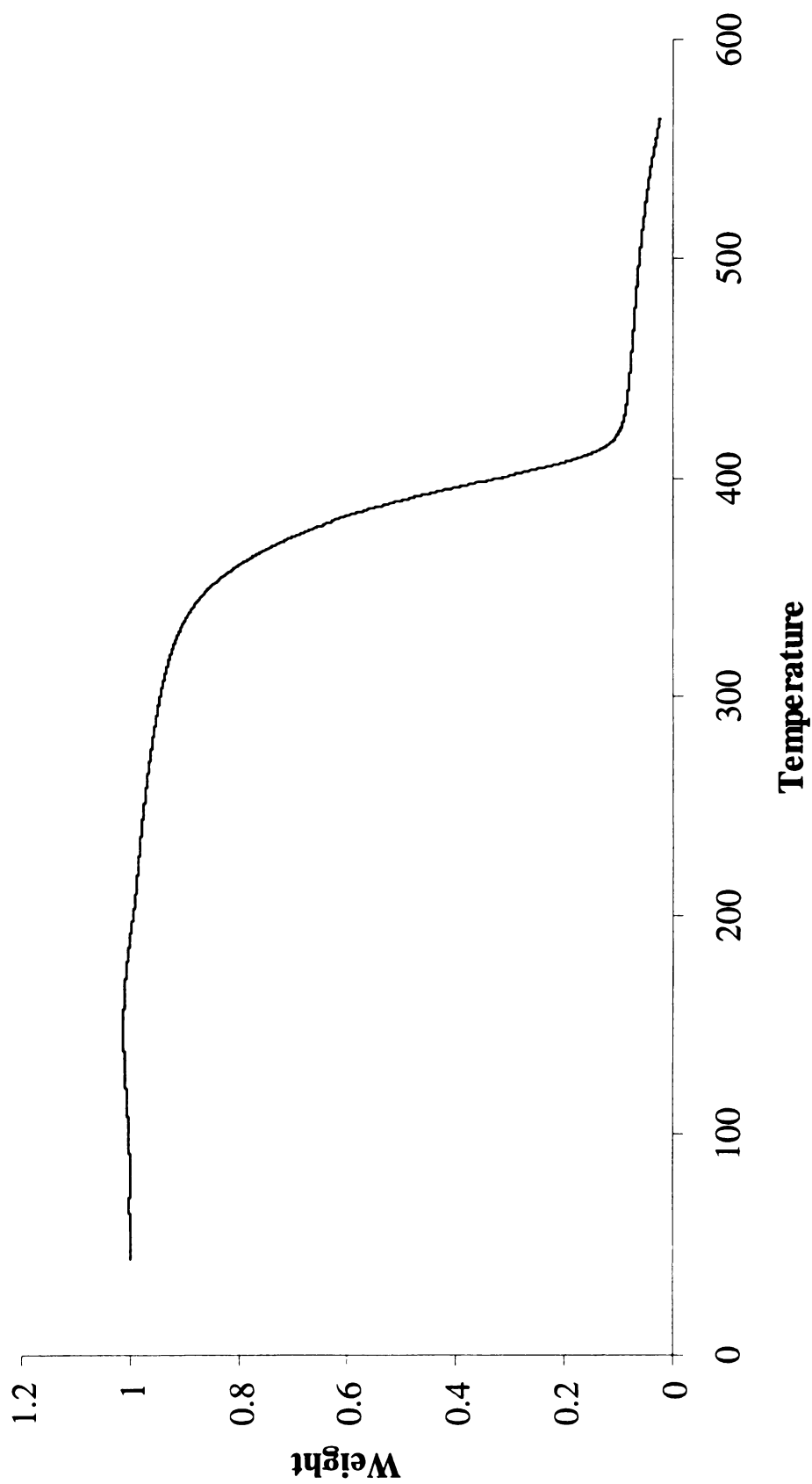
PLLA-g-OIPr



PLLA-g-lnPr



PLLA-g-ArPr



MICHIGAN STATE UNIVERSITY LIBRARIES



3 1293 02511 0259